AFCRL-67-0338

DATA TRANSMISSION AND INSTRUMENTATION SYSTEMS FOR SPACE VEHICLES

J. Spencer Rochefort
Lawrence J. O'Connor
Raimundas Sukys
Arthur Glazer

NORTHEASTERN UNIVERSITY
BOSTON, MASSACHUSETTS 02115

Contract No. AF 19(628)-2433
Project No. 7043

FINAL REPORT

1 April 1963 through 31 March 1967
30 April 1967

Contract Monitor
Charles H. Reynolds
Aerospace Instrumentation Laboratory

Prepared
for

AIR FORCE CAMBRIDGE RESEARCH LABORATORIES
OFFICE OF AEROSPACE RESEARCH
UNITED STATES AIR FORCE
BEDFORD, MASSACHUSETTS 01730

AFCRL-67-0338

DATA TRANSMISSION AND INSTRUMENTATION SYSTEMS FOR SPACE VEHICLES

J. Spencer Rochefort
Lawrence J. O'Connor
Raimundas Sukys
Arthur Glazer

Northeastern University
Boston, Massachusetts 02115

Contract No. AF 19(628)-2433
Project No. 7043

FINAL REPORT
1 April 1963 through 31 March 1967
30 April 1967

Contract Monitor
Charles H. Reynolds
Aerospace Instrumentation Laboratory

Prepared
for

AIR FORCE CAMBRIDGE RESEARCH LABORATORIES
OFFICE OF AEROSPACE RESEARCH
UNITED STATES AIR FORCE
BEDFORD, MASSACHUSETTS, 01730

ABSTRACT

This report summarizes the main work carried out under this contract (April 1, 1963 through March 31, 1967). The contract effort can be grouped under programs concerned with an orbiting vehicle, a re-entry vehicle, field support for certain sounding rockets and balloons, evaluation of commercial telemetry system components, and system studies and developments related to telemetry and weather radar. The orbital vehicle effort is concerned with a telemetry subsystem, a data storage system, aspect instrumentation and determination and a commutator. The discussion of the instrumentation of a Trailblazer II rocket for a re-entry experiment includes treatment of an s-band pulsed system, an x-band PPM telemeter and certain probes. A tabulation is given of commercial airborne telemetry components tested and evaluated since detailed results are published in scientific reports which are available to authorized agencies. The field support rendered in connection with the various programs is tabulated. Specific discussion is given to a PAM/FM system, temperature studies of balloon telemetry systems, and the modification of a weather radar.

TABLE OF CONTENTS

INTRODUCTION

This report summarizes the work which was accomplished under this contract. The material has been organized so that each chapter is reasonably independent of the others although much of the material is related on the program level. The two major programs were concerned with orbital vehicles and re-entry vehicles respectively. Other effort was associated with field support for certain rockets and balloons, evaluation of commercial components, and system studies related to telemetry and weather radar. The contract effort has been grouped into six chapters.

The first two chapters are concerned with the satellite program. The first chapter is system and hardware oriented and embodies discussions of systems, components, circuit design and development and overall performance. The second chapter is essentially mathematical and computer oriented. It deals with the determination of sensor aspect from telemetered information taken by the airborne magnetic aspect system.

Chapter three deals with the instrumentation of a Trailblazer II rocket intended to gather data in a re-entry physics program. The discussion is mainly concerned with a pulsed system operating at s-band, certain probes, and an x-band telemeter.

Field support in connection with satellites, sounding rockets and balloons is the subject matter of the fourth chapter. Most of the travel documented in this chapter was preceeded by numerous preliminary discussions with experimenters and then several months of system development and testing. The travel indicated was then taken so that final field tests or actual support during launch could be carried out.

The fifth chapter is concerned with the evaluation of commercial radio telemetry components. This program is of a continuing nature and scientific reports have been issued on an annual basis. The chapter deals with the components tested and the development of a transmitter test unit.

The sixth chapter contains discussions of system studies which were complete in themselves and not directly related to the material in the other chapters.

CHAPTER I

ORBITAL VEHICLE PROGRAM

The instrumentation design of the support subsystems has been completed on the Atmospheric Composition Satellite (ATCOS). This spacecraft, shown in Figure 1-1, is one of six managed by Air Force Cambridge Research Laboratories as a project in the USAF Aerospace Research Support Program. The official designation is OV3 - 5 and it is designed and fabricated by AFCRL.

The satellite and onboard components are used to facilitate the acquisition and transmission of scientific data to earth. A scout launch vehicle will be used to place the satellite into earth orbit from the Western Test Range, California, on January 31, 1967 with Northeastern personnel assisting in the field test supported under a follow-on contract from Air Force Cambridge Research Laboratories.*

The orbit will be near polar with an apogee of 1000 km and a perigee of 300 km to meet the requirements of two basic experiments. Two Mass Spectrometers and three Ion Density Gauges form one basic experiment and an Impedance Probe the other.

The Mass Spectrometers are used to determine upper atmospheric structure including the composition number densities, partial pressures, and temperature of the charged and uncharged gaseous constituent. Included in the experiment objective is a determination of the physical and chemical processes which create this structure.

The Density Gauges are used to measure neutral atmospheric density. The data obtained is to be used to compare direct density values with those calculated from drag; determine the origin, nature, and degree of geophysical phenomena occuring in our atmosphere; to provide data for upgrading the U.S. Standard Atmosphere; and supply evidence for the basis of solar geophysical interaction.

The Impedance Probe will measure electron density and temperature irregularities, both large and small, in and above the F_2 layer of the ionosphere as well as the more pronounced irregularities under disturbed conditions in the auroral zones.

A. Telemetering Subsystems Description

The ATCOS telemetering subsystems diagram is shown in Figure 1-2. There are three telemetering links that provide data encoding for experimental and spacecraft status information into standard IRIG NRZ PAM/FM/FM and PCM/FM systems. The two primary data links contain on-board magnetic tape storage capabilities for the purpose of data storage over complete orbits prior to ground transmission. The record-to-playback ratios for the recorders are 1 to 18 and 1 to 80 respectively, which allow for the acquisition and storage of approximately 100 minutes of data prior to transmission for the former and 600 minutes for the latter. Provision has been made for real time modes of operation in order to assist in spacecraft evaluation.

The first of the telemetry subsystems, Link I, consists of experimental and status data being transmitted as a PAM/FM/FM/ system. This link employs a standard 50.0 kHz reference channel for tape speed compensation and seven IRIG bands: 16, 15, 14, 13, 11, 10, and 8. The reference channel as well as bands 16, 15, 14, 13, and 11 are reproduced from the tape recorder as previously stored data, and bands

* Contract AF 19 (628) - 5140, April 1, 1965

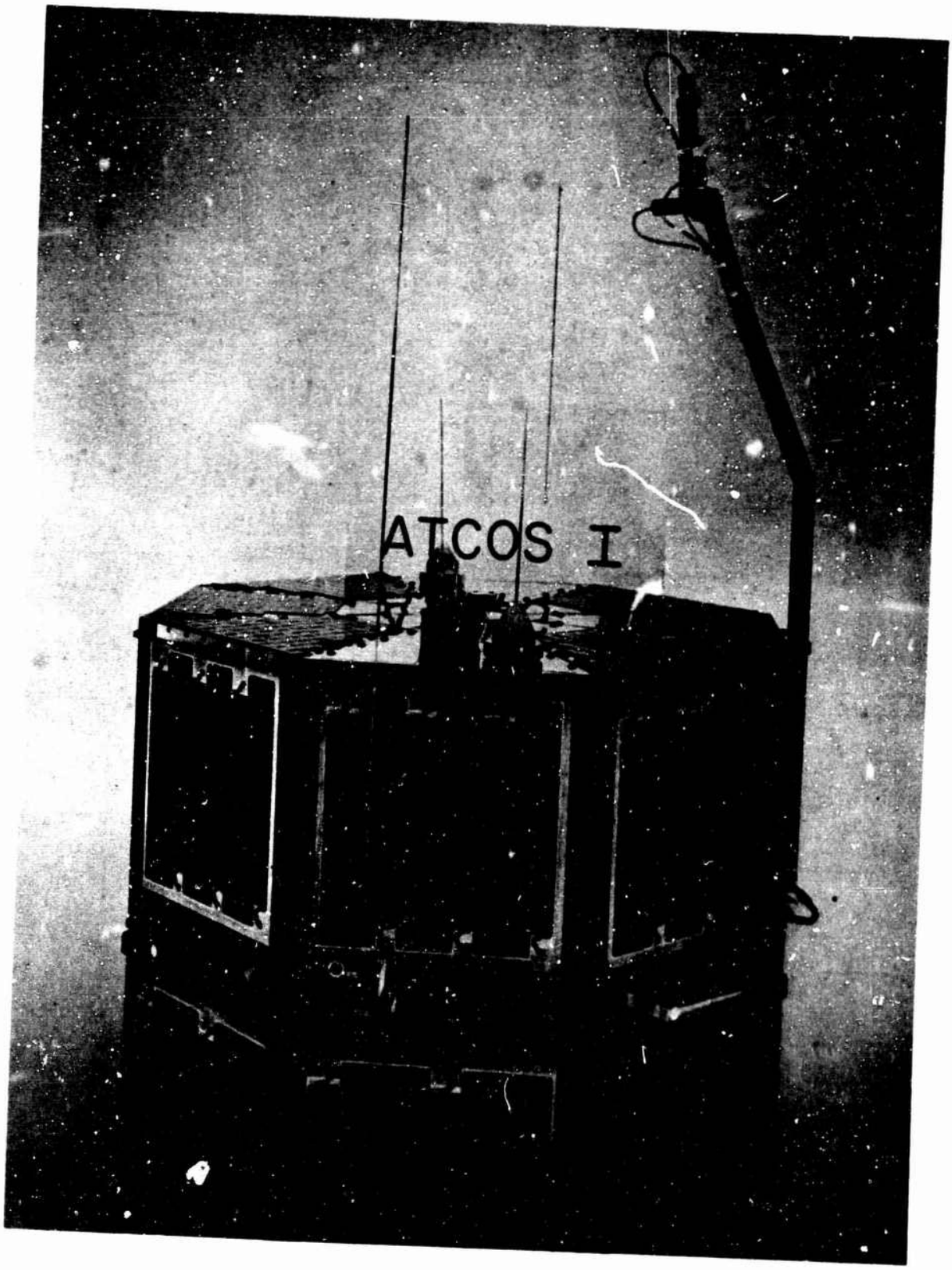

FIGURE 1-1. ATMOSPHERIC COMPOSITION SATELLITE

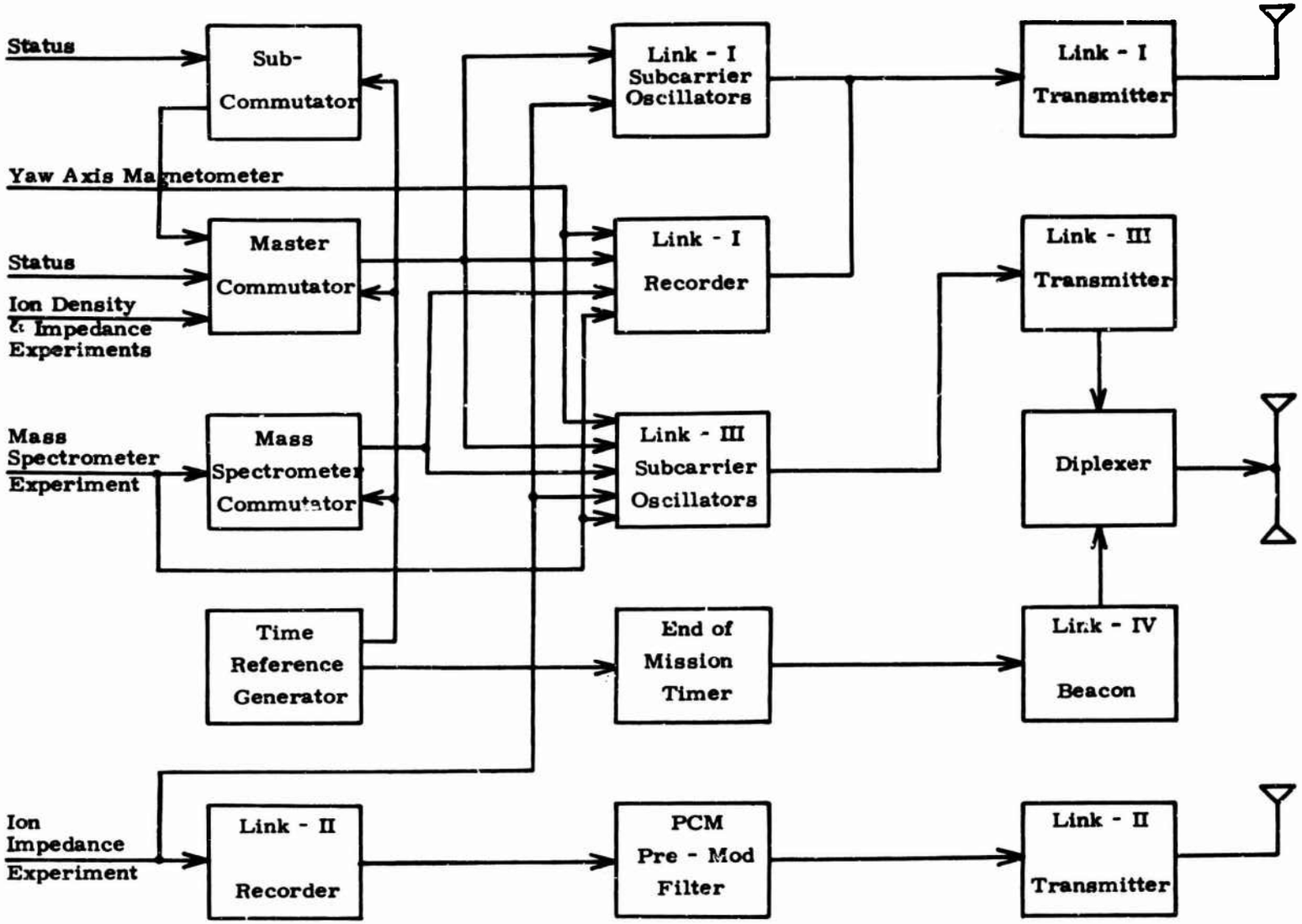

FIGURE 1-2. BLOCK DIAGRAM-TELEMETRY SUBSYSTEMS

10 and 8 are real time data only as shown in Figure 1-3. Band 16 is the Master Commutator for experimental data, "red line" functions, and is subcommutated with spacecraft status data. This commutator is also transmitted in real time on Band 8. Bands 15, 14, 13, 11, and 10 are experimental data with band 13 being commutated.

LINK I (Recorded Data)

Data Channel	Frequency	Function	Transmitter Deviation
--	50.0 kHz	Reference Oscillator	10 kHz
16	40.0 kHz	Recorded Commutator	35 kHz
15	30.0 kHz	Spectrometer I	25 kHz
14	22.0 kHz	Spectrometer II	20 kHz
13	14.5 kHz	Spectrometer Commutator	15 kHz
11	7.35 kHz	Magnetometer	7 kHz
10	5.4 kHz	Real Time PCM - NRZL	7 kHz
8	3.0 kHz	Real Time Commutator	7 kHz
		Total Transmitter Deviations	126 kHz

LINK III (Real Time Evaluation Data)

10	5.4 kHz	PCM - NRZL	15 kHz
8	3.0 kHz	Commutator	10 kHz
6	1.7 kHz	Spectrometer I	6 kHz
5	1.3 kHz	Spectrometer II	6 kHz
4	0.96 kHz	Spectrometer Commutator	6 kHz
3	0.73 kHz	Magnetometer	6 kHz
		Total Transmitter Deviations	49 kHz

FIGURE 1-3 SUBCARRIER OSCILLATOR ASSIGNMENTS & TRANSMITTER DEVIATIONS

Link II has experimental data recorded on magnetic tape for a ten hour period in a PCM-RZ format and is reproduced at a 20,000 bps rate.

Link III is a real time data system intended for the purpose of spacecraft evaluation or possible use in the event of tape recorder failure. There are six data channels, IRIG bands 10, 8, 6, 5, 4, and 3, two of which are commutated (bands 8 and 4) as shown in Figure 1-3.

Link IV is a low power CW oscillator for the purpose of spacecraft tracking and acquisition.

A typical mode of operation, assuming one complete data read-out each day, would be to command on the beacon as the spacecraft comes over the horizon. Then once acquired, by separate commands, to turn on Link II and Link I in that order to dump their stored data. (During this phase of operation, the beacon can be commanded off if the on command was locked in.) After respective data transmission periods of 7.5 and 5.5 minutes the recorders turn off their transmitters,

leave their experiments on and automatically revert into the record modes. After one complete orbit the Link I recorder shuts down with its experiments and stores the data. This shut down also resets the command encoder for the next read-out. The Link II recorder continues to record until at least six consecutive orbits of data are stored on the tape, then it also resets its encoder. The spacecraft then reverts to the charging mode until the batteries have been restored. Simple checks on solar panels, etc. can be performed by using band 8 on either Link I or Link III in the real time mode for spacecraft status.

The components that are used to comprise the spacecraft telemetry subsystems are described briefly in the sections which follow.

1. Time Reference Generator

The Time Reference Generator, manufactured by Adcole Corporation, contains the master timing functions for the satellite subsystems. Basically the unit is a twenty-four hour clock which continuously provides time in both binary (i.e. base 2) form and a format which combines octal base 16 (i.e. least significant digit as base 16 and all other digits as base 8). Outputs are also taken from appropriate points in the unit to provide time pulses for the commutators, the Pulse Code Generator, and an "end of mission" output. A storage register is also included within the unit to store the time of a "sun hit" on the aspect eye. This time information is then made available in terms of base 8 and base 16 digits. The basic timing accuracy is dependent upon a 23,520 Hz crystal oscillator (0.005% accuracy), resulting in a generator base accuracy of 1 part in 10,000 or approximately 9 seconds per day. This accuracy will be improved once the spacecraft temperature has stabilized and the characteristics of the generator drift are established.

The output of the crystal oscillator is used for the basic clock rate in the magnetic aspect electronics and also is counted down to 30 Hz and an output derived to trigger the 60 channel commutator and the 40 segment commutator. The 30 Hz is then further counted down to a signal with a 2 second period. This output is used to synchronize to 60 channel and 40 channel commutators and to trigger the 30 channel subcommutator. It is then counted down in a succession of 16 binaries and the output which occurs at a 24 hour rate is used to reset the entire clock. The outputs of the first four of the 16 binaries are coded into a 16 step staircase as shown in the voltage/time output table in Figure 1-4. Thus the first staircase will code 32 seconds in a 2 second

Level	Voltage	TRG-1	Level	Voltage	TRG-2	TRG-3	TRG-4	TRG-5
0	4.6	0	0	5.0	0	0	0	0
1	4.3	2						
2	4.0	4	1	4.3	32	256	2048	16384
3	3.7	6						
4	3.4	8	2	3.6	64	512	4096	32768
5	3.1	10						
6	2.8	12	3	2.9	96	768	6144	49152
7	2.5	14						
8	2.2	16	4	2.2	128	1024	8192	65536
9	1.9	18						
10	1.6	20	5	1.5	160	1280	10240	81920
11	1.3	22						
12	1.0	24	6	0.8	192	1536	12288	*
13	0.7	26						
14	0.4	28	7	0.1	224	1792	14336	----
15	0.1	30						

FIGURE 1-4. TIME REFERENCE GENERATOR, VOLTAGE/TIME OUTPUTS

* Clock Recycles After 86,400 Secs. (24 Hours)

increments. Similarly the next staircase output will code 256 seconds in 32 second increments, the next 2048 seconds in 256 increments, the next 16,384 seconds in 2,048 second increments, and the last 86,400 seconds (24 hours) in 16,384 second increments. The outputs of each of the eighteen binaries from the one second output to the 24 hour output are isolated and brought out for use in the PCM time coding.

The "end of mission" output is derived by following the 24 hour output by eight binaries used as scalars to give an output after 256 days. This output is amplified so as to be able to drive a latching relay in the control logic and thereby turn off the appropriate equipment.

The time occurence of the solar aspect command pulse is established by setting the clock time into a storage register when the pulse occurs. Seven bits are used in the storage register which allows the time to be determined to within one part in 120 with respect to the commutator period (two seconds).

Synchronization is accomplished between the command pulse and the clock by a controlling binary. The command pulse sets the binary and the next 60 Hz trigger resets the storage register with the time code inserted.

The seven outputs of the register are coded into a sixteen bit staircase and an eight bit staircase similar to that shown in Figure 1-4. Since 120 is not a binary number the staircase outputs are weighed somewhat differently than those in a binary system. The sixteen bit staircase is weighted such that each step below 5 volts corresponds to 1/120 of the commutator two second period. The eight step staircase, however, is weighted as follows:

Level	Volts	Weighted Time (T=2 seconds)
0	5.0	0
1	4.3	16/120 T
2	3.6	30/120 T
3	2.9	46/120 T
4	2.2	60/120 T
5	1.5	76/120 T
6	0.8	90/120 T
7	0.1	106/120 T

Zero time corresponds to the end of the frame sync pulse and therefore coincides with the beginning of the first information channel. As an example, suppose the first staircase has a level of 0.7 volts and the second a level of 2.9 volts. The time of occurrence of the solar aspect command pulse will then have been 13/120 + 46/120 = 59/120 of the commutator period.

2. Master Commutator

The Master Commutator, manufactured by Adcole Corporation, is a solid state 60 position commutator that is driven by the 30 Hz signal from the Time Reference Generator. A two second signal from the Time Reference Generator synchronizes the commutator with the master clock. Calibration voltages are derived from within and provided on the appropriate segments as 0%, 50% and 100% of full scale. Also provided is a command pulse inhibit signal so that aspect data cannot be changed during the readout period.

3. Subcommutator

The Subcommutator, manufactured by Adcole Corporation, is a 30 position solid state commutator similar to the 60 position commutator previously described. A two second signal from the Time Reference Generator drives the counting chain

and synchronizes the sampling with the Master Commutator so that it can be read-out over one position of the Master Commutator.

4. Mass Spectrometer Commutator

The Mass Spectrometer Commutator, designed and developed at Northeastern University, is a 40 position solid state commutator with its timing signals derived from the Time Reference Generator. The primary use of this commutator is for experimental data systems monitoring and it will be discussed in detail in a later section of this report.

5. Subcarrier Oscillators

Standard IRIG subcarrier oscillators are used to modulate the transmitters and provide for the FM encoding of the data. There are two configurations of subcarrier oscillators used in the spacecraft. One set, manufactured by Dorsett Electronics Incorporated, supports the real time modes of operation and the other set is contained within the Link I recorder. They record on the magnetic tape at center frequencies such that when they are reproduced at 18 times the recorded rate they represent standard IRIG bands. A complete listing of these subcarrier oscillators are shown in Figure 1-3 along with the appropriate transmitter deviations.

6. Transmitters

The telemetry transmitter used for Link I is a solid state, crystal stabilized, true FM unit, manufactured by Dorsett Electronics Incorporated, operating at 249.9 megahertz with a stability of ± 0.01% and a nominal power output of 3 watts into a matched load. Each subcarrier oscillator is set to individually deviate the transmitter as tabulated in Figure 1-3. These deviations were chosen to approximately equalize the signal-to-noise ratios in the subcarrier channels. Total r-f bandwidth required (and thus total instantaneous deviation) was determined for the maximum acceptable slant range.

The telemetry transmitter used on Link II is the same as that used on Link I except that it operates at 245.3 megahertz. This is a PCM/FM system and the appropriate premodulation filtering is used as required by IRIG standards. The deviation of this transmitter was also chosen from maximum acceptable range.

Link III is a solid state, crystal stabilized, true FM transmitter, manufactured by Conic Corporation, operating at 255.1 megahertz with a stability of ± 0.01% and a nominal power output of 0.5 watts into a matched load. This unit is modulated in the real time mode only by subcarrier oscillators as indicated in Figure 1-3.

The tracking beacon (Link IV) is a solid state, crystal stabilized unit, manufactured by Conic Corporation, which operates at 258.5 megahertz with a stability of ± 0.005% and provides a CW signal at a nominal power of 150 milliwatts into a matched load. The beacon is used as an aid in spacecraft acquisition and for determination of the emphemerides. The beacon will be commanded off after the first few orbits following the launch. Thereafter the unit will radiate for twenty seconds following each address command.

7. Antennas

The antenna systems for the OV3-5 spacecraft were designed and developed at the Physical Sciences Laboratory of New Mexico State University and are such that Links I and II each have a canted monopole with a maximum gain of - 3 db over 94% of their patterns when diversity combining is used at the receiving stations. The antenna system for Link III is a quadraloop with a maximum gain of - 10 db over 92% of its

pattern and is tuned to 255.1 megahertz for Link III. This antenna system is also used for Link IV at 258.5 megahertz through the use of a diplexer load matching network.

8. R-F System Parameters

The operating parameters of the r-f system were selected from worse case considerations. Certain parameters were relatively inflexible (such as available) power from off-the-shelf IRIG transmitters, ground station antenna gains, receiver thresholds, etc.). Consequently available i-f bandwidths at receiver sites and transmitter deviations were chosen to maximize signal-to-noise ratios as much as possible. The pertinent equations are tabulated below and the selected r-f system parameters are tabulated in Figure 1-5.

Free Space Loss, $L_{fs} = \left[\frac{4\pi}{c} f_c d\right]^2$

where L_{fs} = free space loss, db

f_c = carrier frequency = 250.0 MHz

c = speed of light = 5.55×10^5 nm/sec

d = slant range at 10^o elevation = 1621.0 nm

then $L_{fs} = 37.8 + 20 \log f_c + 20 \log d = 150.0$ db

NOTE: The actual flight frequences, listed in Figure 1-5, are within ± 0.25 db of the free space loss for 250.0 MHz.

Received Power, $P_r = P_t + G_t + G_r - L_x - L_{fs} = P_t + G_t - 125$

where P_r = received power, dbw

P_t = transmitted power, dbw

G_t = transmitter antenna gain, db

G_r = receiver antenna gain including polarization loss = 27 db

L_x = miscellaneous system losses = 2 db

Carrier to Noise Power Ratio, $CNR = P_r - P_n$

where P_n = noise power, dbw = $10 \log \left[k T_s B\right] = -197.85 + 10 \log B$

and k = Boltzman's constant = 1.38×10^{-23} joules / ^oK

T_s = receiver system noise temperature = $T_a + T_r = 1190^oK$

T_a = antenna temperature referred to receiver input = 320^oK

T_r = receiver noise temperature = $290^oK\ (\overline{NF}-1)$

NF = receiver noise figure = 6 db

B = bandwidth, Hz

	LINK I	LINK II	LINK III	LINK IV
Function	PAM/FM/FM	PCM/FM	PCM/PAM/FM/FM	CW - Tracking
Frequency	249.9 MHz	245.3 MHz	255.1 MHz	258.5 MHz
Stability	± 0.01%	± 0.01%	± 0.01%	± 0.005%
Deviation	± 125 kHz	± 50 kHz	± 50 kHz	--------
Transmitter Power	3.0 watts	3.0 watts	0.5 watts	0.15 watts
P_t, dbw	+ 4.78	+ 4.78	- 3.0	- 8.23
G_t, db	- 3.0	- 3.0	- 10.0	- 10.0
P_r, dbw	- 123.22	- 123.22	- 138.0	- 143.23
B	500 kHz	200 kHz	100 kHz	50 kHz
10 log B, db	57.0	53.03	50.0	47.0
P_n, dbw	- 140.85	- 144.82	- 147.85	- 150.85
CNR, db	+ 17.63	+ 21.60	+ 9.85	+ 7.62

FIGURE 1-5. R-F SYSTEMS PARAMETERS

B. Data Storage Systems

The data storage system of the OV3 - 5 spacecraft consists of two magnetic tape recorders in support of the complete experimental requirements for the program. The "Design Specifications for the ATCOS-AFCRL Flight Spacecraft Recorder / Reproducers" prepared by Northeastern personnel and dated November 1, 1964 was a direct result of experimental requirements and technical discussions between Northeastern University, Air Force Cambridge Research Laboratories, Upper Air Research Laboratories of the University of Utah, and prospective suppliers of the recorders. Due to the limitations of the prospective suppliers a subsequent document was prepared entitled "Deviations to Design Specifications for the ATCOS-AFCRL Flight Spacecraft Recorder / Reproducers" and dated February 18, 1965.

The first of the recorders was developed under a subcontract from Northeastern to the Ralph M. Parsons Electronics Company. This recorder, used in conjunction with Link I, uses standard analog FM techniques, records six tracks of information from subcarrier oscillators at approximately 1.875 ips for 100 minutes and plays the data back at an accelerated rate of 33.75 ips in approximately 5.5 minutes. The playback mode of the recorder is performed in the oposite direction than that used for recording. This reverses the time sequence during playback, that is, the last data recorded will be the first data presented when the recorder is in the playback mode. Reel end sensors are included within the recorder to provide signals to the command logic to turn off the recorder after a complete recording cycle. An automatic system is provided to control the transmitter during the reproduce cycle and sequence the recorder into its record mode from which it will then revert to a passive mode after recording for a complete cycle. The spacecraft will then remain in this mode until the next reproduce command is given from any ground station.

The second of the recorders was developed under a subcontract from the University of Utah to the Ralph M. Parsons Electronics Company. This recorder, used in conjunction with Link II, uses standard digital recording techniques. PCM-RZ data is recorded on a single track at 250 bps at approximately 0.3 ips for 600 minutes and plays back at an accelerated rate of 24 ips in approximately 7.5 minutes. The logical operation of the recorder is similar to that of the previously described system of Link I.

1. Recorder System Philosophy

The OV3 - 5 satellite recorder system was designed in support of the experiments previously described. The objectives of the experiments are such that data must be sampled frequently enough to eventually obtain almost total coverage of the earth's atmosphere within the limits of the orbital parameters. The National Range has the responsibility for support. Since there are a limited number of receiving stations available, on-board data storage must be utilized in order to obtain data of an uninterrupted nature around the earth.

The Mass Spectrometer - Density Gauge experiment required data of a continuous nature over one orbit with an overlap over the next orbit. This requirement will indicate any data correlation for an approximate position at the time of orbital overlap. The Impedance Probe experiment is more statistical. Data is required for at least six consecutive orbits during any given twenty-four hour period.

Storage of the spacecraft status data such as time, voltage, current, temperature, and control logic position is required for evaluating the condition of the spacecraft at any time. The satellite receiving stations are well equiped for the receptions

of an FM/FM signal. Therefore, the best utilization of the support stations is realized with an FM/FM signal. In order to transmit all data within a single pass, some of which was recorded for at least six orbits, requires a high reproduce-to-record ratio. The high ratio in itself isn't too bad but the resulting bandwidth would be above the capacity of airborne recorders. There would be at least four data channels required to support this mission. They would be as follows:

Channel	Data Requirements
1	Commutated, NRZL, 60 Samples/second
2, 3	Continuous, 18 Hz per channel
4	Commutated, NRZL, 10 Samples/second

The spacecraft power supply would be operating under heavy load for ten hours unless means were provided for turning off the experiments not required after the first orbit. Power profiles of the satellite indicate that the depth of discharge on the storage cells would be too great for continued operation under this condition. An alternate method would be to lower the reproduce-to-record ratio and transmit the data in consecutive passes. The limitation of this method would be the practicality of turning off the recorder before the satellite went over the horizon. There would also be a loss of data due to the stop and start times of the recorder system.

In order to be within spacecraft power supply limitations and recorder bandwidth capacity the experiments were separated into two groups. The Mass Spectrometer-Density Gauge group to have data stored for more than one orbit, and the Impedance Probe group to have data stored for at least six orbits. Considering all factors these requirements seemed to indicate the need for two tape recorders.

The Impedance Probe instrumentation, designed and constructed at the University of Utah, conditions its data in a format readily adaptable to digital data. Therefore experimental data from the Impedance Probe would be stored best on a digital machine. The development of this recorder was carried out under sub-contracts from the University of Utah. Once separation of experiments had been made it seemed logical to utilize a second transmission link for this digital data.

It was decided to store and transmit the remaining experimental and spacecraft status data with a separate machine and transmission link. Further discussions between Northeastern University, Air Force Cambridge Research Laboratories, and recorder manufacturers indicated that it was best to utilize the availability of the FM/FM receiving sites. This required a tape recorder with outputs which were FM in nature. Five data channels were chosen for the competent fulfillment of the scientific mission. These channels are listed as follows:

Channel	Data Requirements
1	Commutated, NRZL, 30 Samples/second
2, 3	Continuous, 18 Hz per channel
4	Commutated, NRZL, 10 Samples/second
5	Continuous, 5 Hz

This type of data on a tape recorder is susceptible to variations in tape speed which appear as frequency changes simulating data. IRIG Standards require a reference oscillator so that tape speed compensation techniques can be used at the receiving sites.

Special subcarrier oscillators were designed by the sub-contractor with center frequencies and bandwidths such that when reproduced at eighteen times the recorded speed they were at the IRIG frequencies for bands 16, 15, 14, 13 and 11. The reference oscillator was reproduced as 50.0 kHz, the required frequency for compensating up to and including IRIG band 16*,[1]. The recorder output also had to have the necessary amplitude per channel available to set up a transmitter deviation schedule for optimal signal to noise considerations. This deviation schedule is shown in Figure 1-3.

2. Performance

During the development phases of the recorder system the primary problems were concerned with sum and difference frequencies due to the nonlinearity of the reproduce amplifiers, interchannel crosstalk, and harmonic frequencies of the data channels and power inverter. These problems were greatly improved by better grounding techniques, and power line RFI filtering.

The analog data accuracy after filtering was approximately 4% p-p. Subsequently further testing exhibited the ineffectiveness of the Tape Speed Compensation system as designed. Randomly increasing data errors when modulating signals were applied to all channels led to investigations to correlate the time of occurance. Whenever the 40.0 kHz data channel was modulated toward its higher band edge, "spiking" occurred in the demodulated output of the subcarrier discriminators. Discussions were held with the manufacturers of the "ground stations" which led to tests and experimenting with levels and bandwidths. The standard 50.0 kHz reference tuning unit supplied by most manufacturers has an input passband wide enough to allow signals from the upper band edge of the 40.0 kHz channel to get in and "capture" the reference channel, thereby sending a false correction signal to all data channels. Reference to the deviation schedule in Figure 1-3 shows that the 40.0 kHz channel amplitude is 10 db larger than that of the 50.0 kHz reference oscillator. Laboratory tests proved that this signal when attenuated by the filter characteristics of the Reference Tuning Unit, was at times large enough in amplitude to actually "capture" the reference channel.

3. Recommendations for Future Systems

In order to eliminate the "capture" effect from the present recorder, and any subsequent machines purchased on contract AF 19 (628)-5140, the level of the Reference Oscillator must be increased. The amplitude of the Reference Oscillator should not be greater than double that of the 40.0 kHz data channel without resulting in cross-channel interference. Laboratory tests indicate errors produced in the 40.0 kHz were as high as 6% when the 40.0 kHz was at upper band edge and the recorder had high flutter deviation. Also, care must be taken to insure that the amplitude of the Reference Oscillator is not so large that most of the transmission bandwidth would be required. Discussions and tests indicate that the best solution would be to utilize a completely linear taper, which would result in an amplitude of 320 mVrms from the Reference Oscillator. The relative level of the Reference Oscillator would then be 2 db greater than the 40.0 kHz data channel or a net gain of 12 db over the original conditions.

Consideration was given to two alternatives which were later discarded because they led to a major redesign of the recorder system and possible program delays. One was to replace the 50.0 kHz Reference Oscillator with one at 100 kHz and the other was to eliminate the 40.0 kHz data channel and substitute a 10.5 kHz data channel. The first possibility would utilize a larger percentage of transmission bandwidth and the lead time on crystal procurement was extensive. The latter possibility would have resulted in a degradation of data due to information bandwidth compression.

*Numbered superscripts refer to the references in the Bibliography.

If future systems of this type are pursued, then consideration should be given to the availability of the outputs of the individual channels prior to the record amplifiers, in order that system testing can be more readily performed. Also there should be provisions for adjustment of the channel band edges and amplitudes.

C. Aspect Instrumentation

An aspect determining system is provided on the OV3 - 5 spacecraft in order to define vehicle attitude and provide data on the angle of attack of any instrument with respect to the velocity vector of the spacecraft. This system as shown in Figure 1-6, consists of a triaxial magnetometer sensor, a solar sensor, and associated conditioning electronics. The analysis and use of the data from this system will be discussed in Chapter II.

1. Magnetic Sensoring System

The magnetic sensoring system consists of a triaxial magnetometer mounted on a boom that extends out of the side of the spacecraft as shown in Figure 1-7. The sensors are of the Schonstedt Heliflux type with a total field sensitivity of $\pm$ 600 milligauss per sensor. Each sensor is fed into its respective amplifier, the outputs of each are then sampled by an analog-to-digital converter whenever the solar eye acquires the sun. This information is required simultaneous with sun acquisitions and is sequentially read out over the telemeter link. This requirement dictated a system capable of parallel sampling and storage with serial read out. To provide additional information one of the transverse axis magnetometers is read out continuously over a clear subcarrier oscillator.

Analog-to-Digital Converter - The design and development of the electronics for conditioning the magnetic field data was accomplished by the investigation of two possible approaches. The first of these approaches was an analog sample and hold system[2] and the second was an analog-to-digital-to-analog conversion technique. The latter was selected due to its unlimited storage time and the increased accuracy of digital data. The method of successive approximation was chosen becouse of its ability to encode the input signal within seven clock pulses (140 μsec). The input signals were encoded into seven bits per signal in order to obtain a system accuracy of $\pm$ 35 millivolts, which corresponds to a field sensitivity of $\pm$ 10 milligauss.

A block diagram is shown in Figure 1-8 and the wave forms are shown in Figure 1-9. The internal clock is actually a square wave output of the Time Reference Generator at 23.52 kHz and determines the logic sequencing rate. This signal triggers the clock pulse generator to give two square waves 180° out of phase with each other. Also by preset functions, care is taken to insure that CP_1 is initally low and that CP_2 is high. The preset generator is triggered by the solar eye command pulse. The outputs from this generator preset the logic and storage binaries so that they are ready to encode the data.

The open-ended counter generates seven sequential pulses which gate the logic at the proper intervals. Once the seven pulses are transmitted the counter disables itself until the next preset pulse.

The function of the channel comparator, of which there are three, is to compare the amplitude of the magnetometer signal with that of a precision reference voltage and determine the larger of the two by forming a logic "1" or "0". The reference voltage is the resulting states of the seven storage binaries. The preset pulse

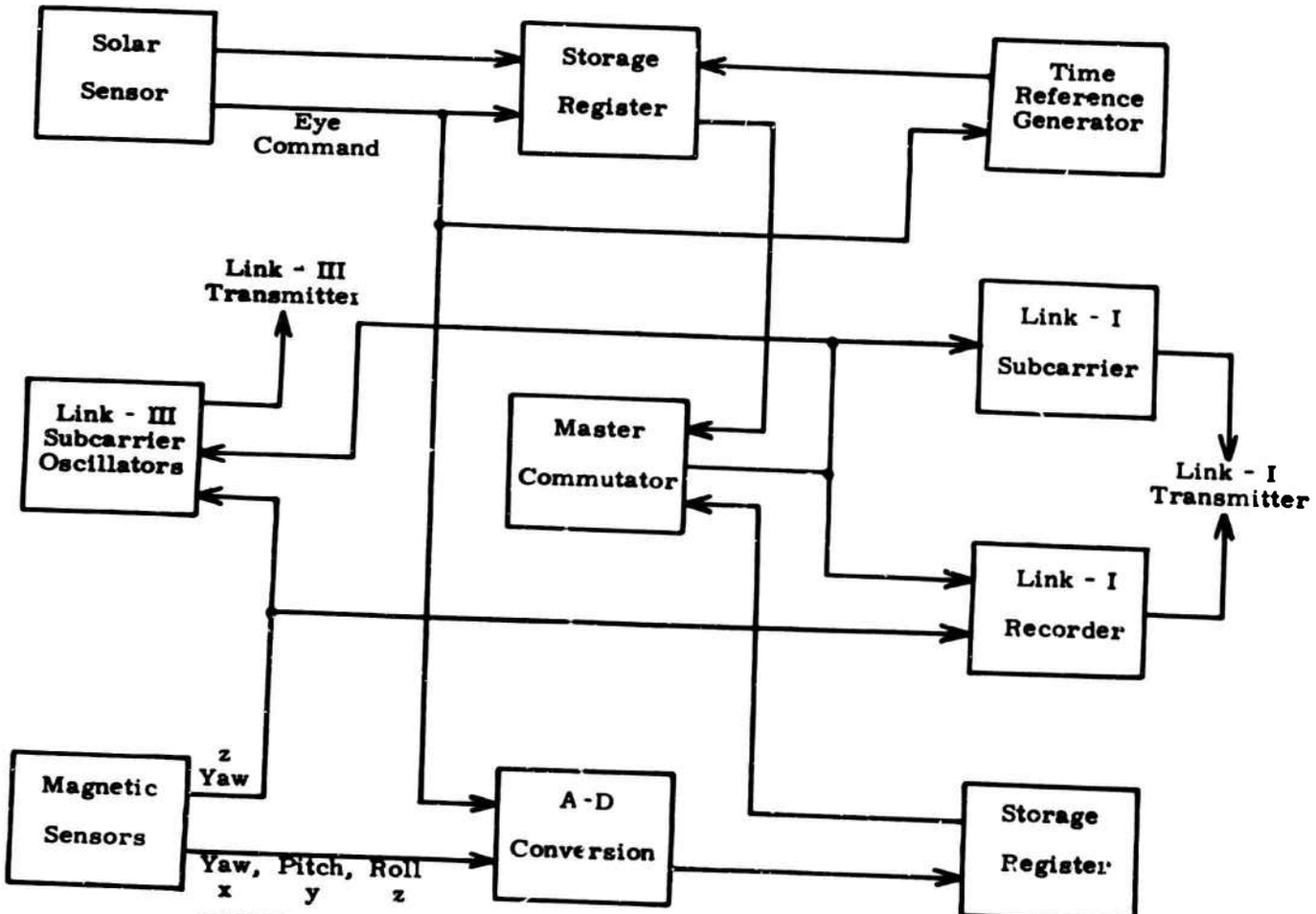

FIGURE 1-6. BLOCK DIAGRAM-ASPECT SYSTEM

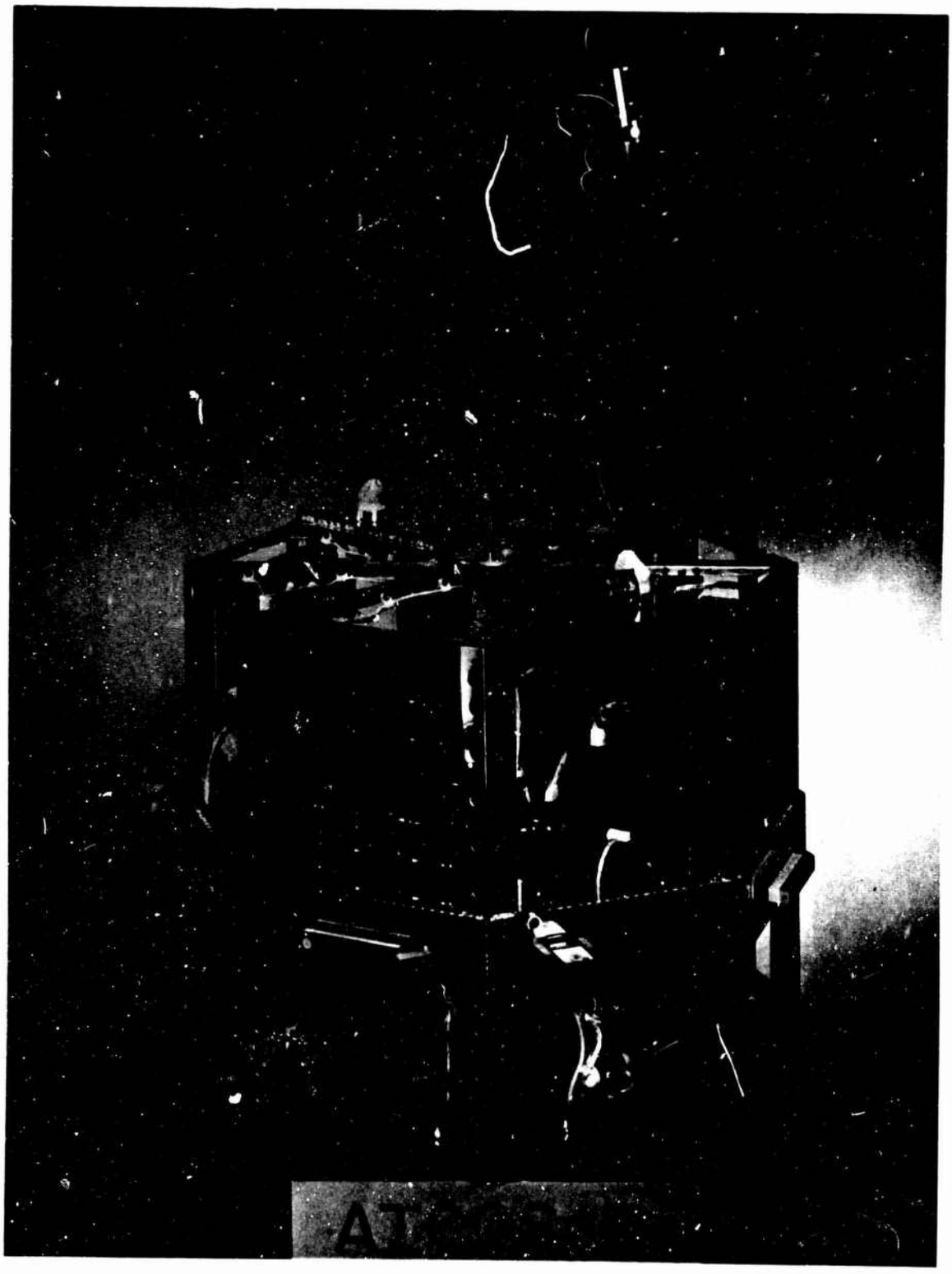

FIGURE 1-7. ATCOS ASPECT SENSORS & ASSOCIATED ELECTRONICS

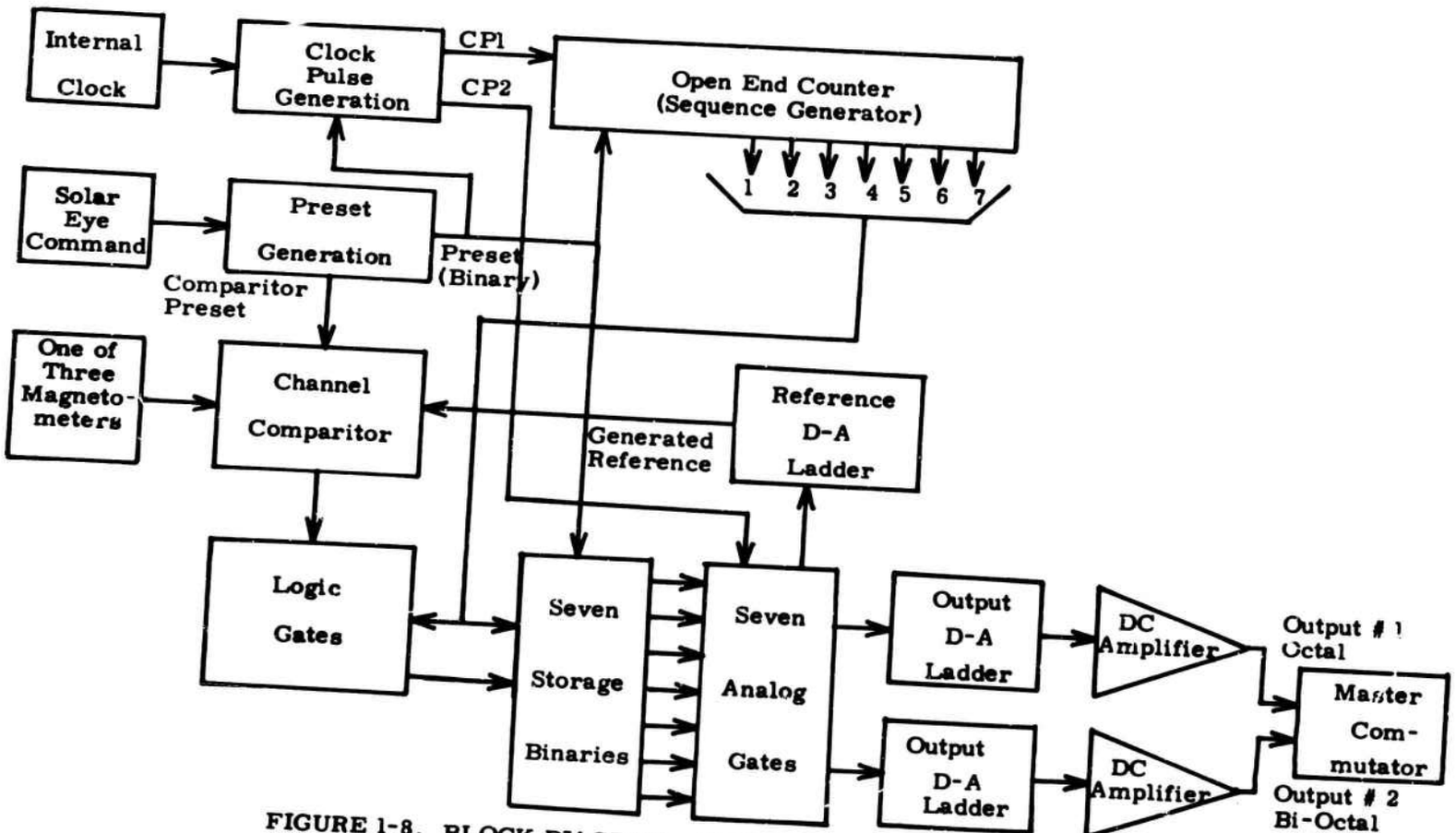

FIGURE 1-8. BLOCK DIAGRAM, ANALOG-TO-DIGITAL CONVERTER

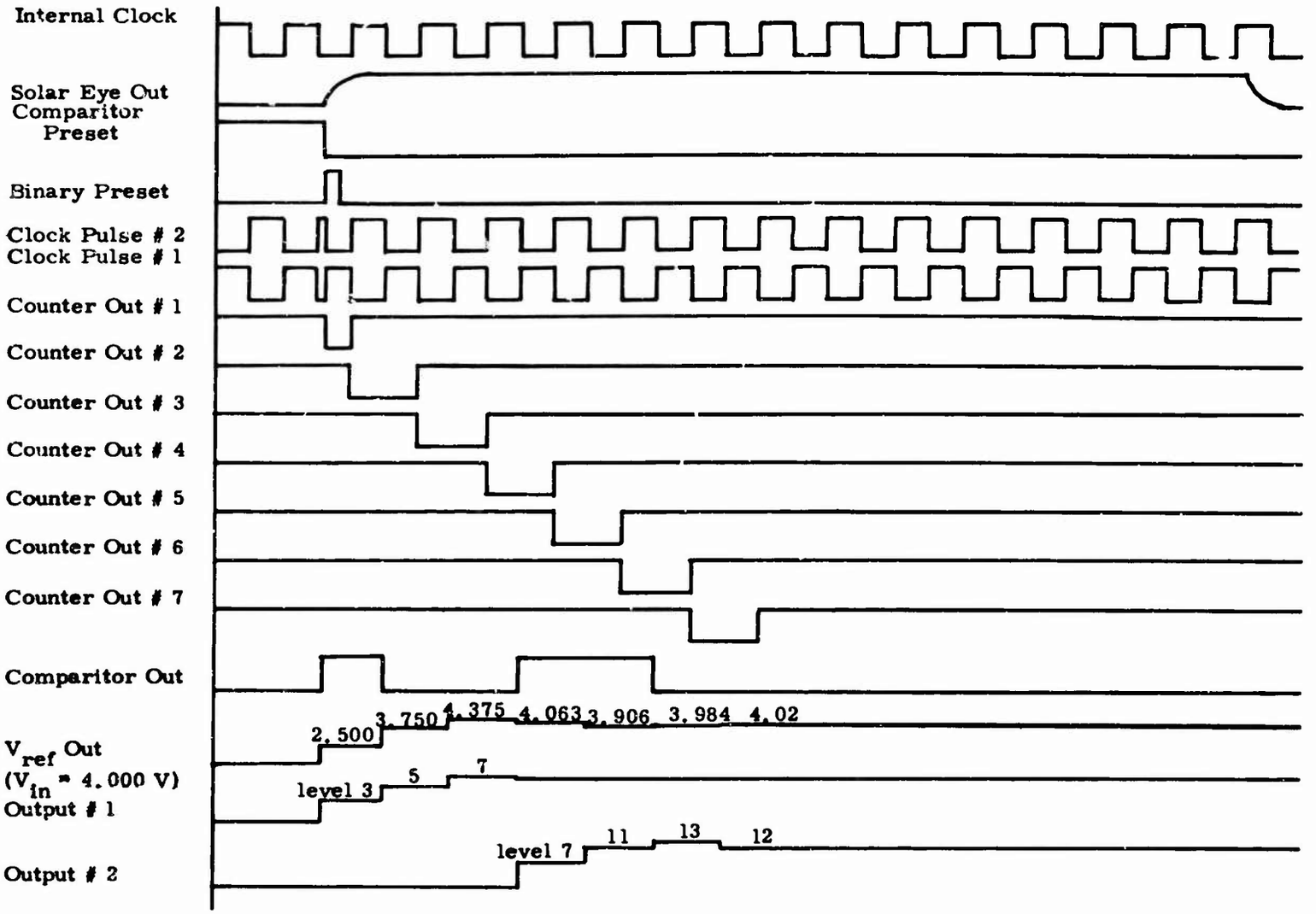

FIGURE 1-9 WAVEFORMS, ANALOG-TO-DIGITAL CONVERTER

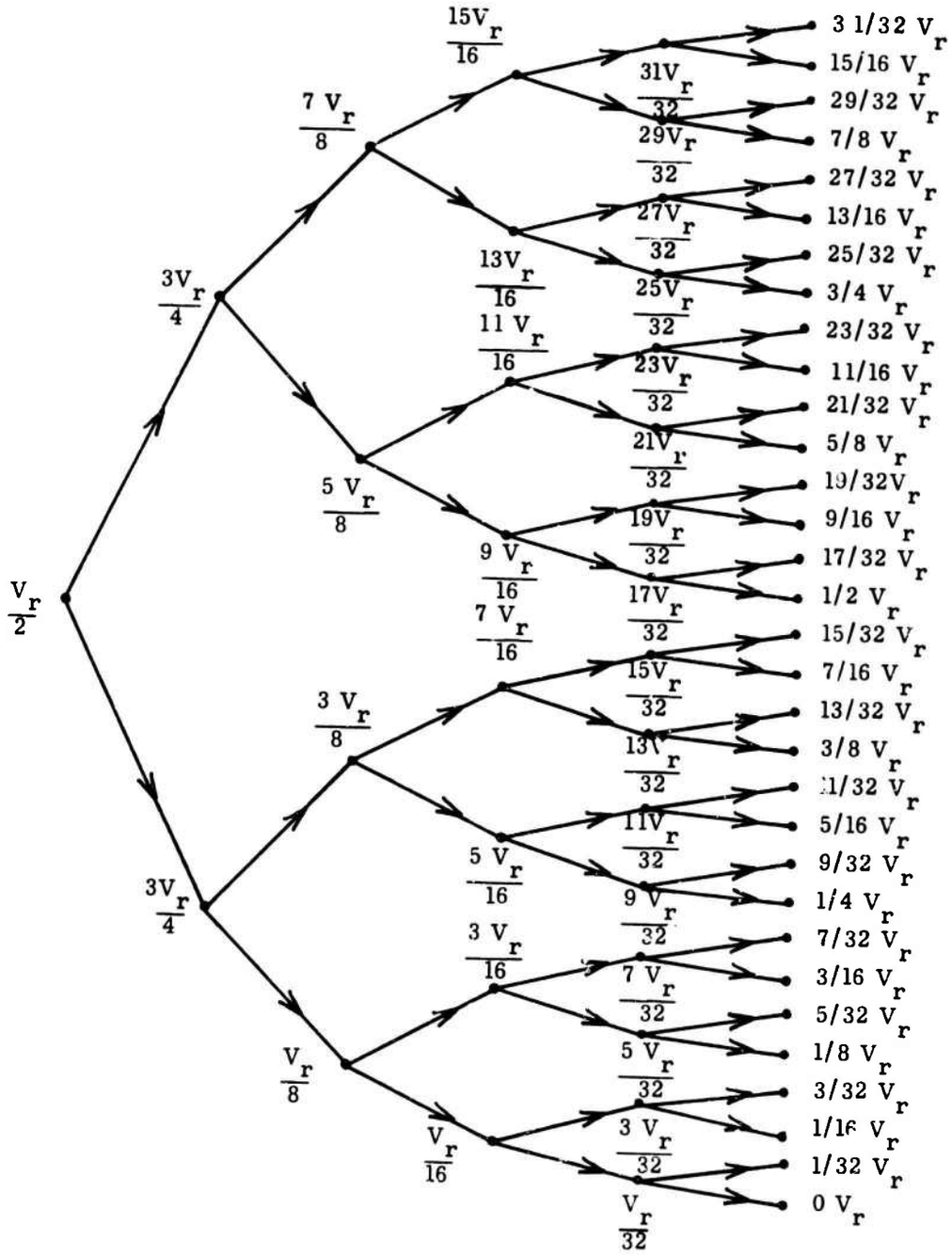

FIGURE 1-10. EXAMPLE OF SUCCESSIVE APPROXIMATION

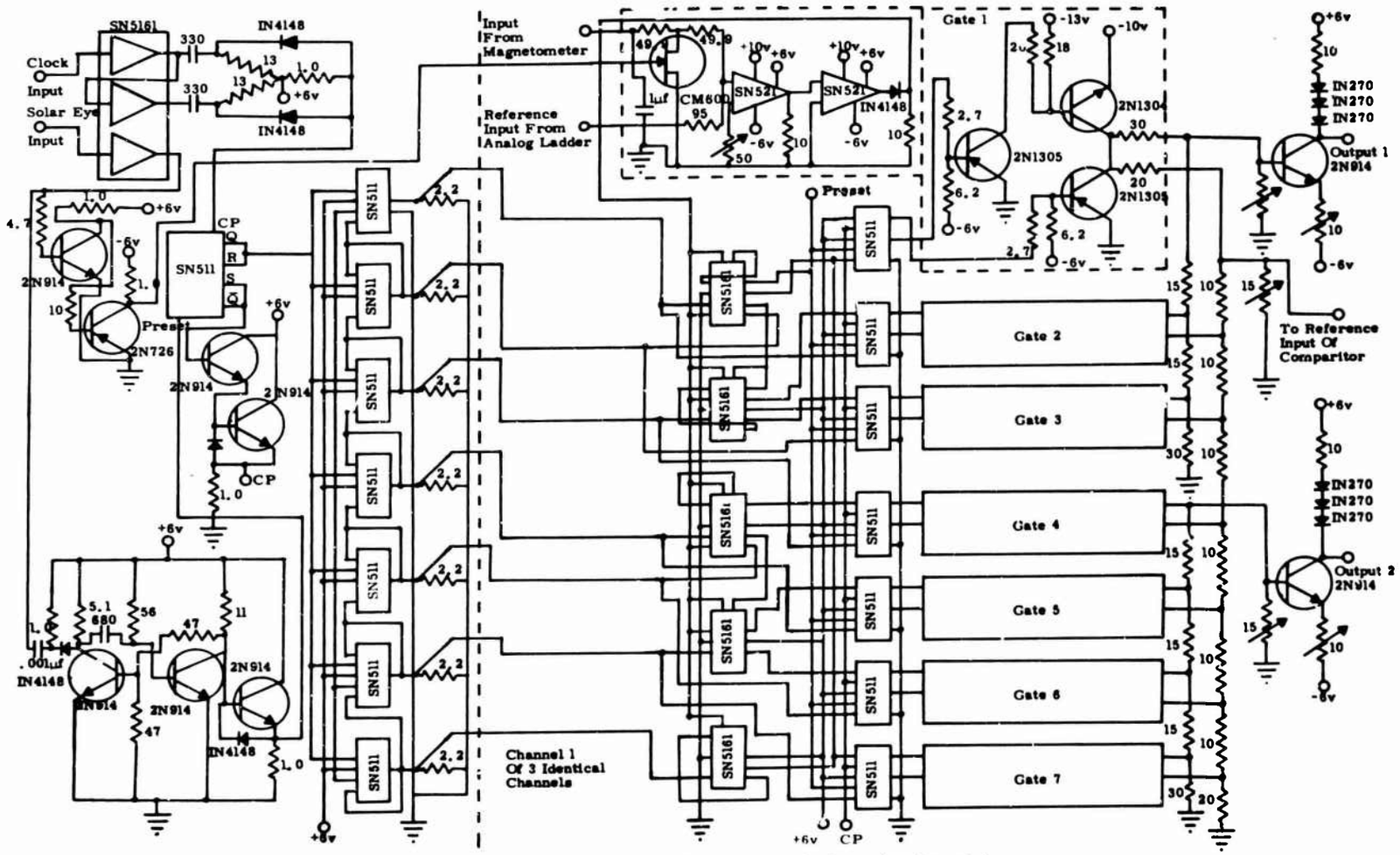

Note: All resistors in Kohms and all capacitors in pf unless otherwise noted.

FIGURE 1 - 11. ANALOG-TO-DIGITAL CONVERTER

turns the first binary "on" and the remaining six "off". The reference ladder output is now $V_{r/2}$, this is sent to the comparitor for comparison with the input signal. If $V_{r/2}$ is larger than the input signal the logic gates will allow binary number one to remain "on" and turn "on" binary number two thus generating $3V_{r/4}$. But if $V_{r/2}$ is smaller than the input the logic turns "off" binary number one and turns "on" binary number two, generating $V_{r/4}$, which is then sent to the comparitor for further comparison. This process continues until all binaries have been used in a comparison resulting in a generated reference which is within $\pm V_{r/128}$. Figure 1-10 is an example of a five binary system of successive approximation. A seven binary system would continue until 128 output levels were available. Note that the dots signify decision states and the arrows the possible directions of decision.

The states of the binaries are now decoded into the output ladders. The first three binaries are coded into eight quantized levels and the remaining four are coded into sixteen quantized levels. The outputs of each of these digital-to-analog ladders are then conditioned in a direct coupled amplifier for read out on the main commutator.

The schematic of the complete analog-to-digital converter system is shown in Figure 1-11. The integrated circuits were described as blocks previously, leaving only the comparitors, analog gates, and ladders.

The channel comparitor shown in Figure 1-12 consists of two high gain operational amplifiers, a zero adjustment network, a voltage adder, and a function control switch. Operationally the Field Effect Transistor, CM 600, is kept "on" until a preset

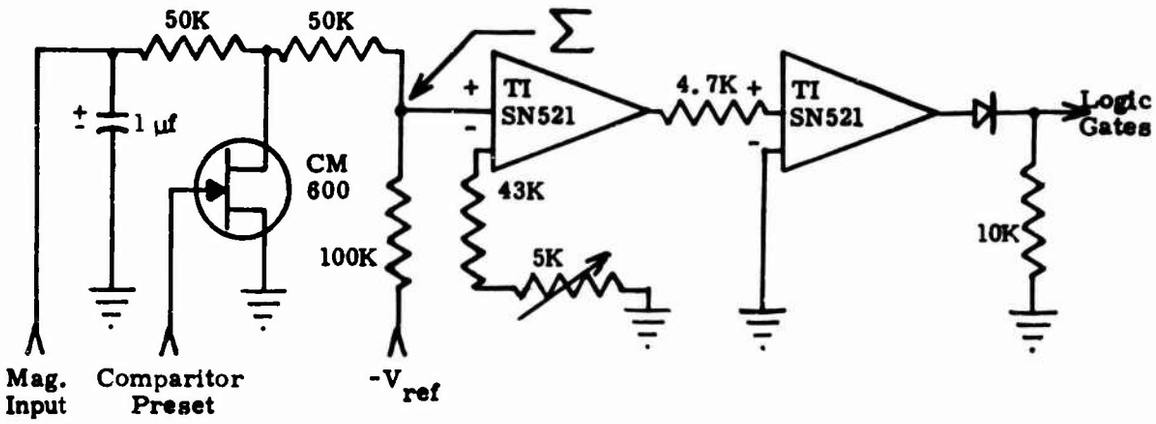

FIGURE 1-12. CHANNEL COMPARITOR

pulse arrives. During this time the 1.0 μf capacitor and the 50 Kohm resistor provide the proper load for a calibrated magnetometer. The preset pulse opens the Field Effect Transistor switch and allows the summing point to add both the input signal and the generated reference input. If the net result is positive, the operational amplifiers saturate and produce a logic "1" which indicates that the input signal is larger than the reference. Alternately, if the net result is negative, the operational amplifiers produce a logic "0" indicating that the reference is larger. The next clock pulse operates on the signal and so on until all binaries have been into the comparitor.

The analog ladder as shown in Figure 1-13 is typical of the one incorporated into the system. Operationally, as each of the seven inputs are connected to either V_r

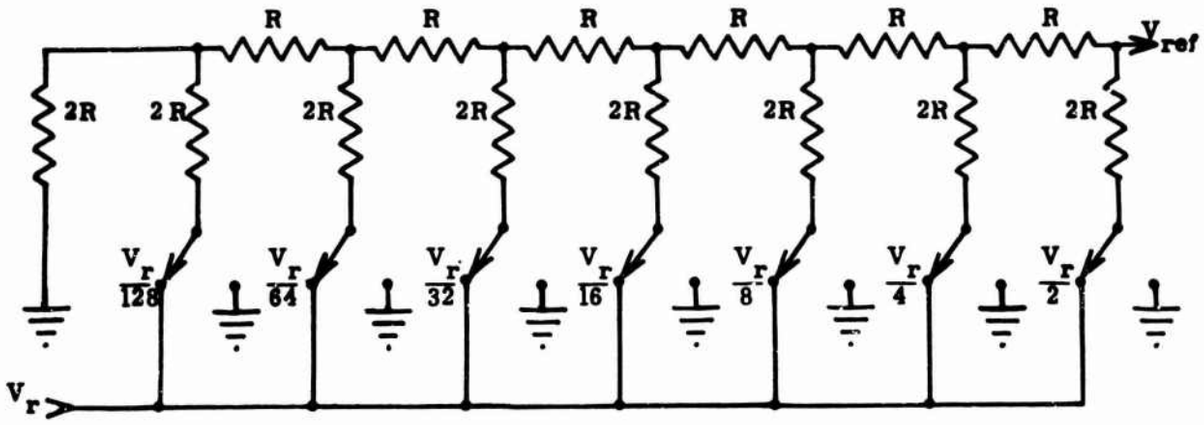

FIGURE 1-13. ANALOG LADDER

or ground the contribution of each input to V_{ref} is either zero or the weighted value shown. These inputs are linearly added to the V_{ref} output. By proper switch position selection any output ranging from zero volts to 127/128 V_r can be acquired. Within the system are seven analog gates to provide this switching. A typical circuit to perform this is shown in Figure 1-14. The position of the switch is dependant on the state of the

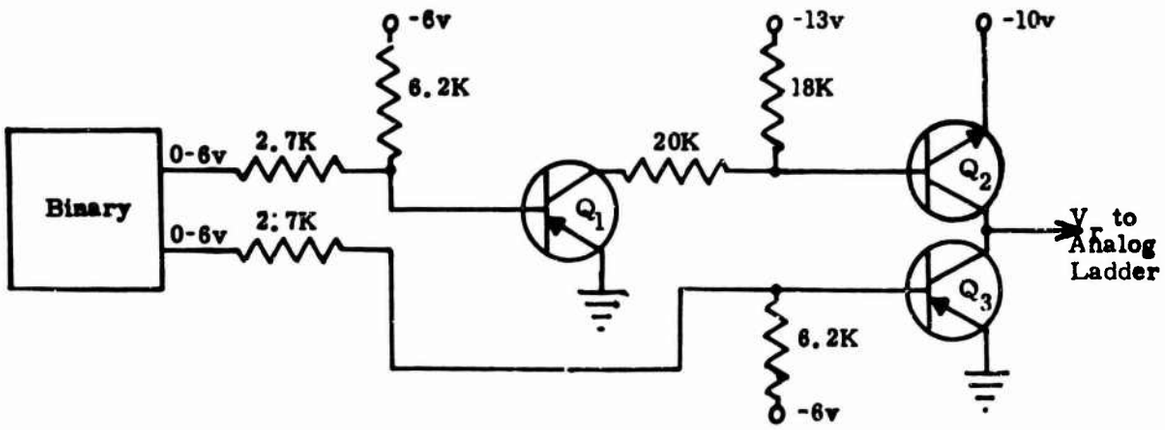

FIGURE 1-14. ANALOG GATE

binary which in turn saturates either Q_2 or Q_3 resulting in V_r volts or zero volts to the analog ladder input.

The completed system was enclosed in a polished aluminum box 3 1/2 inches by 9 inches by 3 3/4 inches and weighed approximately three pounds. The spacecraft power required, to operate the system, was seven watts. The photograph of ATCOS, Figure 1-15, shows a view of the Analog-to-Digital Converter mounted inside the structure of the satellite. The six outputs of the Analog-to-Digital Converter are on the main commutator along with five segments of time and solar eye data. An inhibit pulse from the commutator prevents a solar eye command pulse from occurring during the read out periods, and thus insuring that the aspect data will remain fixed during this time.

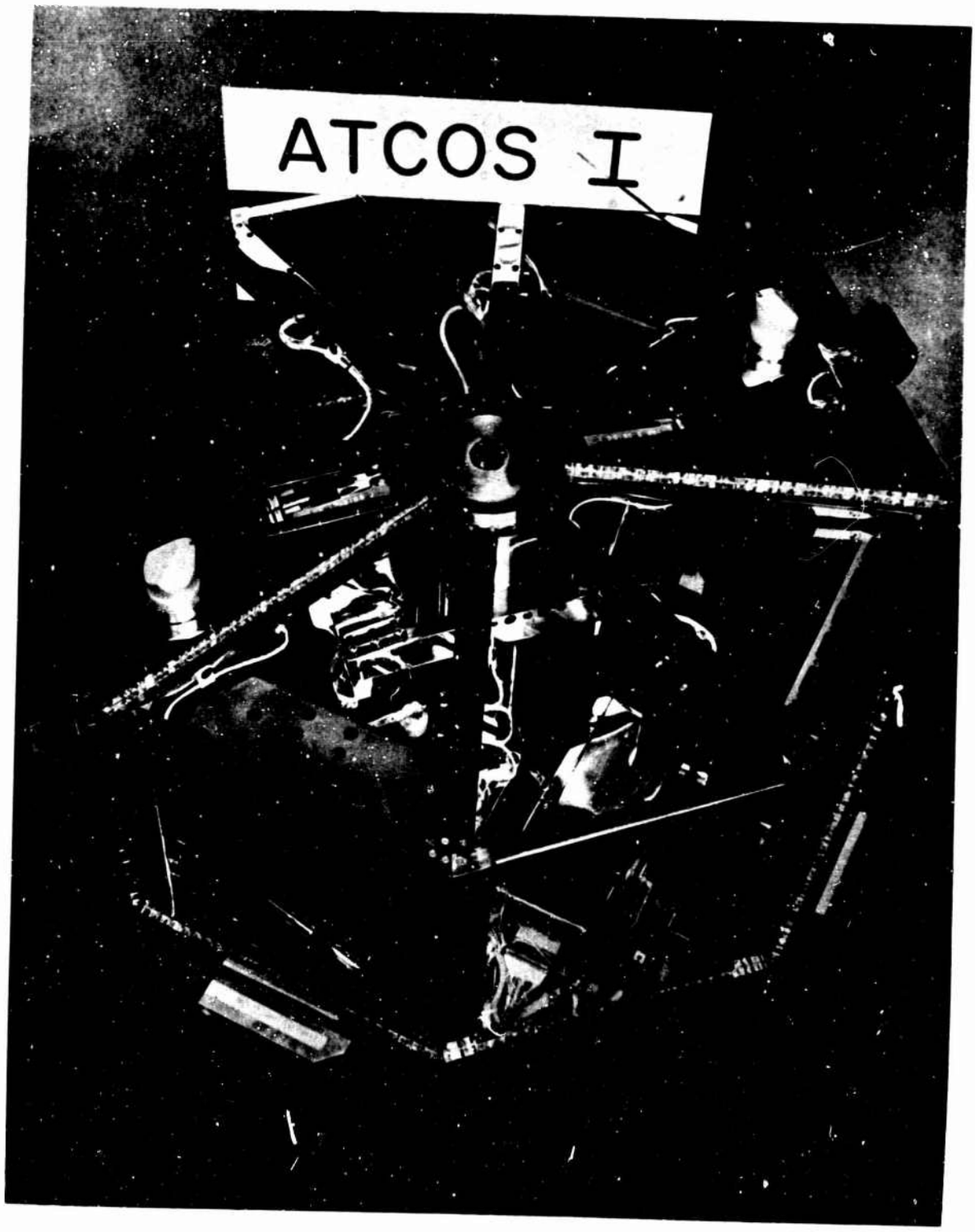

FIGURE 1-15. ATCOS ANALOG-TO-DIGITAL CONVERTER ELECTRONICS

Calibration of the Analog-to-Digital Converter - The calibration of the Analog-to-Digital Converter was accomplished by initially adjusting each of the three channel outputs to the zero level when the signal inputs were grounded. Then the dc output amplifiers were temperature compensated to maintain zero volts over the temperature range of $0^{o}F$ to $90^{o}F$. The next step was to adjust the amplifier output of the first amplifier to five volts at eighth level and of the second amplifier to five volts at the sixteenth level. This resulted in steps of 0.625 volts for the eight level staircase and 0.3125 volts for the sixteen level staircase. The twenty-four output levels were then recorded at temperatures of $0^{o}F$, $55^{o}F$, and $90^{o}F$.

In order to calibrate the analog-to-digital section the input voltage to each channel was varied slowly over the range of magnetometer calibration. When the output levels changed, at approximately every 35 millivolts of input voltage, the absolute input voltage was recorded. This procedure was followed for each of three channels at each of the three temperatures. This resulted in particular sets of output levels as a function of input voltage. The curve that represents this data can be approximated by a second order equation in the form:

$$V_{in} = a_o + a_1 L + a_2 L^2$$

where L represents the output levels numbered 0 through 127. Solution of the expression results in the coefficients which describe each of the two complete systems. The following table lists the coefficients for each channel in each Analog-to-Digital Converter System.

System Serial No.	Channel	a_0	a_1		a_2
1	x	$.12560212 \times 10^{-1}$	$.35395177 \times 10^{-1}$	-	$.53752649 \times 10^{-6}$
1	y	$.17240058 \times 10^{-1}$	$.35211105 \times 10^{-1}$	-	$.28049445 \times 10^{-6}$
1	z	$.33652990 \times 10^{-1}$	$.35367001 \times 10^{-1}$	-	$.31239278 \times 10^{-6}$
2	x	$.11914493 \times 10^{-1}$	$.35411273 \times 10^{-1}$	-	$.48796544 \times 10^{-6}$
2	y	$.11923131 \times 10^{-1}$	$.35214075 \times 10^{-1}$	+	$.96907670 \times 10^{-6}$
2	z	$.14868820 \times 10^{-1}$	$.35144360 \times 10^{-1}$	-	$.11546669 \times 10^{-6}$

2. Solar Sensoring System

The digital solar aspect system, manufactured by the Adcole Corporation, consists of a sensor and its associated electronics. The solar aspect system is shown in the block diagram of Figure 1-16. The sensor, as seen in the photograph of Figure 1-7, is mounted to measure the angle between the spin axis of the spacecraft and the sun.

The sensor is composed of two command reticles and two gray-coded reticles through which light passes before impinging upon photocells of one solar constant. When the sun is in the plane that is normal to one of the command eye reticles, gates are opened from the corresponding gray-coded reticles to a storage register to store the gray-coded angle information. At the same time information from the Time Reference Generator and the Magnetic Sensoring System are stored in their respective registers.

The solar aspect storage register output has eight binaries containing information that is coded into three digits. The outputs of the first six binaries are amplitude coded into two output digits of eight discreet levels each. The most signifi-

cant bit and an identification binary are combined into a four level digit output. The eighth binary is the sensor identification. It represents a logic one or zero depending on which of the gray-coded reticles is activated. An inhibit gate, generated by the Master Commutator, prevents a command pulse from resetting the storage registers during the read-out period, thus insuring that data will remain fixed during this time.

D. Mass Spectrometer Commutator

The two Mass Spectrometers on board the ATCOS satellite use two calibration sweeps each of which would have had to be telemetered on a separate subcarrier oscillator channel. The availability of only one channel due to recording bandwidth limitations necessitated the design of a non-return to zero commutator to sample the sweeps. In order to fully utilize this information additional segments were provided for monitoring bias and current signals from both Mass Spectrometers, as well as the two second staircase output of the Time Reference Generator.

In order to allow flexibility in matching the band pass capabilities of a particular low frequency channel, the number of segments per frame can be varied to 60, 40, or 30 while the frame duration is held constant at 4 seconds.

The format of the frame begins with a standard five segment frame sync consisting of a zero reference, three five volt reference segments, and followed by a 2.5 volt segment. The next five segments are separate information channels which will monitor bias, current and Time Reference Generator staircase outputs. After these ten segments, the commutator samples alternately the two Mass Spectrometer sweeps until the end of the frame.

1. System Operation

A block diagram of the commutator is shown in Figure 1-16. Pulse trains of 1/2 pps and 30 pps, available from the Time Reference Generator, are used to time the operation of the commutator. The 1/2 pps is applied to the Master flip-flop, which divides by two, to give a "start frame" command once every four seconds. The 30 pps signal is fed to a frequency divider which generates the internal clock pulses and determines the segment duration. Division by 2, 3, or 4 will result in segment durations of approximately 66 msec, 100 msec, or 133 msec. For a frame duration of 4 seconds, this division gives the commutator 60, 40, or 30 segments for data.

The "start frame" command pulses an open ended ring-counter which is stepped by the clock pulses. There are ten positions in the ring-counter which sequentially applys the signal on their input gates to the output bus. The first five gates have 0v, 5v, and 2.5v reference voltages on their inputs to make up a frame sync as defined by IRIG standards. The last five gates are used to telemeter Mass Spectrometer bias and current monitors. When the tenth gate turns off, a pulse is coupled to start the Sampling flip-flop which is also gated by the clock pulses.

The Sampling flip-flop stage has the two calibration sweeps of the Mass Spectrometers as inputs to its gates. The sweeps are alternately switched to the output and continue to be sampled until a new "start frame" command pulse arrives turning off the Sampling flip-flop and starting a new frame.

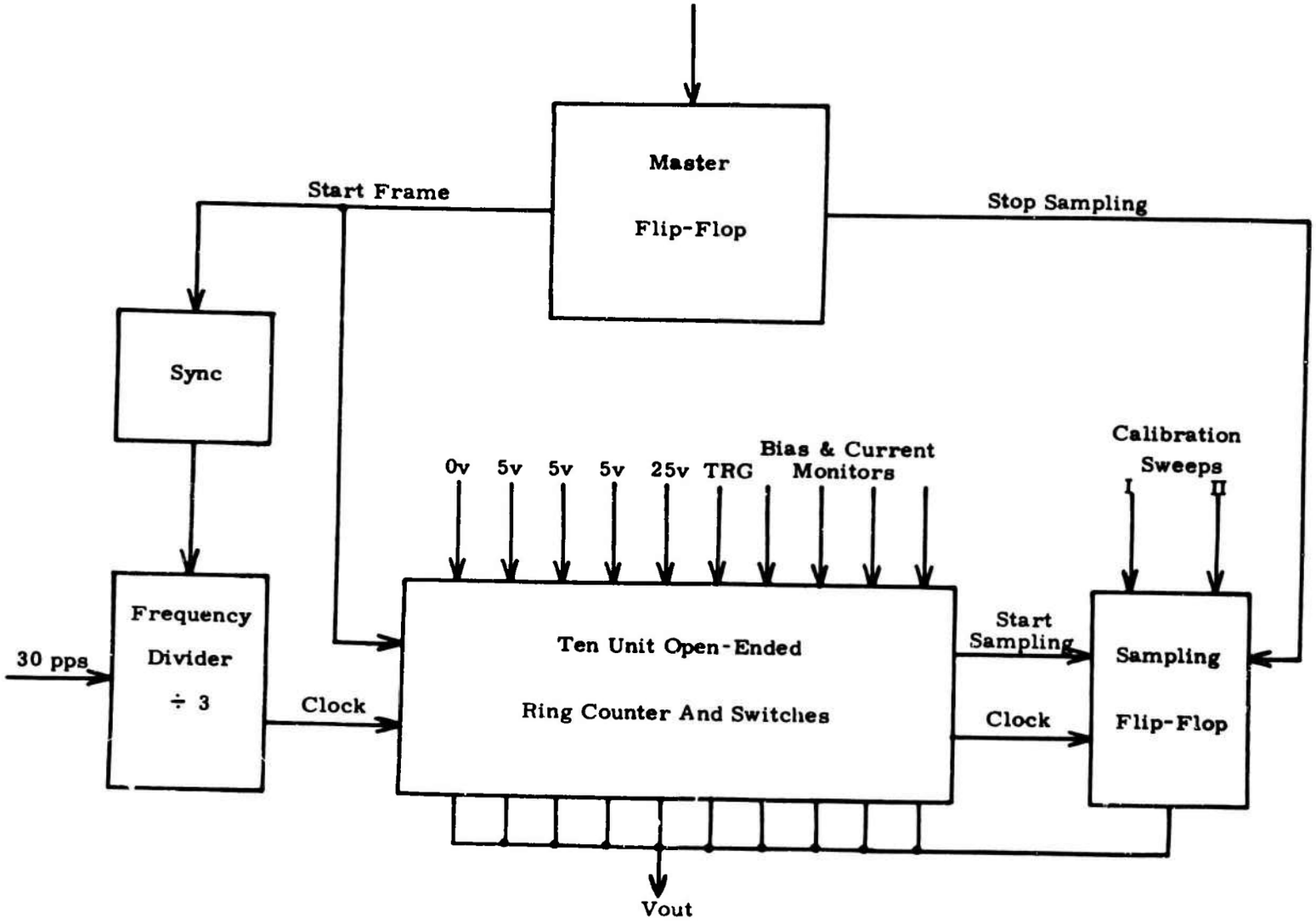

FIGURE 1-16. BLOCK DIAGRAM, MASS SPECTROMETER COMMUTATOR

2. Circuit Operation

The schematic diagram of the entire commutator is shown in Figure 1-17. The 1/2 pps signal triggers the Master flip-flop while the 30 pps signal is fed through an isolation - driver stage, Q_1, to the frequency divider. These pulses are used to step charge capacitor C_1 through the variable resistor R_1. By adjusting R_1, C_1 can be charged to the unijunction firing voltage on either the second, third or fourth pulse resulting in a frequency division. Presently R_1 has been adjusted so that the unijunction fires once for every three pulses from the 30 pps signal yielding at the base one of the unijunction, positive pulses at the rate of 10 pps. This output is applied to Q_2 which provides the negative clock pulses for the rest of the commutator.

A synchronizing circuit was included in the clock generator to keep the 10 pps output in step with the 1/2 pps. Although the 30 pps and 1/2 pps signal were synchronized, the 10 pps is not necessarily slaved to the 1/2 pps signal since any one of three pulses could start the charging process. The Q_4 side of the Master flip-flop is used to pulse Q_3 and discharge C_1 to the voltage set by the resistive divider R_{10} and R_{11} which is adjusted to equal the unijunction residual voltage.

The commutator output format is primarily achieved through the use of eleven trigistors. The trigistor is a p-n-p-n device which approximates the circuit function of a conventional flip-flop. The trigistor is turned "on" (made to conduct) by a positive pulse at the base and once "on" it will remain "on" without the need for continued base current. It is triggered "off" by a negative going pulse at the base and will remain "off" until triggered "on" again. The preferential state of the trigistor is "off".

Ten trigistors form an open ended ring-counter which operates in the following manner. When the Master flip-flop is triggered into the "one" position (Q_4 off, Q_5 on) point A goes from zero to 15v, coupling a large positive pulse into the base of T_1, turning it "on" and lowering its collector (n-p-n sense) to zero. The 0.047 µf capacitor C_2, quickly charges to 15v. This then allows the diode with the clock pulses on its cathode to conduct at the next negative going pulse from the frequency divider. The negative pulse couples through C_2 turning T_1 back "off". As the collector of T_1 switches back to 15v, the next trigistor, T_2, is turned "on" in the same manner as T_1, and is turned "off" 100 msec later by the next clock pulse. Each successive clock pulse steps the ring-counter through to T_{10}. While each trigistor is "on" the associated transistor gates Q_6 through Q_{16}, are saturated in sequence causing any zero to 5 volt signal on their emitters to be switched to the output.

As trigistor T_{10} is turned back "off", T_{11} is turned "on" and through gate Q_{17} applies power to the Sampling flip-flop. A small capacitor, C_{18}, and series resistor, R_{18}, insure the initial turn "on" of Q_{20} thereby allowing the "off" transistor Q_{18} to saturate gate Q_{19} switching sweep one to the output. Then as the internal clock triggers the Sampling flip-flop, the output is switched between sweeps one and two on Q_{19} and Q_{21}. This sampling continues while the Master flip-flop is switched to the zero state (Q_4 on, Q_5 off) by the second pulse of the 1/2 pps signal. After four seconds a third 1/2 pps pulse resets the Master flip-flop to "one". The switching of Q_5 from "off" to "on" couples a negative pulse turning trigistor T_{11} "off" and through Q_{17}, stops the Sampling flip-flop. Simultaneously the Q_4 side of the Master flip-flop initates a new frame by restarting the ring-counter.

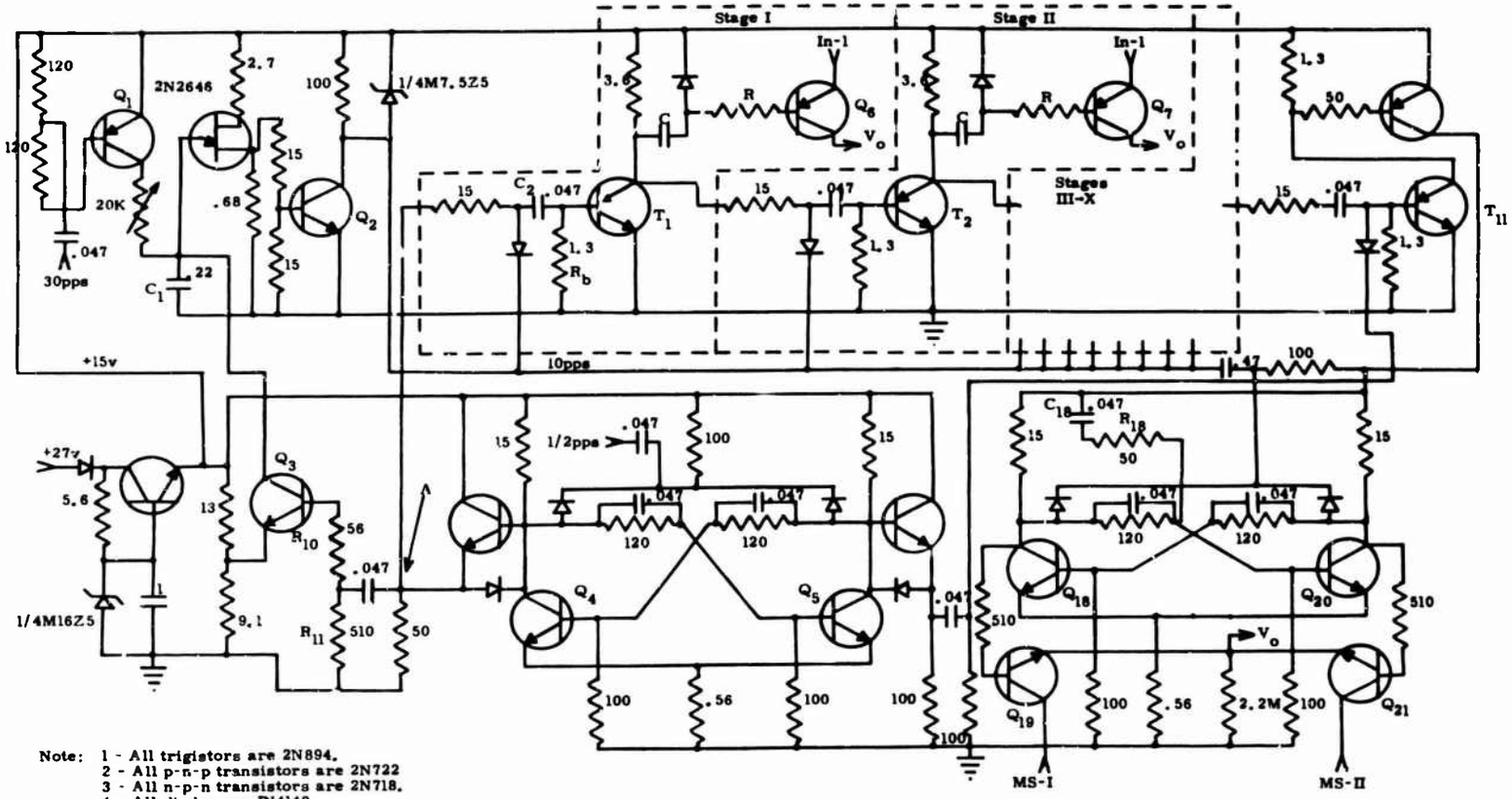

Note: 1 - All trigistors are 2N894.
2 - All p-n-p transistors are 2N722
3 - All n-p-n transistors are 2N718.
4 - All diodes are IN4148.
5 - All resistors in Kohms and all capacitors in uf unless otherwise noted.
6 - Values of C&R vary for given data channels; when Z_{in} is large, C=1 uf, R=10Mohm; when Z_{in} is small, C=10 uf, R=50Kohm.

FIGURE 1 - 17. MASS SPECTROMETER COMMUTATOR

3. Performance

Two Mass Spectrometer Commutators have been constructed and calibrated. The maximum offset error of any gate was less than 50 millivolts. The commutators met specifications over a temperature range of - 30°F to + 150°F with a power supply variation of ± 6 volts from the nominal value of + 28 volts. The power required for each was less than 0.6 watts. They were enclosed in chrome plated boxes 3.5 inches by 3 inches by 1.125 inches and weighted 8.75 ounces. The commutator can be seen mounted in the spacecraft in the photograph of Figure 1-7.

CHAPTER II

THE ASPECT DETERMINING SYSTEM

A. Introduction

In general, gyroscopic devices are required to determine the aspect of space-vehicle sensors with respect to the vehicle's trajectory. However, in the case of sounding rockets and low-altitude satellites, the aspect can be readily computed if in-flight measurements are made of the earth's magnetic field and relative position of the sun. This type of system is relatively inexpensive to develop and fly, and is the type employed on the satellite discussed in Chapter I. During this contract the hardware system was developed, the main program for aspect calculation envisioned in skeletal form, and the necessary sub-programs written and perfected. The final main program is now undergoing final development under follow-on contract AF 19 (628)-5140. In what follows effort is made to explain the requirements and objectives of the system as well as the individual sub-programs. The specific detail of the programs themselves will be published later in a Scientific Report prepared under contract AF 19 (628)-5140.

B. Magnetic Aspect System Philosophy

The satellite contains three magnetometers mounted mutually perpendicular with one magnetometer lined-up with the spin axis of the vehicle. The readings of these three sensors allow the projections of the magnetic field along each body axis to be measured. Later this telemetered information can be used to determine a cone with the magnetic field along its major axis and the spin axis of the satellite being used to generate the cone's surface.

The solar eye working in conjunction with the spacecraft clock determines the time at which the sun is in the plane of the eye and also the angle between the longitudinal axis and the sun. This telemetered information can be later used to establish a cone with the sun along its major axis and the longitudinal (spin) axis being used to generate the cone's surface.

In general these two cones, which have a common vertex point, intersect along two elements, or lines. However, the ambiguity can be resolved from the knowledge of the magnetic field projections along the body axis of the vehicle. (If the two cones are tangent the one solution is obvious. If the two cones coincide, then, the unlikely event of the magnetic field vector pointing toward the sun has occured and a specific solution cannot be obtained.) The correct line of intersection between the two cones determines the direction of the longitudinal axis of the vehicle relative to the magnetic field vector and the vector pointing toward the sun. Once the actual magnetic field vector and sun direction are known for the point in question on the vehicles trajectory, the aspect of the longitudinal and transverse magnetometers are known. The location of each on-board sensor with respect to these axes is known and consequently their aspect is also determined. Furthermore, since the angle between the vehicle's velocity vector and its spin (longitudinal) axis can be determined from orbital information, the angle of attack between each sensor and the velocity vector can be obtained.

Successful determination of the aspect of any satellite sensor, then, requires telemetered information with respect to the readings of the three magnetometers, the sun angle and the reading of the satellite clock at those instants when the sun was in the plane of the aspect eye. When the vehicle is well behaved, continuous

aspect information can be obtained by interpolating between successive eye hits by the sun. This telemetered information must be augmented by a determination of: (1) the true time at which the telemetered data was taken, (2) calculation of the latitude, longitude, altitude and velocity vector of the satellite from orbital parameters, (3) calculation of the magnetic field vector at the point in question and (4) calculation of the position of the sun relative to the point in question.

In the main program which is summarized in the following section subprograms are utilized to calculate the needed quantities. The approach used is to project the calculated magnetic field onto a set of body axes and compare these values with the measured readings. This allows the determination of a set of Euler angles which, when combined with trajectory data, yields the angle of attack of the vehicle.

As discussed in Chapter I, a commutator with a frame period of two seconds is used to commutate the pertinent airborne data. The angle-of-attack is computed for each frame read-out. One of the transverse magnetometers is also monitored continuously on a seperate telemetry subcarrier channel and can be used to accurately determine the spin rate of the vehicle under conditions of well behaved performance. This allows an interpolation to be performed for specific time between successive read-outs of the commutator.

C. The Main Program

The main program which is flow-charted in Figure 2-1 is intended to: (1) process the input data, (2) control the order of computations and (3) supply the desired output data.

1. The Input Data

Orbital Parameters - The orbital parameters used are specified by AFCRL data analysis branch on form No. 1 for CRMXA element data set-six. Specifically, the parameters* used are:

a) Ω (2); right ascension of ascending node
b) ω (2); argument of perigee
c) e (2); eccentricity
d) i (1); inclination
e) n (3); orbit frequency
f) a (2); semi-major axis
g) modified Julian days; reference day and time of ascending node.

Coefficients for Magnetic Field - The coefficients used for calculating the earth's magnetic field are the Leaton Evans coefficients for epoch 1965.0. These coefficients can be found in the Goddard Space Flight Center publication No. X-611-64-316 entitled "Computation of the Main Geomagnetic Field from Spherical Harmonic Expansions." They are given in Schmidt normalized form with time coefficients. Due to changes made in the magnetic field program, the coefficients were changed to Gauss normalized and updated to epoch 1967.0.

Magnetometer Calibration Coefficients - The A/D converter divides each magnetometer voltage reading into 128 levels. A quadratic equation relates the level to the actual voltage reading. This is given by:

*The number in parentheses indicates the order of the time derivatives used in a Taylor series expansion for extrapolation.

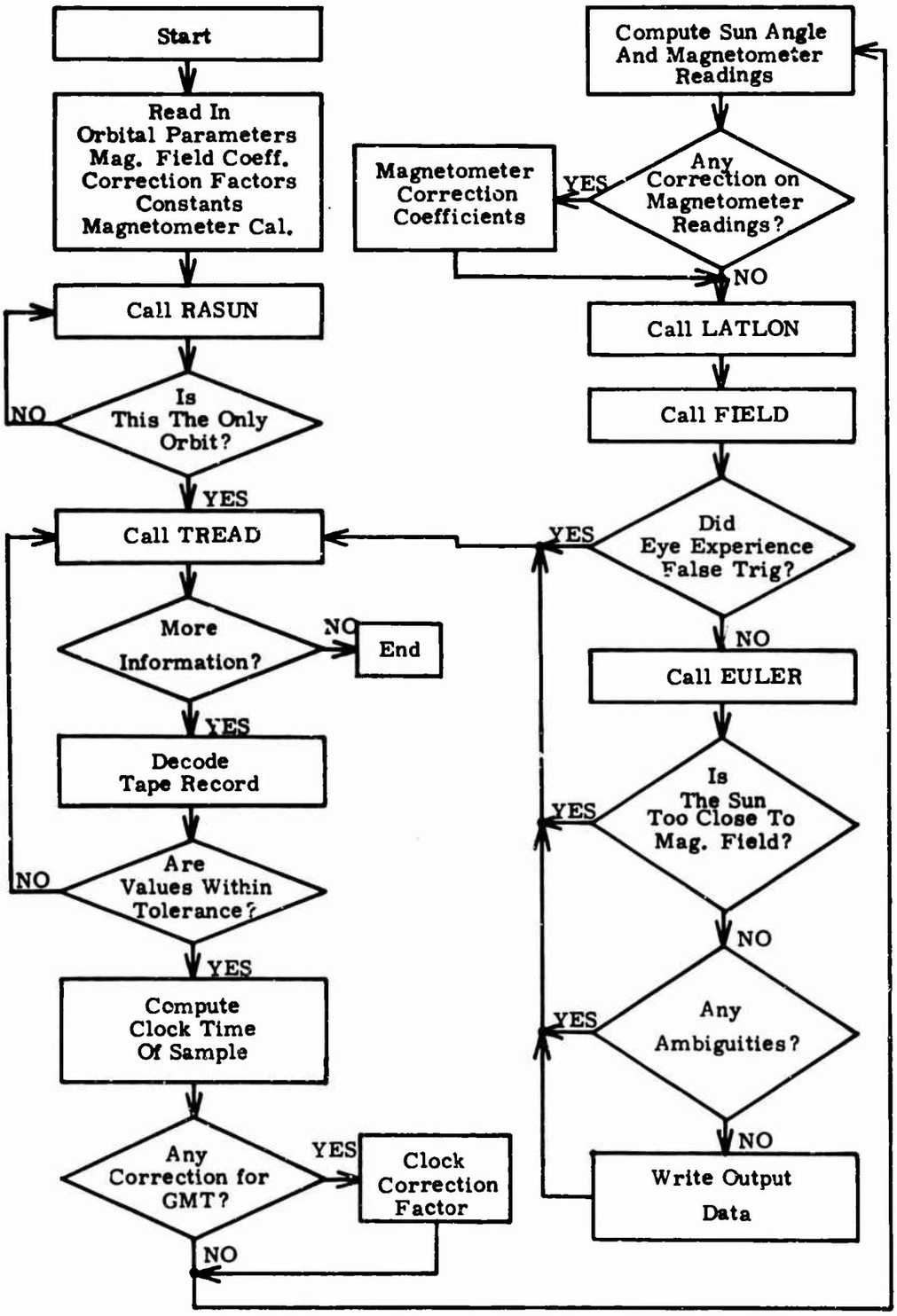

FIGURE 2-1. FLOW CHART OF MAIN PROGRAM

$$\text{Vol}(I) = a_0(I) + a_1(I)\,L(I) + a_2(I)\,L^2(I) \qquad (I = 1, 2, 3)$$

Another quadratic equation is used to convert the magnetometer voltage in volts to milligauss. This is given by:

$$EM(I) = a_{0m}(I) + a_{1m}\text{Vol}(I) + a_{2m}[\text{Vol}(I)]^2 \qquad (I = 1, 2, 3)$$

Magnetometer Saturation Values - In order to account for a possible faulty magnetometer, an upper limit is established for each magnetometer. These limits can be set so that each reading from a faulty magnetometer would be rejected and therefore save computer time.

Satellite Stray Magnetic Field Correction Coefficients - A series of measurements were made and compared to reference data in order to compute the necessary correction factors to account for stray fields present in the satellite. The correction is accomplished by multiplying the magnetometer values by a 3x3 matrix.

$$\begin{bmatrix} M(1) \\ M(2) \\ M(3) \end{bmatrix} = \begin{bmatrix} 3\text{x}3 \\ \text{Magcoe} \end{bmatrix} \begin{bmatrix} EM(1) \\ EM(2) \\ EM(3) \end{bmatrix}$$

Time Factors - It is necessary to know the day and time at the start of the particular orbit of interest. For the case of real time data reduction only a partial orbit is considered, but for the tape recorder channel prior read-out information is necessary. In order to correlate clock time with universal time corrective constants must be inserted into the program.

Binary Tape - a binary tape will be received from the recording site which will contain the telemetered values of the magnetometers, sun angle, and the clock. The commutator used has 60 segments which results in a PAM tape format of 11 revolutions per record. The reading-in of the tape is controlled by subroutine TREAD which was written by the AFCRL computer group.

2. Sequence of Computations

The sequence of control operation performed by the main program is illustrated by the flow-chart given as Figure 2-1. The various subprograms are called for when needed to perform specific calculations. The purpose of each program is indicated in somewhat cryptic form by the subprogram call name.

RASUN is used to compute the right ascension and declination of the sun for a given day and universal time.

TREAD is used to read the binary angle tape which contains the telemetered data from the satellite. This is an AFCRL machine language program.

LATLON is used to compute the location and velocity of the satellite in its orbit on a given day at a specific time.

FIELD is used to calculate the components of the magnetic field at the point in the orbit determined by LATLON.

EULER combines the information available on the magnetic field and the sun with measured values of the field and the angle between the vehicle spin axis and the sun to produce a set of Euler angles.

3. Output Data

In general the output data will consist of a set of Euler angles and the angle of attack. The angle of attack can be found from the dot product of the velocity vector with the axis of interest for any particular sensor.

D. Subprogram RASUN

Subprogram RASUN is used to compute the right ascension and declination of the sun for a given day and universal time. The necessary constants*, describing the rotation of the earth about the sun, for this computation are:

Eccentricity = e = 0.01672297
Mean Longitude of Perigee = ω_o = 282.37288°
Mean obliguity = ϵ = 23.44358°
Time of perigee (days after Jan. 1) = DAFJ10 = 3.1828

All calculations will be referenced to the celestial sphere as shown in Figure 2-2.

The mean anomaly is computed on the assumption that the sun rotates at a constant rate around the earth and is given by:

$$MA = 2\pi(\text{Date} + \text{GMT} / 86400 - \text{DAFJ10}) / 365.2422$$

where Date = day of interest
GMT = universal time on day of interest
365.2422 = tropical year

The true anomaly can be found by adding the mean anomaly to the equation of the centre and is given by:

$$TA = MA + 2e \sin(ma) + (5/4)e^2 \; n\,[2(ma)] + (e^3/12)\,[13 \sin(3ma) - 3\sin(ma)] + \ldots$$

The right ascension of the sun as measured in the plane of the ecliptic is given by:

$$RAE = TA + \omega$$

The right ascension and declination can now be found from triangle SVE. Spherical trigonometry yields:

$$\frac{\sin(Decs)}{\sin(\epsilon)} = \frac{\sin(RAE)}{\sin(n\pi/2)}$$

*All constants are subject to small corrections due to the passage of time.

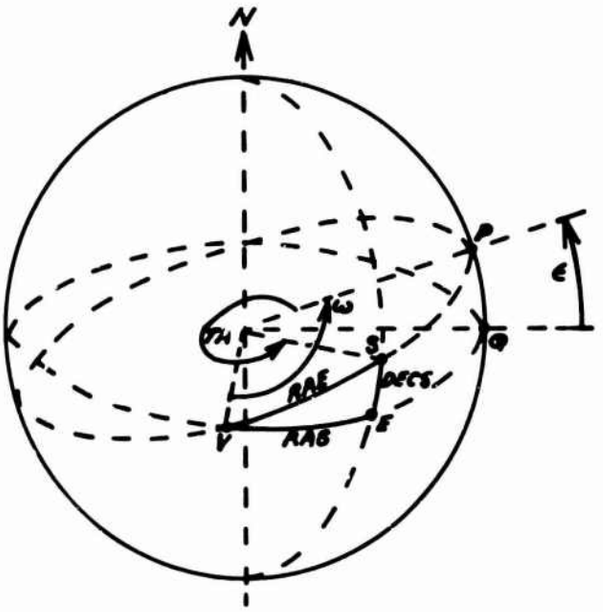

N = North Celestial Pole
V = Vernal Equinox
P = Perigee of Sun
S = Sun
VEQ = Equitorial Plane
VSP = Ecliptic Plane

FIGURE 2-2. POSITION OF SUN ON CELESTIAL SPHERE

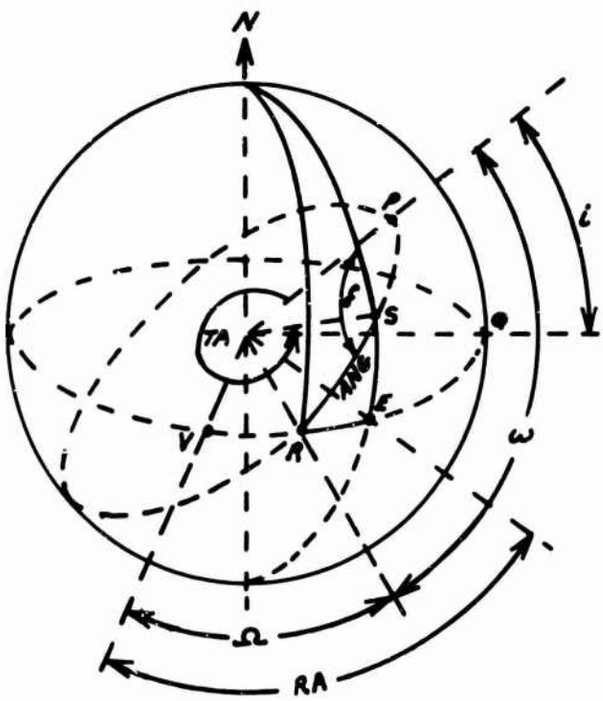

N = North Celestial Pole
V = Vernal Equinox
P = Perigee of Satellite
S = Satellite
R = Ascending Node
VEQ = Equitorial Plane
RSP = Orbit Plane

FIGURE 2-3. POSITION OF SATELLITE ON CELESTIAL SPHERE

from which

$$Decs = \sin^{-1}[\sin(\epsilon)\sin(RAE)]$$

also

$$\cos(RAE) = \cos(Decs)\cos(RAS) + \sin(Decs)\sin(RAS)\cos(n\pi/2)$$

from which

$$RAS = \cos^{-1}\left[\frac{\cos(RAE)}{\cos(Decs)}\right]$$

E. Subprogram LATLON

Subprogram LATLON is used to compute the location and velocity of a satellite in orbit on a given day at a specified time. The calculations are made first with respect to an inertial coordinate system and then referred to an earth referenced system. The necessary input data are:

1. day of interest = date (day)
2. universal time of interest = GMT (sec)
3. right ascension of Greenwich meridian on Jan. 1 at 0 hrs GMT = Vern where Vern = 99.95712^{0}
4. Orbital parameters*
   a. semi-major axis = a (nautical miles)
   b. eccentricity = e
   c. argument of perigee = ω (deg)
   d. right ascension of ascending node = Ω (dec)
   e. revolutions per day = N (rev/day)
   f. reference time for measurement of orbital parameters = To (sec)
   g. reference day for orbital parameters = DT_{to} (day)
   h. inclination = i (deg)

The pertinent parameters are indicated on Figure 2-3.

The orbital parameters must be updated before any calculations can be made. At the ascending node, the eccentric anomaly is given by:

$$E = 2\pi - \cos^{-1}\left[\frac{e + \cos\omega}{1 + e\cos\omega}\right]$$

The mean anomaly at the ascending node can be found by solving Kepler's equation:

$$MA = E - e\sin E$$

The mean anomaly at any time can be generated from

$$M = 2\pi N(TTT) + MA$$

*Associated time derivatives are also necessary to update the orbital parameters.

where TTT = total time (days) elapsed from To (which is taken at ascending node). The true anomaly is found by adding the equation of the centre to the mean anomaly.

$$TA = M + 2e \sin M + (5/4)e^2 \sin 2M + (e^3/12)\,[13 \sin 3M - 3 \sin M] + \ldots\ldots$$

If ANG is used to designate the longitude of the satellite measured east along the orbit plane then:

$$ANG = TA + \omega$$

The latitude can now be found using triangle SRE.

$$\frac{\sin (Lat)}{\sin (i)} = \frac{\sin (ANG)}{\sin (\pi/2)}$$

from which

$$Lat = \sin^{-1}[\sin (i) \sin (ANG)]$$

also

$$\cos (ANG) = \cos (Lat) \cos (RA - \Omega) + \sin (Lat) \sin (RA - \Omega) \cos \pi/2$$

from which

$$RA = \Omega + \cos^{-1}\left[\frac{\cos (ANG)}{\cos (Lat)}\right]$$

Celestial latitude and earth referenced latitude are the same. The earth referenced longitude measured east from the Greenwich meridian can be found from the celestial longitude and the right ascension of the Greenwich meridian and is given by:

$$lon = RA - RAGM$$

where

$$RAGM = 2\pi\left[\frac{(date - 1 + \frac{GMT}{86400})}{365.2422} + \frac{GMT}{86400}\right] + Vern$$

From the geometry, the geocentric distance to the satellite is given by:

$$R_{nm} = \frac{a(1-e^2)}{1+e \cos (TA)}$$

The geodetic altitude can be found by using the flatness factor and is given by:

$$Alt_{nm} = R_{nm} - 3440\,[\,1 - f \sin^2 (Lat)]$$

where

$$\text{flatness} = f = \frac{1}{298.34}$$

Energy relationships[4] yield the following:

$$h = \text{specific angular momentum} = \left[62746.8a\,(1-e^2)\right]^{1/2}$$

$$\frac{T}{2} = \text{Specific kinetic energy} = 62746.3\left(\frac{1}{R_{nm}} - \frac{1}{2a}\right)$$

The tangential velocity is given by:

$$HV = \frac{h}{R_{nm}}$$

and the radial velocity by:

$$\dot{R} = \left[T - (HV)^2\right]^{1/2}$$

As shown in Figure 2-3, the angle α can be found using triangle RSN.

$$\cos\frac{\pi}{2} = \cos\left(\frac{\pi}{2} - \text{Lat}\right)\cos(\text{ANG}) + \sin\left(\frac{\pi}{2} - \text{Lat}\right)\sin(\text{ANG})\cos\alpha$$

from which

$$\alpha = \cos^{-1}\left[-\frac{\sin(\text{Lat})\cos(\text{ANG})}{\cos(\text{Lat})\sin(\text{ANG})}\right]$$

The tangential velocity can now be resolved into two components.

$$\text{clond} = \text{celestial azimuthal velocity} = HV\cos\left(\alpha - \frac{\pi}{2}\right)$$

and

$$\text{Latd} = \text{celestial (or earth) polar velocity} = -HV\sin\left(\alpha - \frac{\pi}{2}\right)$$

The velocity vector can now be expressed in terms of spherical coordinates with respect to a celestial reference as*:

$$\vec{V}_I = (\dot{R})\,\hat{r} + (\text{Latd})\,\hat{\theta} + (\text{clond})\,\hat{\phi}$$

In order to find the velocity with respect to earth, the azimuthal component has to be corrected for the earth's rotation. The period of rotation is that of a sidereal day. Hence:

$$\text{Lond} = \text{earth referenced azimuthal velocity}$$

$$= \text{clond} - \frac{2\pi R_{nm}\cos(\text{Lat})}{86164.1}$$

*$\hat{\ }$ indicates unit vector

The velocity vector with respect to the earth is now given by:

$$\vec{V}_e = (\dot{R})\hat{r} + (Latd)\hat{\theta} + (Lond)\hat{\phi}$$

F. Subprogram Field

The magnetic field can be calculated for any point close to the earth's surface by a spherical harmonic expansion as depicted by Chapman and Bartels[5]. This method is based on a set of measured coefficients and is discussed for computer applications by Cain et al[6]. As indicated under section C2 of this chapter, Cain's program was simplified for this specific application. Leaton Evans coefficients for epoch 1965.0 were updated to epoch 1967.0 and changed to Gauss normalized form.

Subprogram FIELD used the modified NASA program developed by Cain to calculate the components of the magnetic field at the point in the orbit specified by LATLON. The field is resolved into a radial component, BR, which is directed toward the zenith, a latitude-tangent component, BP, which is directed toward the east and longitude-tangent component, BT, which is directed toward the south. Additional calculations are then undertaken to arrive at the output quantities B, RAM and Decm. Figure 2-4 indicates many of the quantities used in the following material.

$$B = [(BR)^2 + (BP)^2 + (BT)^2]^{1/2}$$

$$BVert = BR \sin(Lat) - BT \cos(Lat)$$

$$BHR = BR \cos(Lat) + BT \sin(Lat)$$

The declination of the magnetic field, Decm, can now be expressed by:

$$Decm = \arcsin(BVert/B)$$

The longitude of the magnetic field, BML, measured from the BVert-BHR plane can be expressed by:

$$BML = \arctan(BP/BHR)$$

The right ascension of the magnetic field, RAM, can be expressed in terms of the right ascension of the Greenwich meridian, GAGM, the longitude of the satellite, Lon, and BML by:

$$RAM = RAGM + Lon + BML$$

G. Subprogram EULER

Subprogram EULER combines the information available on the magnetic field and the sun with measured values of the field and the angle between the vehicle spin axis and the sun to produce a set of Euler angles. This is accomplished by performing two sets of coordinate transformations. The first transformation refers the magnetic field to a coordinate system with the sun as the zenith axis. This is shown in Figure 2-5 and the components are given by:

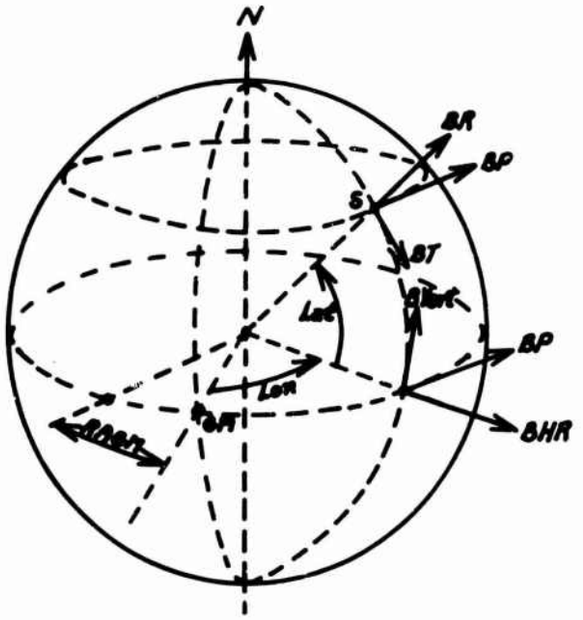

N = North Celestial Pole
S = Satellite
V = Vernal Equinox
NGM = Greenwich Meridian

FIGURE 2-4. COMPONENTS OF MAGNETIC FIELD

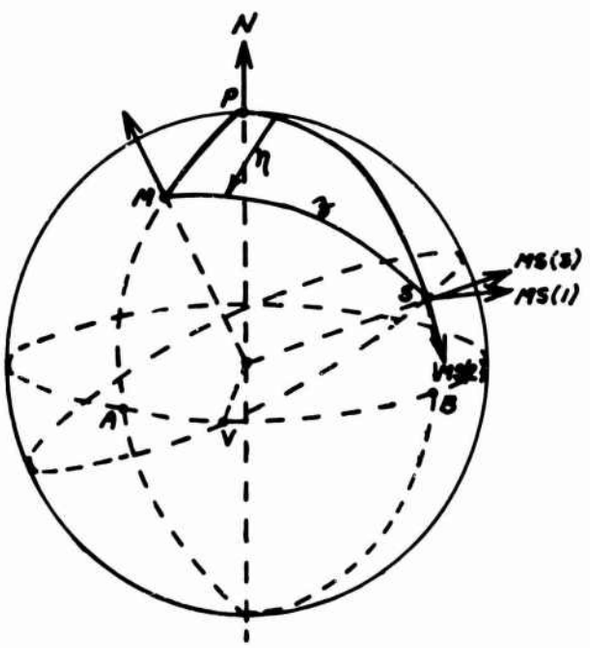

N = North Celestial Pole
S = Sun
V = Vernal Equinox
M = Magnetic Vector
arc AM = Decm
arc BS = Decs
arc VB = Ras
arc VBA = Ram

FIGURE 2-5. MAGNETIC COMPONENTS IN SUN ORIENTED SYSTEM

$$MS(1) = -|M| \sin(z) \sin(\eta)$$
$$MS(2) = -|M| \sin(z) \cos(\eta)$$
$$MS(3) = |M| \cos(z)$$

or in matrix form:

$$M = \begin{bmatrix} -|M|\sin(z)\sin(\eta) & -|M|\sin(z)\cos(\eta) & |M|\cos(z) \end{bmatrix} \begin{bmatrix} \hat{MS}(1) \\ \hat{MS}(2) \\ \hat{MS}(3) \end{bmatrix}$$

Since the location of the sun and field are known the angles z and η can be found from triangle PSM.

$$z = \cos^{-1} [\sin(Decs) \sin(Decm) + \cos(Decs) \cos(Decm) \cos(Ras-Ram)]$$

and

$$\eta = \cos^{-1} \left[\frac{\sin(Decm) - \sin(Decs) \cos(z)}{\cos(Decs) \sin(z)} \right]$$

The second transformation refers the sun referenced coordinate system to that of the satellite axis. This is accomplished by two rotations which are illustrated in Figure 2-6. The first rotation is (90 + α) degrees about MS(3) this gives:

$$\begin{bmatrix} \hat{MS}(1) \\ \hat{MS}(2) \\ \hat{MS}(3) \end{bmatrix} = \begin{bmatrix} -\sin\alpha & \cos\alpha & 0 \\ -\cos\alpha & -\sin\alpha & 0 \\ 0 & 0 & 1 \end{bmatrix} \begin{bmatrix} \hat{MS'}(1) \\ \hat{MS'}(2) \\ \hat{MS'}(3) \end{bmatrix}$$

The second rotation is (sang) degrees about MS'(2) where sang is the angle between the satellite spin axis and the sun. This gives:

$$\begin{bmatrix} \hat{MS'}(1) \\ \hat{MS'}(2) \\ \hat{MS'}(3) \end{bmatrix} = \begin{bmatrix} \cos(sang) & 0 & \sin(sang) \\ 0 & 1 & 0 \\ +\sin(sang) & 0 & -\cos(sang) \end{bmatrix} \begin{bmatrix} \hat{z} \\ \hat{y} \\ \hat{x} \end{bmatrix}$$

The two above equations can be combined to yield:

$$\begin{bmatrix} \hat{MS}(1) \\ \hat{MS}(2) \\ \hat{MS}(3) \end{bmatrix} = \begin{bmatrix} -\sin\alpha\cos(sang) & \cos\alpha & -\sin\alpha\sin(sang) \\ -\cos\alpha\cos(sang) & -\sin\alpha & -\cos\alpha\sin(sang) \\ +\sin(sang) & 0 & -\cos(sang) \end{bmatrix} \begin{bmatrix} \hat{z} \\ \hat{y} \\ \hat{x} \end{bmatrix}$$

The magnetic field can be expressed as:

$$M = \begin{bmatrix} MS(1) & MS(2) & MS(3) \end{bmatrix} \begin{bmatrix} \hat{MS}(1) \\ \hat{MS}(2) \\ \hat{MS}(3) \end{bmatrix}$$

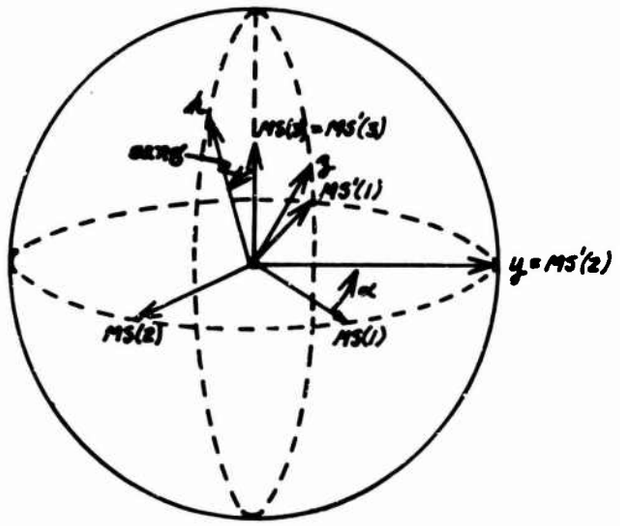

FIGURE 2-6. TRANSFORMATION OF SUN REFERENCED SYSTEM

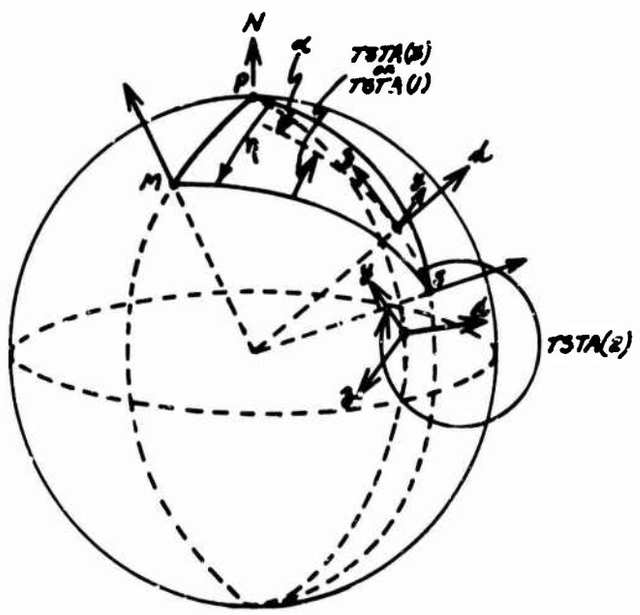

FIGURE 2-7. ILLUSTRATION OF TEST ANGLES

or

$$M = \begin{bmatrix} M(1)\ M(2)\ M(3) \end{bmatrix} \begin{bmatrix} \hat{z} \\ \hat{y} \\ \hat{x} \end{bmatrix}$$

Where M(1), M(2) and M(3) are the readings of the three magnetometers aligned with the satellite axis. Combining the three previous equations yields:

$$\begin{bmatrix} M(1)\ M(2)\ M(3) \end{bmatrix} \begin{bmatrix} \hat{z} \\ \hat{y} \\ \hat{x} \end{bmatrix}$$

$$= \begin{bmatrix} MS(1)\ MS(2)\ MS(3) \end{bmatrix} \begin{bmatrix} -\sin\alpha\cos(sang) & \cos\alpha & -\sin\alpha\sin(sang) \\ -\cos\alpha\cos(sang) & -\sin\alpha & -\cos\alpha\sin(sang) \\ +\sin(sang & 0 & -\cos(sang) \end{bmatrix} \begin{bmatrix} \hat{z} \\ \hat{y} \\ \hat{x} \end{bmatrix}$$

This equation represents three equations with the only unknown angle being α. The general form of these equations is:

$$PP(I)\cos\alpha(I) + QQ(I)\sin\alpha(I) + RR(I) = 0 \qquad (I = 1, 2, 3)$$

If this equation is differentiated with respect to α and the absolute value taken, then:

$$DAL(I) = \left| -PP(I)\sin\alpha(I) + QQ(I)\cos\alpha(I) \right| \qquad (I = 1, 2, 3)$$

DAL(I) can be used to select one of the three values of α. In general PP(I) and QQ(I) are functions of η, z and sang, while RR(I) is a function of η, z, sang and M(I). Only M(I) depends on α, therefore:

$$\frac{\partial M(I)}{d\alpha(I)} = \frac{1}{DAL(I)}$$

To minimize the error, the value of α that yields the maximum DAL(I) is chosen. The solution for $\alpha(I)$ requires some explanation since a second degree transcendental equation must be solved. For example:

$$P(I)\cos^2\alpha(I) + Q(I)\cos\alpha(I) + R(I) = 0$$

The solution of this equation yields four values of $\alpha(I)$, two of which can be eliminated by substituting into the general equation. The final choice for $\alpha(I)$ can be made by introducing a test angle for each $\alpha(I)$. These will be designated by:

$$\text{test angle } (I) = TSTA(I) \qquad (I = 1, 2, 3)$$

TSTA(1) or TSTA(3) is the angle measured counterclockwise from the (M-S) plane to the (x-z) plane. TSTA(2) is the angle measured counterclockwise from the (M-S) plane to the (x-y) plane. These are indicated on Figure 2-7.

It can be seen that when TSTA(1) and/or TSTA(3) are greater than 180^{o}, M(2) which is located along the y-axis will yield a negative reading (the angle between the magnetic field and magnetometer (2) is greater then 90^{o}). Similarly when

$$TSTA(2) + 90^{o} > 180^{o}$$

M(2) is again negative.

The component of the magnetic field measured perpendicularly to the sun in the (x-z) plane is shown in Figure 2-8, and is given by:

$$HM = - [M(3)\sin(sang) + M(1)\cos(sang)]$$

Inspection of Figures 2 - 7 and 2 - 8 indicates that when TSTA(2) is greater than 180^{o}, HM is greater than 0.

Since TSTA(I) is a function of $\alpha(I)$, the previously mentioned conditions can be used to determine the proper value for $\alpha(I)$ to be used.

Once α has been found, the Euler angles can be determined. These are shown on Figure 2-9. From triangle PST.

$$\cos\theta = \cos\left(\frac{\pi}{2} - Decs\right)\cos(sang) + \sin\left(\frac{\pi}{2} - Decs\right)\sin(sang)\cos\alpha$$

From which,

$$\theta = \cos^{-1}[\sin(Decs)\cos(sang) + \cos(Decs)\sin(sang)\cos\alpha]$$

Also,

$$\cos(sang) = \cos\left(\frac{\pi}{2} - Decs\right)\cos\theta + \sin\left(\frac{\pi}{2} - Decs\right)\sin\theta\cos(RAS - \phi)$$

From which,

$$\phi = RAS - \cos^{-1}\left[\frac{\cos(sang) - \sin(Decs)\cos\theta}{\cos(Decs)\sin\theta}\right]$$

and finally,

$$\cos\left(\frac{\pi}{2} - Decs\right) = \cos\theta\cos(sang) + \sin\theta\sin(sang)\cos\left(\frac{3\pi}{2} - \psi\right)$$

From which,

$$\psi = \frac{3\pi}{2} - \cos^{-1}\left[\frac{\sin(Decs) - \cos\theta\cos(sang)}{\sin\theta\sin(sang)}\right]$$

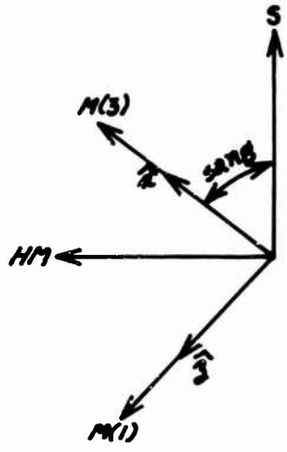

FIGURE 2-8. VECTOR DIAGRAM OF HM

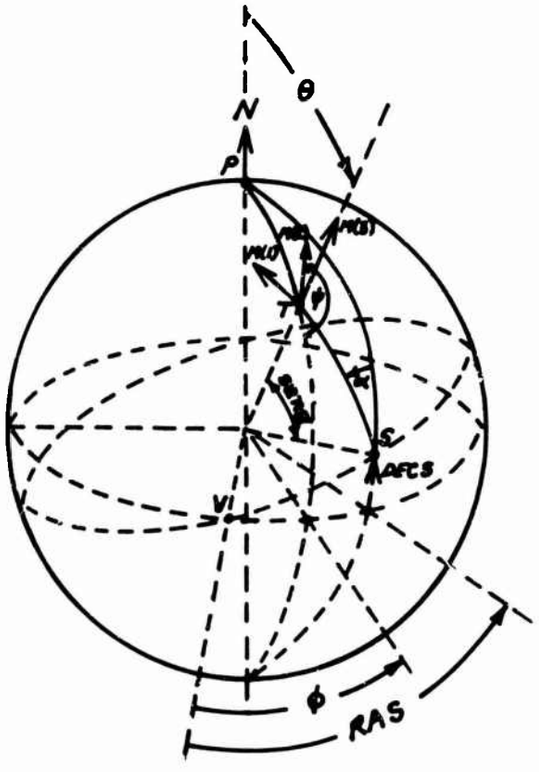

FIGURE 2-9. ILLUSTRATION OF EULER ANGLES

CHAPTER III

RE-ENTRY PHYSICS PROGRAM

The acquisition of data from a vehicle entering the Earth's atmosphere is dependent upon the ability of the communication systems to transmit information to the ground stations. This requirement is dependent not only on the proper functioning of the electronic communications equipment, but also on the ability of the signal transmitted from the vehicle to arrive at the receiver in an adequate strength.

Ionization of the atmosphere in the vicinity of the entering body affects the propagation of the electromagnetic waves. The plasma which surrounds the vehicle in certain ranges of atmospheric density and vehicle velocity attenuates electromagnetic waves that may be incident upon it by absorption and reflection. The attenuation may reach such proportions that a complete blackout of communications occurs during some critical phase of re-entry. Since the plasma effects are exhibited over broad bands of radio frequencies, operation of the communications link above the expected plasma frequency has only limited application.

Measurement of the plasma sheath properties and their effects on the microwave signals during an actual flight can lead to the development of theories predicting an optimum choice of communication system parameters for a given vehicle configuration and trajectory.

A. Experiment Instrumentation

Two instrumentation systems have been designed for a re-entry flight on the Trailblazer II vehicle from NASA Wallops Station, Virginia. The objectives of the instrumentation are to determine the electron density profile of the plasma and to measure the plasma sheath effects on a pulsed microwave system operating at a fixed s-band frequency.

The s-band system has been designed to measure nonlinear pulse distortion, interantenna coupling, antenna impedance mismatch and voltage breakdown, antenna pattern distortion and signal attenuation in the presence of plasma. These measurements will be made by monitoring sensors in the vehicle through a telemetry link and from the s-band signal data received by the ground stations.

Electroacoustic probes operating at VHF , UHF and L-band frequencies and Langmuir probes have been selected for electron density profile measurements.

For the transmission of physical data gathered by the various experiment sensors in the vehicle a PPM telemetry system operating at x-band frequency has been chosen. A block diagram of the instrumentation is shown in Figure 3-1.

The instrumentation package will be carried in a re-entry nose cone on a Trailblazer II vehicle. The nose cone is a hemisphere-cone combination fabricated of aluminum without the protective covering of ablative materials. It is expected that the re-entry vehicle will reach a velocity of 18,000 ft. per second producing a desired test period between 350,000 ft. and 150,000 ft. of about 11 seconds duration and a self destruction by aerodynamic heating at approximately 125,000 ft.

B. S-Band System

The s-band instrumentation which forms the primary multipurpose experiment can be subdivided into two functional blocks: The transmitter and the receiver. The transmitting link consists of a s-band transmitter, digital diode attenuator, two directional couplers and an antenna located at the stagnation point. The receiving link

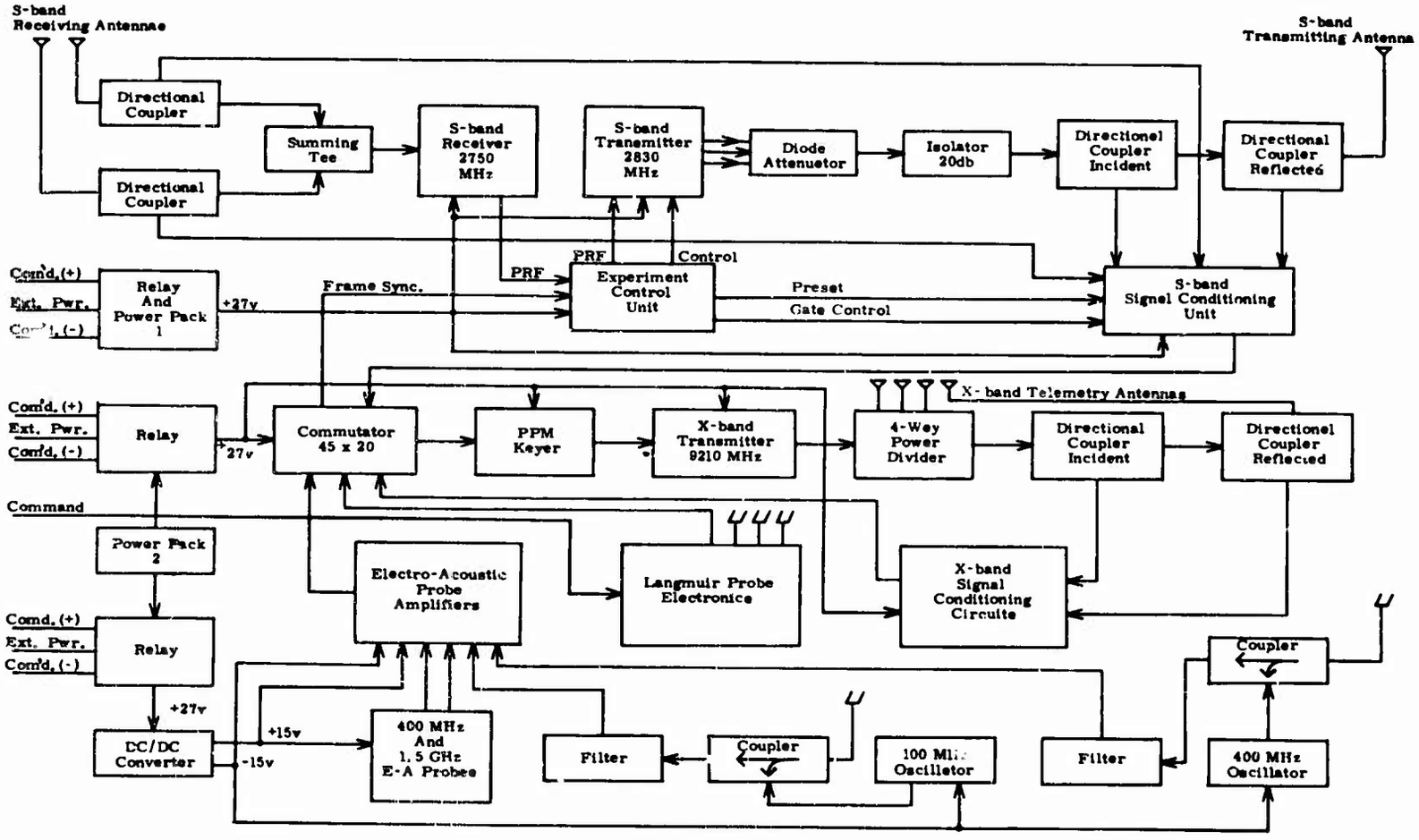

FIGURE 3 - 1. BLOCK DIAGRAM, RE-ENTRY INSTRUMENTATION

has two antennas located 180° apart on the sides of the re-entry nose cone, two directional couplers and a receiver. Both links have the necessary signal conditioning and experiment control circuits.

1. Transmitter

The s-band transmitter operates at a frequency of 2380 MHz with a PRF of 320 pps and a 6 μsec pulse width. To measure the effects of the plasma sheath on the pulse shape distortion and the antenna voltage breakdown, the transmitted peak power is switched sequentially from 1000 to 500 to 125 watts at a rate of 10 Hz by the digital diode attenuator. It is expected to observe the antenna voltage breakdown at the 1000 watt and possibly at the 500 watt levels. No breakdown is expected at the 125 watt level.

Antenna voltage breakdown is evidenced by the errosion of the trailing edge of the transmitted pulse and a considerable increase of the reflected power in the transmission line. The effects of the antenna impedance mismatch due to the voltage breakdown or the plasma sheath can be determined from the incident and reflected powers at the transmitting antenna by detecting the outputs of two directional couplers.

The output of the incident power directional coupler is peak detected to observe the power level changes in the transmitter. The reflected power pulses are peak detected and also integrated over the pulse width by the signal conditioning circuits. The outputs of the integrating circuits are proportional to the energy contained in the microwave pulse. Comparison of the peak detector and the integrator circuit outputs gives a good indication of the severity of pulse distortion during antenna breakdown. In the event of the antenna impedance mismatch without pulse distortion the calibrated outputs of the two circuits indicate the same pulse power. During the antenna breakdown the width of the reflected power pulse is only a fraction of the normal width resulting in an integrator output which is less than would be expected at a given peak power and a normal pulse width. Comparing the reflected peak power obtained from the peak detector with the integrator output an average reflected pulse width can be determined.

From the recordings of the signal strength and the photographs of the received pulse shape at the ground stations, additional information can be obtained on the behavior of the vehicle antenna in the presence of plasma. The signal attenuation due to plasma can be determined from the received signal intensity at the ground stations, the knowledge of the actual transmitted power as determined from the directional coupler data and the slant range between the ground receiving antenna and the vehicle. The attenuation can be calculated at the 125 watt power level where no signal distortion due to antenna voltage breakdown is expected.

2. Receiver

The requirement for the received pulse photography on the ground and the synchronization problems associated with it dictated a transponder type s-band system and the PRF of 320 pps. The tracking radar interrogates the s-band system through the two vehicle receiving antennas at 2750 MHz. Each of the receiving antennas are monitored by a directional coupler terminated in a peak power detector and a pulse integrator. Measurements of these outputs indicate the degree of coupling between the vehicle transmitting and receiving antennas as well as the pulse distortion caused by the plasma sheath.

3. Experiment Control Unit

For a meaningful interpretation of the s-band experiment data it is necessary to sample the outputs of all microwave detectors at the same transmitted power

level and within a short period of time of each other. This requirement is met by synchronizing the switching of the transmitter power levels with every other frame pulse of the TLM commutator. Also the sampling gate control and the pulse integrating circuits are preset during each frame pulse producing two independant data samples at each microwave power level. The Experiment Control circuits are shown in Figures 3-2, 3-3, and 3-4.

Auxiliary Trigger Source - The circuit of Figure 3-2 serves as the s-band transmitter triggering source in absence of the radar interogation during system checks and in the event of radar pulse blackout during re-entry. The UJT Q_2 and associated components form a stable relaxation oscillator operating at 310 pps. The pulses are amplified by the transistor Q_3 differentiated and transmitted through the diode OR gate to the s-band transmitter and the gate control circuits. When the system is interrogated by radar at 320 pps, the output pulses of the s-band receiver trigger the transmitter through the diode D_2 and saturate transistor Q_1. The transistor discharges the timing capacitor C_t thus preventing the UJT from firing.

Power Control - The preset and the transmitted microwave power level control pulses are generated by the circuit shown in Figure 3-3. To prevent excessive loading, the commutator frame sync pulse is isolated from other circuits by the emitter follower Q_1. The output pulses of Q_1 are used to preset control and signal conditioning circuits and to trigger an IC binary which with the transistor Q_2 produces 1 usec pulses at a rate of 10 pps to control the power level switch in the transmitter.

Sampling Gate Control - The output pulses of the crystal video detectors monitoring the microwave power in a transmission line are processed by signal conditioning circuits. The 45 segment 20 frame per second commutator and the PRF of 310 - 320 pps allows an integration and storage of eleven pulses during each frame. The stored data is then sampled once near the end of the commutator cycle.

To achieve some synchronization between frame rate and the signal conditioning circuits, the opening and closing of the transmission gates is controlled by the preset and the PRF pulses of the receiver. A block diagram of the sampling gate control circuit consisting of binary and NOR IC's is shown in Figure 3-4.

The preset pulse derived from the commutator frame sync pulse resets all Q terminals of the binaries to a low voltage level. The PRF pulses from the receiver trigger a monostable-inverter combination to produce a delayed pulse train. The delayed pulses are applied to a ripple counter (binaries B_0 , B_1 , B_2 , and B_3) which through the binaries B_4 and B_5 controls the output OR gate. The delay between the PRF and the information pulses to be sampled prevents opening of the transmission gates during an information pulse. A waveform diagram of the control circuit is shown in Figure 3-5.

The PRF pulse following the preset period changes the state of B_0 and B_4. The change in the state of B_4 forces the output of the OR gate into a low voltage state and opens the transmission gates of the signal conditioning circuits. Since the SET terminal of B_4 is connected to a high voltage level (+5v) the binary can not react to the following trigger pulses until it is reset again. After eight PRF pulses the binary B_3 changes its state setting the RESET terminal of B_5 to a low voltage and deactivating itself with a high voltage on both SET and RESET terminals. For the same reason, B_5 could not react to the triggering by B_2 until this time. After the twelveth pulse B_2 and B_5 change their states. The output of the OR gate returns to a high voltage state and the transmission gates close. Eleven information pulses corresponding to the PRF pulses two to twelve have been transmitted through the gates. Further triggering of the ripple counter has no effect on the gates since binaries B_3 , B_4 , and B_5 are "locked".

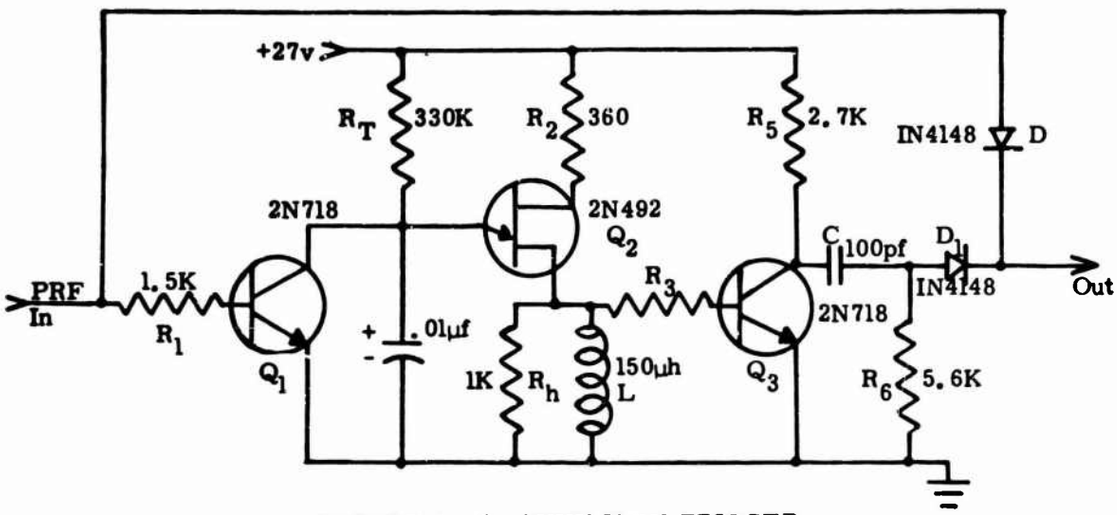

FIGURE 3 - 2. AUXILIARY TRIGGER

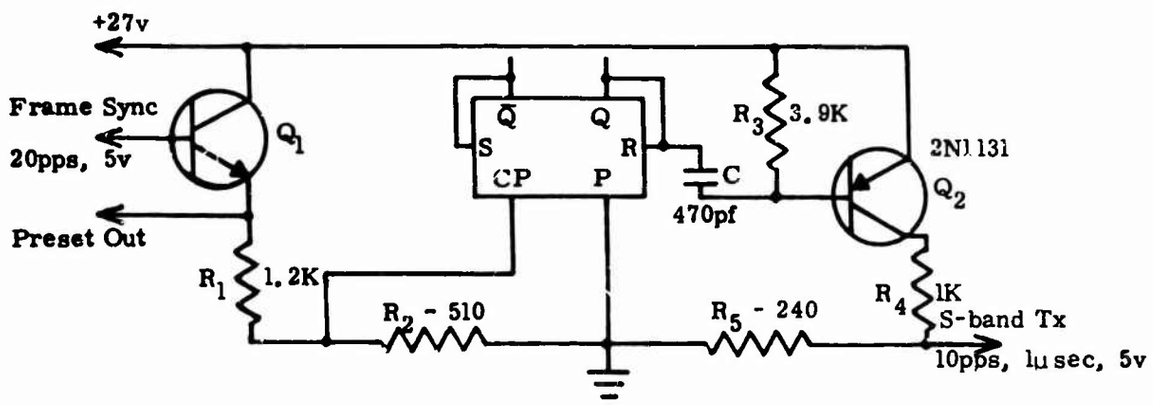

FIGURE 3 - 3. PRESET & R-F CONTROL PULSE GENERATOR

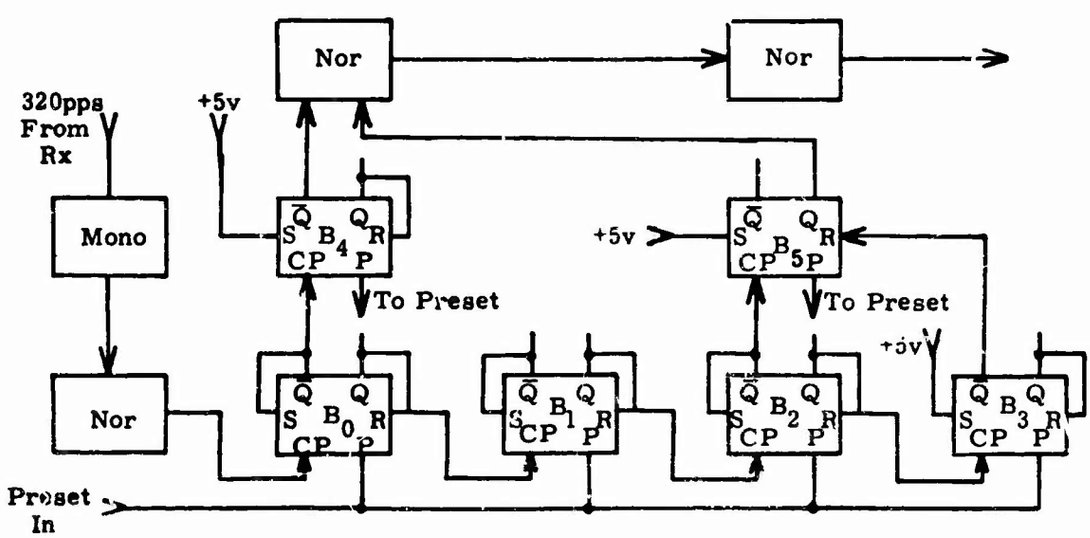

FIGURE 3 - 4. GATE CONTROL LOGIC

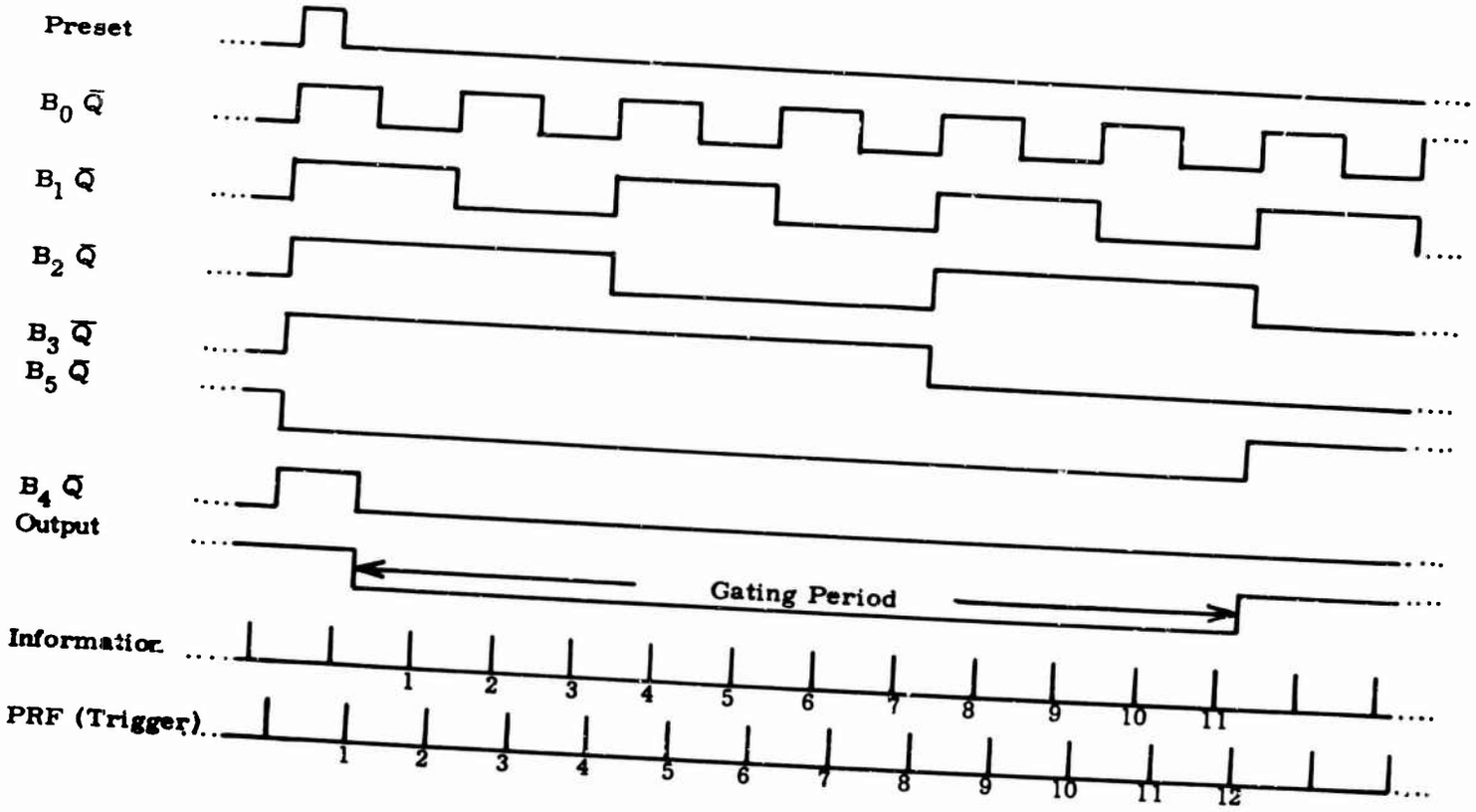

FIGURE 3 - 5. GATE CONTROL WAVEFORMS

4. Signal Conditioning Unit

Integrator - The pulse integrator is shown in Figure 3-6. Transistor Q_1 and the FET Q_2 form a transmission gate for the negative video pulses from the crystal detector. With zero volts at the gate control input the transistor Q_1 and the diode D_1 are cut-off. The gate and the source terminals of the FET are at the same potential permitting the input pulses to arrive at the video amplifier consisting of Q_3 and Q_4. Each amplified pulse turns the transistor Q_5 ON and charges the storage capacitor C_s. The collector of the transistor Q_5 acts as a current source with the instantaneous current proportional to the amplitude of the input pulse. The total charge accumulated by the capacitor during each pulse is proportional to the amplitude and duration of that pulse. The transistors Q_7, Q_8 and Q_9 form an high impedance isolation circuit to prevent the loss of charge by the storage capacitor and to provide a low impedance readout. A pedestal is added to each information pulse at the emitter of Q_3 to compensate for the base to emitter voltage drop required to bring the transistor Q_5 into its active region. The pedestal pulse is derived from the incident power pulse.

The input gate is closed after eleven information pulses have been processed. The storage capacitor retains its charge until the preset pulse derived from commutator frame sync pulse saturates transistor Q_6.

Peak Detector - The pulse peak detector circuit is shown in Figure 3-7. The input pulses are amplified by Q_1 and charge the capacitor C_s through the diode D. It is assumed that no significant change in pulse amplitude will occur during one commutator frame and that any small variations will be averaged by the detector circuit. The capacitor is discharged through the transistor Q_6 by the preset pulse at the end of the commutator sampling period.

Other circuits included in the instrumentation but not shown in this report are: series voltage regulators, a commutator calibration voltage generator, a 30 second dc power delay circuit and various monitor circuits.

C. Electroacoustic Probes

Electroacoustic waves can be generated in a plasma by an electromagnetic wave propagation through the sheath. The waves are logitudinal oscillations of electrons and their wavelengths are much shorter than the free space wavelengths of the electromagnetic waves. The electroacoustic waves do not propagate in plasma where the plasma frequency is greater than the frequency of the wave and are reflected at a surface where plasma frequency equals the wave frequency.

When the distance between the skin of the vehicle and the surface in plasma where the electroacoustic wave is reflected equals an integral number of half wavelengths, standing electroacoustic waves are generated. This condition leads to a decrease in the reflected power of the electromagnetic signal which can be detected.

The number of half wavelengths between the vehicle and the reflecting surface in plasma can be identified from the relative magnitude of the reflected signal. The most pronounced decrease in reflected power occurs when the distance between the reflecting surface in plasma and the vehicle equals to one half wavelength. Since the electron density and collision frequency in the plasma sheath varies during reentry the resonances corresponding to the diffe[illegible] number of half wavelengths occur at different times. Several electroacoustic pr[illegible] operating at different microwave frequencies can measure electron density gra[illegible]nt over a wide range of vehicle altitudes.

The experiment has one probe operating at 100 MHz, one at 1.5 GHz and two probes at 400 MHz. A block diagram of the instrumentation for two probes is

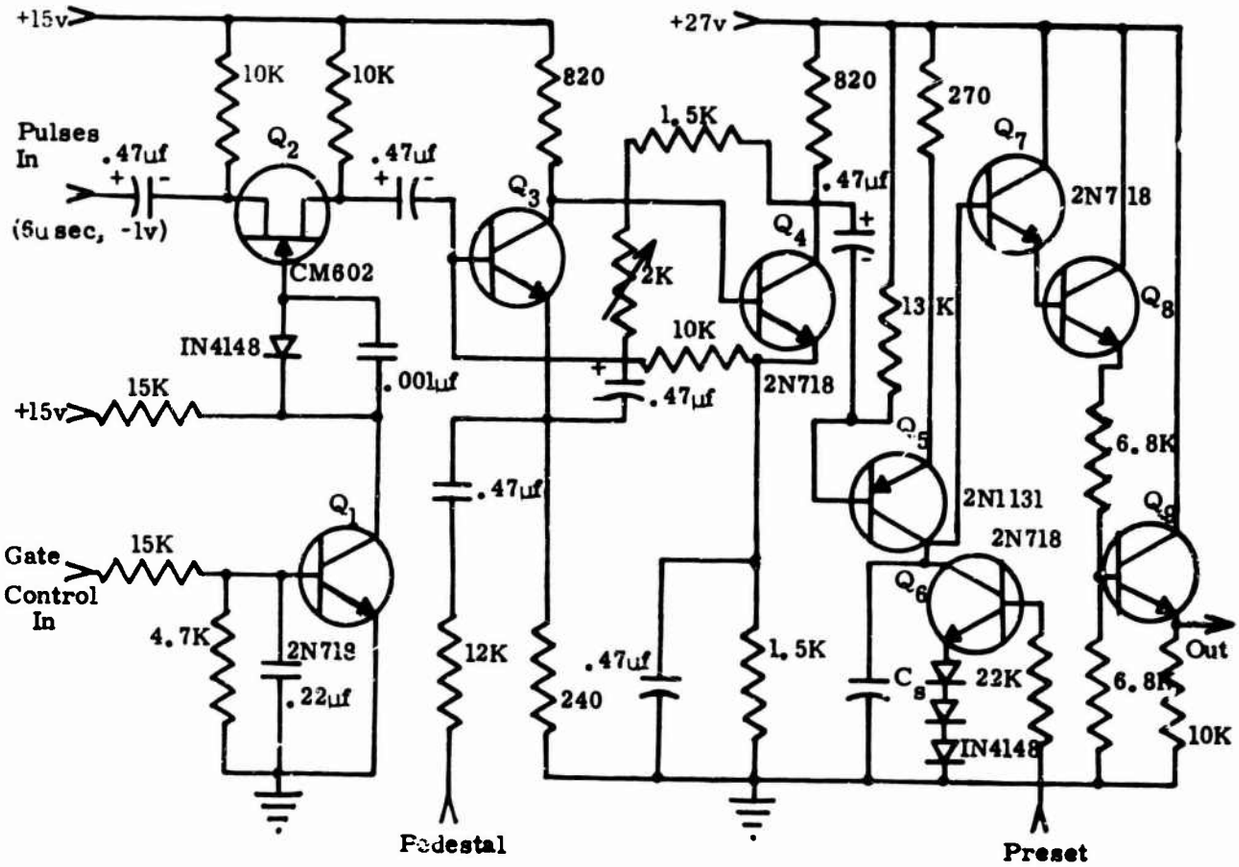

FIGURE 3 - 6. PULSE INTEGRATOR

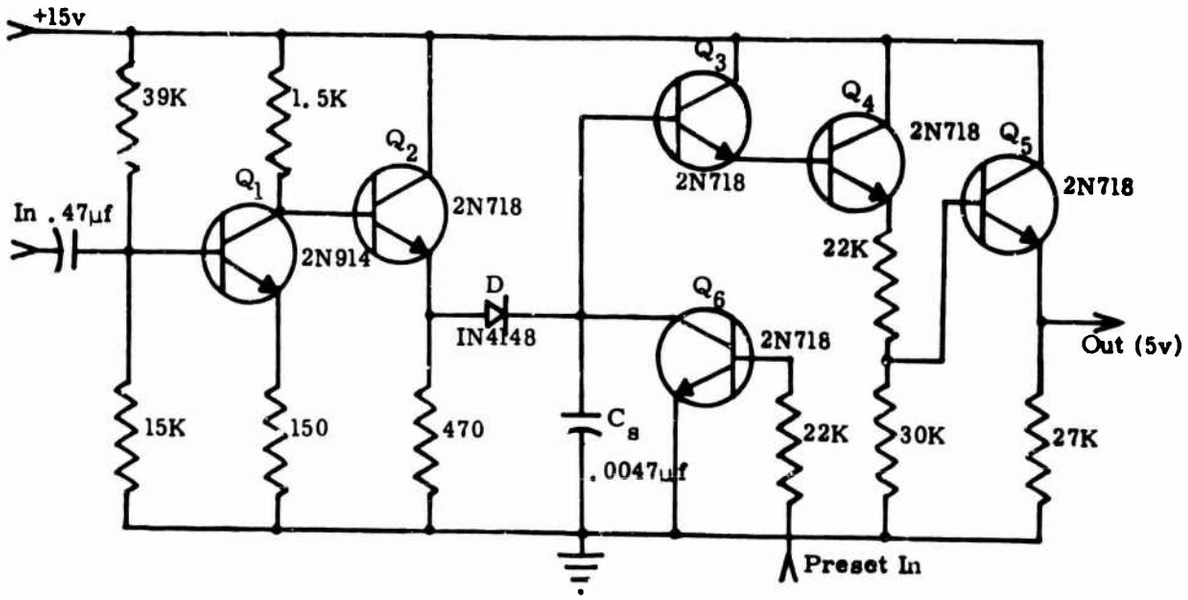

FIGURE 3 - 7. PEAK DETECTOR

shown in Figure 3-1. The microwave oscillator output power of approximately 20 mw is coupled to a probe through a directional coupler with a.20 db coupling coefficient and 20 db directivity. To avoid any influence on the plasma sheath the power of the probe has to be kept well below 1.0 milliwatt. The dimensions of the probe are small compared to a free-space wavelength of the operating microwave frequency and nearly all of the incident power is reflected in absence of plasma.

At the s-band and x-band frequencies the probes can act as reasonably good receiving antennas. Therefore to avoid interference from these high power sources the reflected power from the probe is coupled through a low-pass filter into a crystal detector. The filter has a 30 db attenuation at the s-band and 40 db attenuation at the x-band frequencies used in the vehicle. The detected signal is amplified by a high gain IC operational amplifier. The amplifiers are individually compensated for temperature effects.

The electroacoustic probes which have been designed and tested by the Sperry Rand Research Center are quartz filled co-axial line antennas.

D. Langmuir Probes

The Langmuir probes and associated electric circuits have been supplied by AFCRL Microwave Physics Laboratory. The probes consist of a 0.25 in. flush mounted electrode insulated from the nose cone by boron nitride dielectric. The electrode is made of irridium. The electronics consist of wide dynamic range logarithmic amplifiers.

E. Telemetry

The x-band telemetry system operates at 9210 MHz with four quartz filled slot antennas radiating approximately 25 watts each. The antennas are located near the aft end of the nose cone. The x-band frequency and the location of the antennas will enable the telemetry link to operate without interruption during re-entry.

The data is timed multiplexed by a solid state commutator. Each data sample is converted into a pair of pulses where the time interval between the pulses is proportional to the amplitude of the sample. These pulses are used to trigger the x-band transmitter.

The solid state RZ commutator has a frame rate of 20 Hz and 43 data channels. The PAM output of the commutator is converted into a PPM pulse train by a PDM keyer employing differentiation and inversion of alternate pulses. The maximum spacing for a pair of pulses is restricted to 400 μsec and a minimum spacing to 90 μsec. Therefore the maximum interval between a pair of pulses carrying information is always less than the spacing between adjacent pairs. This arrangement helps to separate the first pulse of a pair from the second pulse in the event that some pulses during a commutator frame are not received. Frame synchronization of the PPM pulse train is accomplished by blanking the pulses during commutator frame synchronization pulse.

To observe the effects of the plasma sheath on the x-band antennas two directional couplers have been placed in the transmission line of one antenna. The output of each coupler is terminated in a crystal detector and a peak power indicating circuit similar to the circuit described in the s-band section.

F. VHF - Beacon

Pointing information from the s-band tracking radars is not available to the x-band receiving site at Coquina Beach, Virginia. Since the x-band receiver cannot aquire the target by itself a CW VHF transmitter operating at 259.7 MHz with

an output of two watts is provided in the vehicle as an aquisition aid. The VHF transmitter will be separated from the re-entry vehicle at apogee.

CHAPTER IV
FIELD SUPPORT

This chapter contains a tabulation of those instances in which field programs required Northeastern University personnel to provide professional and technician level support at field locations.

Satellite programs frequently required working group meetings, testing sessions, system checks and finally the actual launch itself. Because of the multitude of groups involved and geographic locations of the testing centers and ranges, usually a fair amount of field work was associated with orbital vehicles. Balloon programs were also frequently cooperative efforts and so a fair amount of liason was usually required. Whenever overnight travel was needed (as was the case when Georgia Institute of Technology was the experimenter) the trip was classified as field support and is consequently listed below. Sounding rocket support, on the other hand, was usually associated with Northeastern University or AFCRL experiments and thus pre-launch liason was on a local level.

TABULATION OF FIELD SUPPORT

Launch Date or Purpose	Place	Vehicle Type	Designation	Trip Duration	Staff
Mission Working Group Meeting	AF-Space Systems Div. Point Mugu Vandenburg AFB	Orbital Vehicle	Research Satellite for Environmental Sciences - A 015	4/30/63 - 5/3/63	O'Connor
Testing	Goddard Space Flight Center - Blossom Point, Wallops Island	Orbital Vehicle	Research Satellite for Geophysics A 010	5/14/63 - 5/29/63	O'Connor Harding
Testing	Wallops Island	Orbital Vehicle	Research Satellite for Geophysics A 010	6/3/63 - 6/13/63	Harding
Testing	Wallops Island	Orbital Vehicle	Research Satellite for Geophysics A 010	6/19/63 - 6/30/63	Harding
6/29/63	Eglin AFB	Aerobee	AC3.607	6/17/63 - 6/30/63	Sukys Glazer
7/20/63 7/26/63	Fort Churchill	Black Brant IIA Black Brant IIA	ABi7.109 AB17.601	7/8/63 - 7/28/63	Epstein
8/28/63	Holloman AFB	Balloon	Block Assoc. Experimenter: (Cunniff)	8/18/63 - 8/30/63	Nault
8/7/63 8/12/63 8/17/63 8/18/63	Kronagrad, Sweden	Nike Apache Nike Apache Nike Apache Nike Apache	AE5.119 AE5.262 AE5.263 AE5.264	7/6/63 - 8/19/63	Harding
9/3/63	White Sands Missile Range	Aerobee	AD3.374	8/14/63 - 9/5/63	Price
11/14/63	White Sands Missile Range	Aerobee	AD3.324	11/3/63 - 11/15/63	Epstein

TABULATION OF FIELD SUPPORT (Continued)

Launch Date or Purpose	Place	Vehicle Type	Designation	Trip Duration	Staff
Testing	Blossom Point Wallops Island Langley Research Center	Orbital Vehicle	Research Satellite for Environmental Sciences - A 015	12/2/63 - 12/13/63	O'Connor Harding
Mission Working Group Meeting	AF - Space Systems Division, Calif.	Orbital Vehicle	ATCOS - I OV3 - 5	1/27/64 - 1/29/64	O'Connor
Testing	Raytheon Sudbury, Mass.	Orbital Vehicle	Research Satellite for Environmental Sciences - A 015	2/5/64 - 2/10/64	O'Connor Harding
Testing	Point Mugu	Orbital Vehicle	Research Satellite for Environmental Sciences - A 015	5/3/64 - 5/7/64	O'Connor Harding
5/27/64	White Sands Missile Range	Nike Cajun	AE5.118	5/17/64 - 5/28/64	Harding
6/25/64 (failed to orbit)	Vandenburg AFB	Orbital Vehicle	Research Satellite for Environmental Sciences - A 015	5/8/64 - 6/28/64 5/5/64 - 5/17/64 5/7/64 - 6/13/64 6/20/64 - 6/27/64	O'Connor Harding
Testing	Georgia Institute of Technology	Balloon	Toolin	7/22/64 - 7/24/64	Poirier
Testing	Georgia Institute of Technology	Balloon	Toolin	8/5/64 - 8/6/64	Poirier
8/26/64	Holloman AFB	Balloon	Toolin	8/17/64 - 8/27/64	Nault Poirier
10/2/64 10/7/64 10/8/64	Holloman AFB	Balloon Balloon Balloon	Cunniff	9/30/64 - 10/11/64	Nault

TABULATION OF FIELD SUPPORT (Continued)

Launch Date or Purpose	Place	Vehicle Type	Designation	Trip Duration	Staff
Mission Working Group Meeting	Ling-Tempo-Vought	Orbital Vehicle	ATCOS - I OV3 - 5	11/30/64 - 12/2/64	O'Connor
3/6/65 3/13/65	Fort Churchill	Aerobee Aerobee	AD3.313 AD3.312	2/17/65 - 3/14/65	Harding
4/20/65	Wallops Island	Nike Cajun	AD6.841	3/31/65 - 4/21/65	Glazer
Testing	Georgia Tech. Inst.	Balloon	Toolin	5/12/65 - 5/13/65	Nault
6/30/65 7/1/65	Holloman AFB	Balloon Balloon	Toolin	6/15/65 - 7/2/65	Nault
Testing	R.M. Parsons Elec. Company Pasadena	Satellite Tape Recorder	ATCOS - I OV3 - 5	1/25/66 - 1/28/66	Rochefort O'Connor
Testing	Ling-Tempo-Vought	Orbital Vehicle	ATCOS - I OV3 - 5	7/24/66 - 7/27/66	Harding

CHAPTER V

EVALUATION STUDIES OF TELEMETRY SYSTEM COMPONENTS

Evaluation studies and environmental tests of certain airborne telemetry system components have been carried out under this contract. This program was started under the previous contract and has been quite productive. In order to arrive at a comparitive evaluation of commercial equipment, all major manufacturers were invited to submit certain catagories of system components on consignment. The electrical and environmental characteristics were then measured and evaluated, and the results classified as proprietary information and made available to AFCRL and the individual manufacturers concerned. As a sufficient number of units are evaluated, Scientific Reports are issued in order that the results be made available before becoming dated.

The first part of this chapter lists the units tested and references the reports in which detailed information can be found. The second part of the chapter discusses the development of a prototype test unit for automatically performing certain tests on transmitters.

A. Components Tested

Complete results from this contract are contained in Scientific Report No. 1, dated 31 August 1964, and Scientific Report No. 2, dated 31 August 1965, and are available to authorized agencies. A chapter of each report is devoted to one of the three major catagories of system components evaluated to date, namely Voltage Controlled Oscillators, VHF Transmitters, and Electronic Commutators. Each section contains a description of the tests performed, proceedures followed and method of result presentation for these three catagories of system components.

Scientific Reports No. 1 and No. 2 carry the test results of the specific models from each manufacturer as tabulated below.

Scientific Report No. 1

Voltage Controlled Oscillators

Manufacturers	Type	Number Tested
Data-Tronix Corp.	7000-624	1
Data-Tronix Corp.	7003-633	3
Dorsett Electronics Lab., Inc.	0-18G	1
Dorsett Electronics Lab., Inc.	0-18D	2
Sonex, Inc.	TEX-3005C	3
Tele-Dynamics, Inc.	1270A	4
Tele-Dynamics, Inc.	1270AL	14
Vector Manufacturing Co., Inc.	TR-30	12
Vector Manufacturing Co., Inc.	TR-30A	1

VHF Transmitters

Manufacturers	Type	Number Tested
Advanced Electronics Corp.	T-2D/F-26	1
Advanced Electronics Corp.	T-3B/F-6.3	1
Dorsett Electronics Lab., Inc.	TR-20	1
Sonex, Inc.	TEX-3903	1
Tele-Dynamics, Inc.	1062A	1

Electronic Commutators

Manufacturers	Type	Number Tested
Adcole Corp.	202A	2
Dynaplex Corp.	310	1

Scientific Report No. 2

Voltage Controlled Oscillators

Manufacturers	Type	Number Tested
Data-Tronix Corp.	7003-633	31
Dorsett Electronics Lab., Inc.	0-18G	2
International Electronics Res. Corp.	554	2
Scionics Corp.	103	2
Vector Manufacturing Co., Inc.	MMO-10	2

VHF Transmitters

Manufacturers	Type	Number Tested
Vector Manufacturing Co., Inc.	T1127	1
Vector Manufacturing Co., Inc.	T2125	1

B. Transmitter Test Unit

Introduction - In order to speed and facilitate evaluation and acceptance tests of VHF transmitters, a special purpose testing unit was designed to automate most of the repetitive manual proceedures involved. A prototype model was designed to operate in conjunction with a VHF receiver by utilizing the demodulated video output as a direct measure of the test transmitter deviation. Essentially the test unit supplies a set of fixed amplitude, known frequency, modulating signals to the transmitter under test and monitors the amplitude of the corresponding video signals recovered by the receiver. Certain analog operations are then performed on the video signal to derive a dc output, proportional to the desired transmitter parameters, and suitable for driving an external chart recorder.

Of all the tests normally performed on transmitters, modulation response, sensitivity, linearity and deviation ratio measurements are the most time consuming since they require the application of a set of accurately known modulating signals to the transmitter under test. In addition, readings taken from the receiver deviation monitor must be recorded and used to calculate normalized sensitivity and linearity figures for suitable presentation of results. These procedures, repeated at a number of modulating voltages and environmental temperatures, represent a sizeable expenditure of time and effort. It was decided therefore, to design an automated test unit to supply the needed modulating signals and automatically perform the functions of calculating and recording the normalized plot of deviation sensitivity, linearity, etc.

Description - Figure 5-1 illustrates the equipment interconnections used with the transmitter test set and a functional block diagram of the unit is shown in Figure 5-2. A bank of eighteen equal amplitude, IRIG frequency, voltage controlled oscillators are sequentially applied to the modulation input of a test transmitter by a

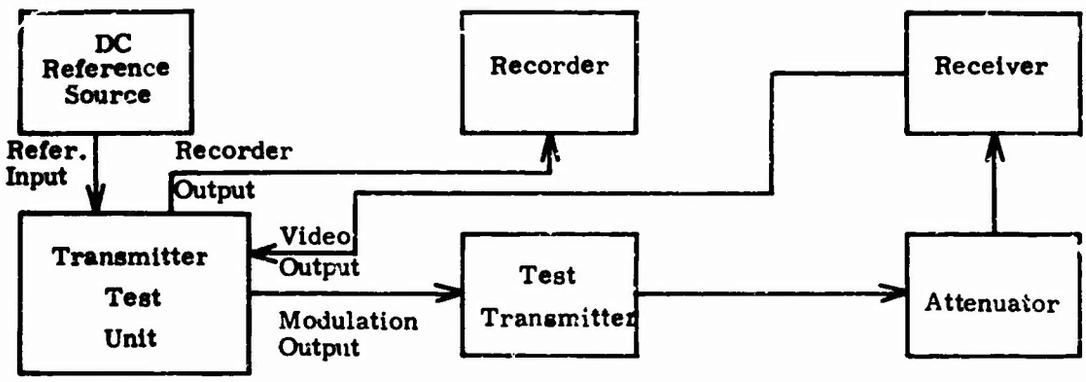

FIGURE 5 - 1. TRANSMITTER TESTING SYSTEM

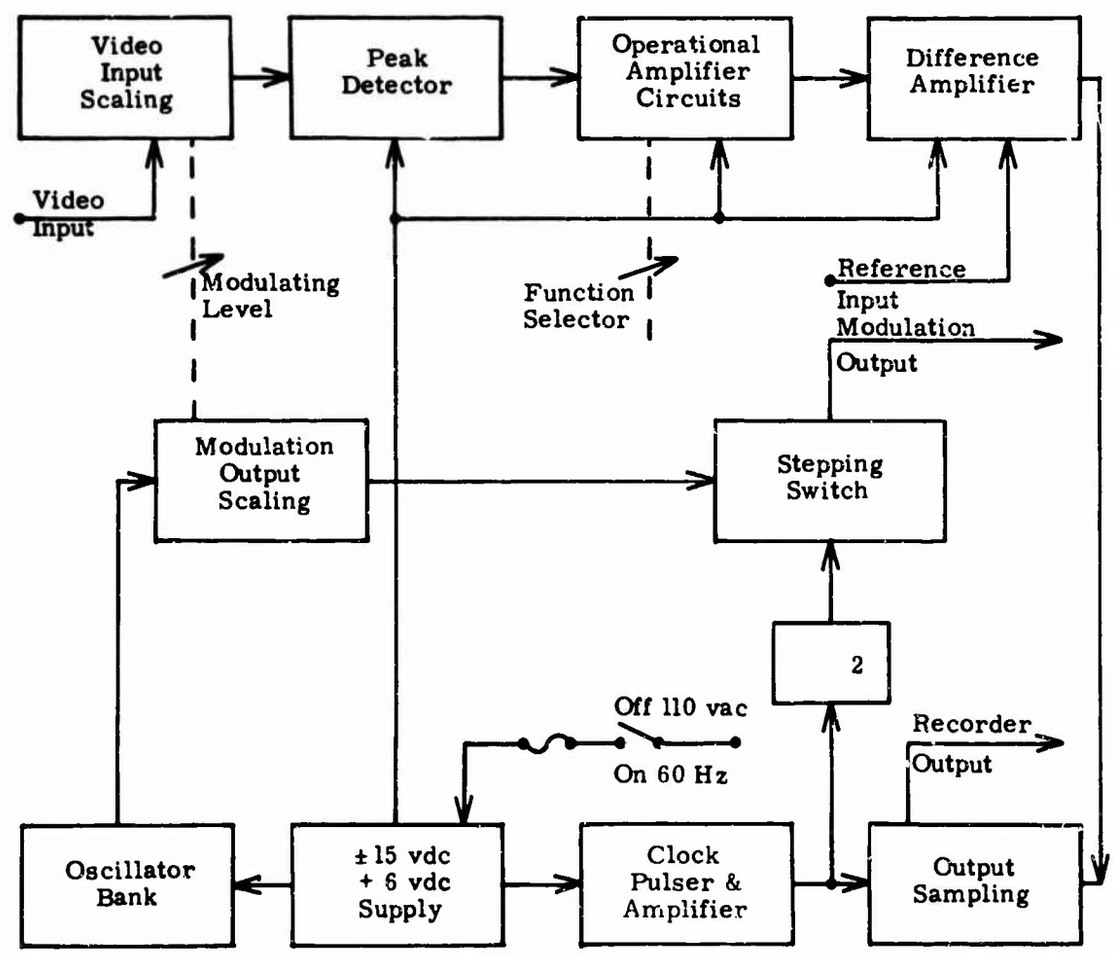

FIGURE 5 - 2. FUNCTIONAL DIAGRAM OF TRANSMITTER TEST SET

motor driven stepping switch. One second clock pulses are generated by a relaxation oscillator circuit and amplified to drive the stepping motor. Two identical gang-tuned voltage dividers form the output and input scaling circuits, and are used to select the desired modulating level and corresponding input sensitivity of the test unit. Thus, as the modulating voltage is increased the input sensitivity is decreased such that an ideally linear transmitter would exhibit a constant deviation sensitivity (constant dc output level from the test unit) throughout the design range of modulating voltages.

The r-f output of the test transmitter is coupled through a fixed attenuator, to the receiver r-f input. The demodulated video output, whose amplitude is directly proportional to the receiver's deviation meter reading, is then ac coupled to the test unit input and peak detected. A function selector switch routes the detected signal to the particular resistance scaling and operational amplifier circuitry needed to implement the desired analog computations. For example, in making deviation ratio measurements for a true FM transmitter, the detected signal is divided in proportion to each modulating frequency by a precision divider network which is controlled by the stepping switch. The resulting range of signals is logarithmic and is therefore compressed to a linear range by a logarithmic amplifier for direct plotting on logarithmically scaled chart paper. Provisions have also been made to accomodate the testing of phase modulated transmitters which require other combinations of analog operations. However, final implementation of these functions were not completed in view of their relatively infrequent use at present. Deviation sensitivity measurements for an FM transmitter are quite straight forward and are essentially obtained directly from the peak detector output. The detected signal is applied to the non-inverting input of a difference amplifier where it is subtracted from an external dc reference voltage in order to provide large dynamic input range and high output sensitivity. This allows the external recorder to be balanced to center scale at any convenient nominal deviation value and maintain the same independant full scale deflection sensitivity. The final output signal is sampled by an output relay during the last half of the stepping switch dwell period in order to prevent switching transients from saturating the recorder. This also provides a convenient zero reference indication to the recorder.

Performance - Initial results from the automated testing of a number of FM transmitters were in close agreement with those obtained by previous manual methods, and achieved a substantial reduction in testing and computation time. However, it became apparent that the long term reliability of the unit was seriously affected by amplitude variations of the oscillators used. In order to keep initial development costs to a minimum, it had been decided that a bank of obsolete voltage controlled oscillators would serve the purpose of generating the desired modulating signals. It was found, however, that these oscillators required more frequent resetting of their voltage levels than anticipated, primarily due to the effects of vibration and long term drifts. The resolution of the wire-wound output potentiometers of the oscillators were found to account for variations as large as 5% in the accuracy of the output voltage settings, resulting in corresponding errors in the amplitude dependant deviation measurements. These errors, added to the inherent system errors of approximately 3%, dictate the need of additional AGC circuitry to maintain amplitude variations below 0.5% and thereby provide the necessary stability and reliability. Plans have been made to make this modification or obtain more stable oscillators in the near future, and conduct a final evaluation of the prototype unit.

CHAPTER VI

SYSTEM PROGRAMS

A. PAM/FM System

The development of a PAM/FM system was undertaken during the previous contract[2] in order to evaluate its use for certain applications at ranges greater than those obtainable with a conventional FM/FM system. The first system developed (Model I) was intended to be flight tested in a piggy-back rocket experiment from WSMR in December, 1962. However, the instrumentation for the prime experiment was found to be very sensitive to the r-f output of the PAM/FM system and consequently the PAM/FM system was not flown. The system was returned to Northeastern and re-worked while awaiting available space upon another flight vehicle. Specifically, the transmitter was returned to the manufacturer for modification to remove spurious emissions and temperature sensitivity. The test signal generator was also modified[2] and the revised PAM/FM system was renamed Model II.

The Model II system was flight tested during the present contract as a piggy-back experiment on board Aerobee rocket AD3.374 from WSMR on 3 September, 1963. Data analysis indicated that the system operated qualitatively throughout the flight. The recovered airborne unit operated accurately in post-flight laboratory tests.

During the flight a Defense Electronics receiver with a 216-260 MHz manually-tuned r-f head, a 100kHz i-f bandwidth, a wide-band FM limiter-discriminator, and a direct-coupled video section was used by the ground station. The receiver was used to drive a $\pm$ 54 kHz wide-band recording module of the Ampex FR-100 tape recorder. Analysis of the recorded data indicated that distortion was encountered at peak signal amplitudes during part of the flight. Since pre-detection recording was not available it is difficult to determine the exact cause of the distortion when the only data available is the result of post-detection recording. However, any signal outside a $\pm$ 1.4 volt range will overdrive the Ampex recorder which was employed and cause the distortion which was observed. Since the distortion was only present for part of the flight and was exclusively associated with peak signals of one polarity, it is concluded that it resulted from relative drift in frequency which took place between the airborne transmitter and the tuned oscillator in the ground receiver as well as a dc drift in the video output of the receiver. It is felt that this distortion could be eliminated on future flight tests by utilizing a crystal-controlled receiver, wider i-f bandwidth at the receiver, and either dc offset at the receiver video output or a recorder with a larger dynamic range.

Post-flight tests run at Northeastern substantiate the above conclusions. Specific data and observations are detailed in the following material.

In the airborne unit a repetitive 200 millisecond pulse train varying from 5.3 to 0 volts was commutated by a 45 x 20 rps solid state commutator. The pulse train consisted of an exponential decay curve and a 6 step descending staircase along with 5 calibration pulses. The commutator output was attenuated and biased such that the input to a solid state transmitter ranged between $\pm$ 0.26 volts. This input signal produced approximately $\pm$ 50 kHz of transmitter carrier deviation.

Analysis of the PAM/FM data indicates that portions of the staircase and exponential signals were transmitted and received with good resolution. Accuracy of these signal levels is easily established since calibration pulses have been transmitted with the signal information.

During the flight, distortion occurred at the 5.2 volt level and later extended through the 4 volt level. During the latter portion of the flight, the distortion at the 4 volt level cleared up. There is also a gradual upward drift of the base line associated with the drift of the upper voltage levels.

No signal information is obtainable from the distorted levels of the flight data. However, all signals having a magnitude less than the distorted levels are reproduced accurately. The distortion has been traced to three different causes, any one of which could have caused the distorted signals. It is very probable that a combination of all three occurred to varing degrees. Those effects which can produce distortion are:

(1) Transmitter frequency drift
(2) Receiver oscillator drift
(3) Receiver dc video output variations causing base line shift

Transmitter Frequency Drift - The transmitting system stability was reinvestigated after the flight data had been scanned. Tests were run examining signal stability of the signal generating circuits, solid state commutator and solid state transmitter. These tests indicated over the temperature range of - 50°C to + 65°C the signal generating circuits, and the Vector commutator were essentially stable, The transmitter exhibits a 5 kHz drift in frequency from turn-on at 7°C in the period of one hour. The transmitter was then subjected to a step change in temperature to 40°C and its drift observed. An additional 6 kHz of drift occurred in 8 minutes time.

Changes in ambient temperature occurring during flight can cause a small shift in the transmitter frequency. This frequency shift will cause the signal to be displaced from the center of the i-f strip bandwidth. A large shift in the relative positions of the transmitter frequency and receiver oscillator frequency can move the signal outside the i-f bandwidth causing distortion. Of course, the change in transmitter temperature during the flight is not known. However, a change in excess of 15°C does not seem likely. A change of this magnitude would account for about a 6 kHz shift in transmitter frequency. Other unknowns could result in additional changes.

Receiver - A Defense Electronics receiver was used at the ground receiving station during the flight. The plug-ins used with this receiver were such that the unit offered r-f tuning over the telemetry band of 216 to 260 MHz, a 100 kHz i-f bandwidth, a wide-band FM limiter-discriminator, and direct-coupled video section. The receiver was manually tuned to the airborne frequency and does not appear to have been re-tuned during the flight.

A similar receiver is available at Northeastern (this receiver is equipped with the wide band tuning head 50 MHz - 260 MHz) and an evaluation of this unit was recently undertaken to determine typical drift data and the like.

In this post-flight evaluation, it was found that the receiver at Northeastern University could be detuned by 20 to 25 kHz during signal transmission before peak distortion was introduced by the i-f band edges. This figure, then, seems to indicate that a relative drift of 20 kHz between transmitter and receiver can be tolerated. Specific drift data on the receiver at Northeastern is not meaningful since the receiver used in the field employed a different r-f head.

It was further determined that the signal format employed caused a video output from the receiver with unequal positive and negative excursions even though the transmitter was symmetrically deviated. An unmodulated r-f carrier from a signal

generator was first used to set the dc video output of the receiver to zero volts. (Any symmetrical signal, varying about a dc level, usually zero, which FM modulates an r-f signal, is reproduced by the FM receiver dc video output as symmetrical about the dc level corresponding to transmitted center frequency.) Next, the transmitter was turned on. In this particular case, the composite signal fed to the transmitter varies between ± 2.6 volts. However, the average dc level is not zero volts but - 0.76 volts due to the unsymmetrical nature of the stairstep, exponential and calibration signals. When the FM receiver reproduces this signal, the dc video output averages about zero volts. The end result of this blocking of the dc level is that the maximum voltage excursion of the varying signal is not equal about the receiver zero point. The signal varies between + 1/3 h to - 2/3 h, where h equals the maximum amplitude of the output signal.

Any change in the dc output of the Defense Electronics receiver will cause the signal to shift from the apparent zero level. Negative going changes in the zero level will cause an even greater offset of the maximum voltage excursion. Since this signal feeds into a ± 54 kHz wide-band recording module of the Ampex FR-100 tape recorder, any signal outside of ± 1.4 volts will overdrive the recorder, thus causing distortion. The stability of the Defense Electronics receiver dc video output has been observed to drift in 1 - 3 seconds by .1 to .2 volts. Occasional step changes in the base line have been observed. These changes are similar to those observed in the flight data.

Receiver Power Supply Variation - Output changes in the dc level have been observed and traced to variations due to the changing line voltage used to power the receiver. Calculations made from the output of the FM discriminator reveal significant variations of the dc video output level coincident with line voltage variations. These variations combined with the drift possibilities mentioned previously can easily cause additional signal distortion by overdriving the Ampex recording module.

B. Temperature Studies of Balloon Telemetry Systems

Balloon borne experiments of the type engaged in by Northeastern generally have a duration of about 4 to 10 hours. The temperature environment experienced by the telemetry system is quite different from the usual 20 Centigrade degree rise encountered during a 6 minute sounding rocket flight. The balloon telemetry system is usually mounted somewhere on an open gondola. During the pre-launch preparation it arrives at a temperature equilibrium with the ambient conditions in existance at the launch site. Over the several hours required for the balloon to reach the float altitude of say 100,000 ft the air temperature may drop to as low as -100°F and then back up to -30°F. The new equilibrium condition at this altitude is one at which convection cooling by the sparce atmosphere is low and radiation cooling (or heating) is dominant. On the down leg of the mission the process is reversed over a shorter period of time since free fall and parachute recovery may be used.

Over a period of several years temperature sensors were attached to telemetry components whenever feasible on balloon flights. Several experimental innovations were tried in telemetry system packaging. As a result of this low-priority type of experimental research a fairly successful telemetry package was developed and finally flight tested on 12 July 1966 on a balloon launch carried out under contract AF 19 (628) - 5140. In what follows, data is presented for the two extremes; an unprotected system, and a final system.

On 26 August 1964 a balloon borne experiment was launched from Holloman AFB, New Mexico. The telemetry transmitter was mounted, in the open, on the ground

plane of the antenna. The subcarrier oscillators were mounted nearby in an unpressurized box. The temperatures measured at various parts of the system are shown in the curves of Figure 6-1. After four hours the balloon reached an altitude of 100, 000 ft and was cut-down. A stable float altitude was never allowed to develop because of difficulties with the prime experiment. However, it is apparent that the transmitter (operating in direct sunlight) had exceeded its rated temperature and life expectancy had become a matter for speculation.

During this particular flight a boom was attached to the gondola to conduct a piggy-back experiment to establish the temperature of three aluminum plates. Each plate was thermally insulated from the boom and each other. The first plate was polished on both sides, the second was polished on the bottom and painted with titanium dioxide on the top, and the third was painted on both sides. Titanium dioxide paint acts as a good reflector to solar radiation and a good emitter for heat which is conducted to it. It was that the bulk of the heating at 100, 000 ft would come from sunlight striking the upper surface of any openly mounted object and the measured data shown in Figure 6-2 confirms this fact.

As a result of data taken in experiments of this type it was concluded that insulation and painted surfaces could be used to maintain the temperature of low-wattage devices such as solid state subcarrier oscillators. High wattage devices such as vacuum-tube transmitters, would require large-surfaces for radiation cooling. These observations were eventually incorporated into a mechanical configuration in which:

1.) The transmitter was mounted to the outside of the telemetry case (that included subcarriers and battery box) in order to prevent the temperature build up inside the telemetry case and allow the transmitter to radiate heat directly to the cold surroundings.

2.) The inside of the telemetry case was lined with one inch styrofoam and the remaining space was filled with water bottles to increase the thermal inertia and thus stabilize the internal temperature.

3.) A sunshade was constructed of sheet aluminum to protect the telemetry case and transmitter from direct solar radiation.

4.) Both sunshade and telemetry case were painted with a white titanium dioxide base paint which previous experiments showed had a high degree of reflectivity to the solar spectrum at these altitudes.

This configuration was developed under this contract. The first opportunity for flight trial occured under contract AF 19 (628) - 5140. The flight was carried out at Holloman AFB, New Mexico, on 12 July 1966. The launch took place at 4:52 AM MST and ground station recorders did not commence recording until approximately 5 AM when the air temperature was rapidly falling as the balloon quickly ascended. The resulting temperature data is plotted in Figure 6-3. The results from this flight show that components inside the instrument case were virtually uneffected by the environment, while the transmitter stabilized at a moderate temperature of 25°C. Consequently all the components stay well within the allowable temperatures set by the manufacturer.

C. Weather Radar Modification

A modification for an AN/CPS-9 radar was developed at Northeastern, experimentally verified at the Maynard branch of AFCRL, and later installed by AF

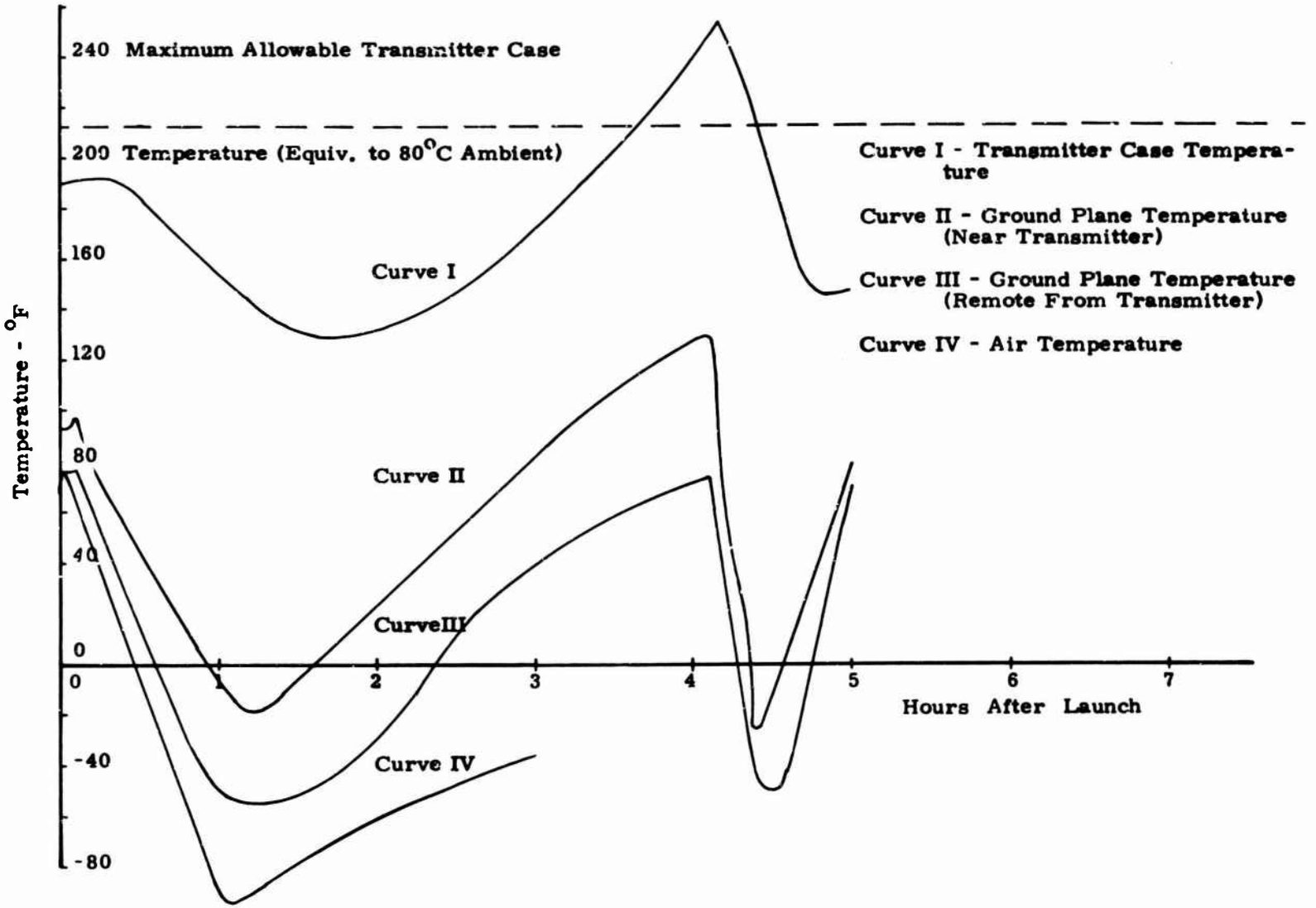

FIGURE 6 - 1. TEMPERATURE MEASUREMENTS BALLOON FLIGHT #1407

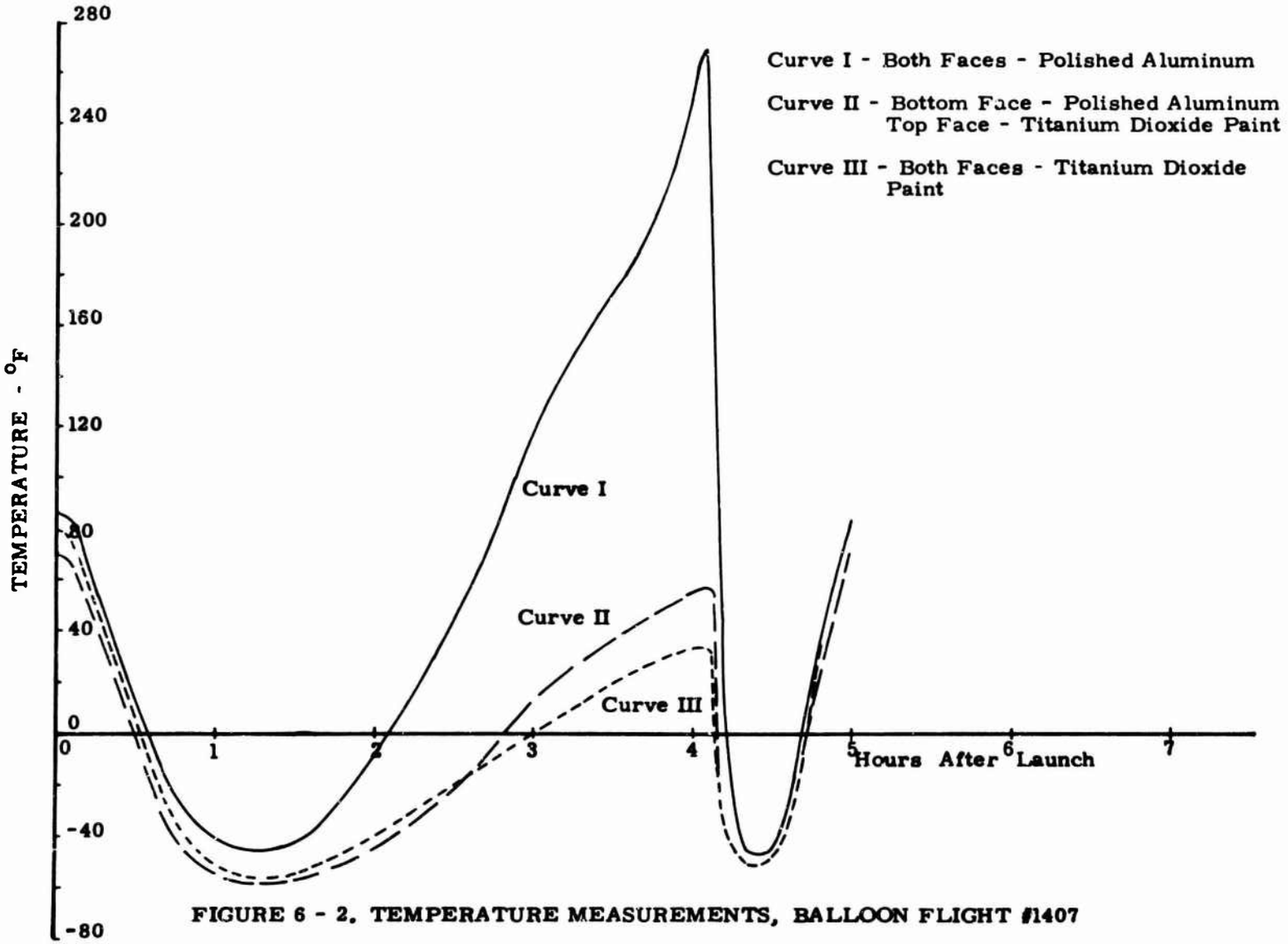

FIGURE 6 - 2. TEMPERATURE MEASUREMENTS, BALLOON FLIGHT #1407

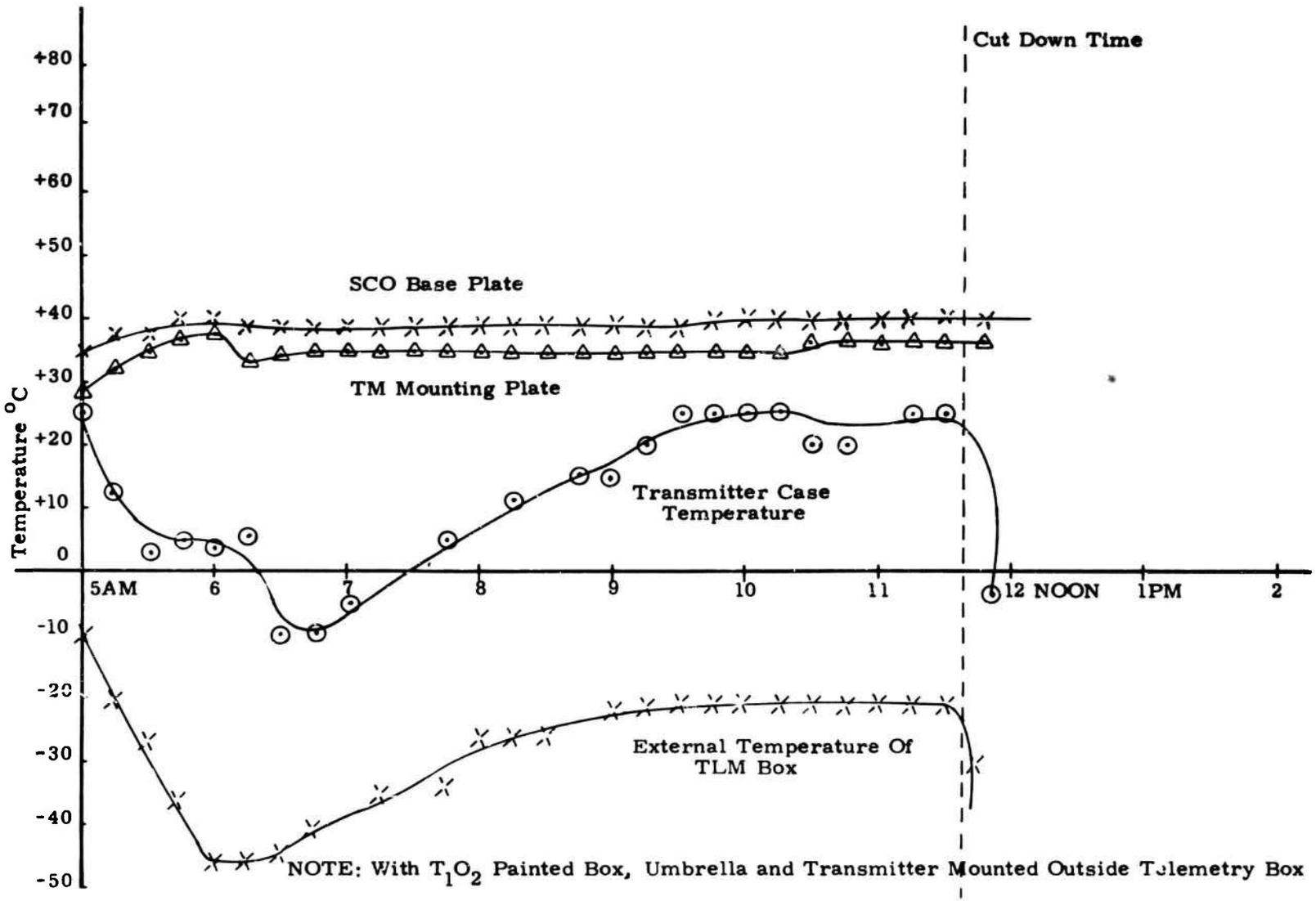

FIGURE 6 - 3. TEMPERATURE MEASUREMENTS BALLOON FLIGHT 12 JULY 1966

personnel in a radar located at Patrick Air Force Base, Florida. The purpose of the modification was to allow areas of high turbulance to be readily seen on a PPI display. This was accomplished by replacing the conventional CRT with a dark trace tube which was blanked out whenever the amplitude of the radar return exceeded a pre-set threshold.

The i-f output of the AN/CPS-9 was routed through coaxial attenuators to an RHG linear-logarithmic amplifier. A switch operated relay allowed the operator to select either output from the amplifier. The linear-amplifier selection returned the signal to the PPI unit unaltered and provided normal operation with dark-tube display. Selection of the logarithmic output of the receiver inserted the iso-echo modification.

The iso-echo modification caused a negative pulse to be generated whenever the log output of the amplifier exceeced a threshold which had been pre-set by the operator. Returns in excess of this threshold indicated regions of high air turbulance. The negative pulse from the iso-echo circuit was then combined in a mixer with the log output to blank out the PPI display. Consequently each region of high turbulance was appropriately indicated on the dark-tube face.

The iso-echo modification was checked-out at AF Maynard in July 1964 and later during the same month installed in an AN/CPS-9 weather radar at Patrick AFB, Florida, by AF personnel.

BIBLIOGRAPHY

1. Telemetry Standards, Telemetry Working Group, Inter-range Instrumentation Group, Range Commanders Council, Document 106-66, Revised March 1966, p. 9.

2. J. Spencer Rochefort, et al, Data Transmission and Trajectory Determining Devices for Research Rockets and Satellites, Final Report, Volume I, Contract AF 19 (604) - 3506, Northeastern University, 30 June 1963.

3. Smart, W.M., Spherical Astronomy, Cambridge University Press, Cambridge 1962.

4. Nelson, W.C. and E.E. Loft, Space Mechanics, Prentice Hall, Englewood Cliffs, 1962.

5. Chapman, S. and Bartels, J., Geomagnetism, Volume 2, Oxford at the Clarendon Press, 1940

6. Cain, J.C., S. Hendricks, W.E. Daniels, D.C. Jensen, Computation of the Main Geomagnetic Field From Spherical Harmonic Expansions, Goddard Space Flight Center, Greenbelt, Md., NASA document X-611-64-316, October 1964.

7. U.S. Government Printing Office, The American Ephemeris and Nautical Almanac.

8. Hosmer, G.L., Pratical Astronomy, John Wiley and Sons Inc., New York, 1956.

9. Arnold, R.N. and L. Maunder, Cyrodynamics, Academic Press, New York and London, 1961.

10. Brouwer, D. and G.M. Clemence, Celestial Mechanics, Academic Press, New York and London, 1961.

11. Nault, J.G. and R.A. Wagner, Evaluation Studies of Telemetry System Components, Scientific Report No. 1, Contract AF 19 (628) - 2433, Northeastern University, 31 August 1964.

12. Wagner, R.A., Evaluation Studies of Telemetry System Components, Scientific Report No. 2, Contract AF 19 (628) - 2433, Northeastern University, 31 August 1965.

PERSONNEL

A list of the engineers and technicians who contributed to the work reported is given below:

J. Spencer Rochefort, Professor of Electrical Engineering, Principal Investigator.

Lawrence J. O'Connor, Assistant Professor of Electrical Engineering, Engineer.

Arthur Glazer, Research Associate, Engineer.

J. Gabriel Nault, Research Associate, Engineer.

Norman Poirier, Research Associate, Engineer.

Charles H. Price, Research Associate, Engineer.

Raimundas Sukys, Research Associate, Engineer.

Ronald A. Wagner, Research Associate, Engineer.

George Schreiner, Research Assistant, Engineer.

Leonard J. Epstein, Graduate Assistant, Engineer.

William D. O'Neil, Graduate Assistant, Engineer.

Joseph F. Santacroce, Graduate Assistant, Engineer.

George Wooley, Graduate Assistant, Engineer.

Robert Cooney, Technician, Electrical Engineering.

Walter Goddard, Technician, Electrical Engineering.

Warren D. Harding, Technician, Electrical Engineering.

Robert Meston, Technician, Electrical Engineering.

Robert Pielage, Technician, Electrical Engineering.

John Shields, Technician, Electrical Engineering.

Michael Tangusso, Technician, Electrical Engineering.

RELATED CONTRACTS AND PUBLICATIONS

AF 19 (604) - 3506	1 April 1958 through 30 June 1963
AF 19 (628) - 2433	1 April 1963 through 30 September 1966
AF 19 (628) - 5140	1 April 1965 through present.

J.G. Nault and R.A. Wagner, Evaluation Studies of Telemetry System Components, Scientific Report No. 1, Contract AF 19 (628) -2433, Northeastern University, 31 August 1964.

R.A. Wagner, Evaluation Studies of Telemetry System Components, Scientific Reprrt No. 2, Contract AF 19 (628) - 2433, Northeastern University, 31 August 1965.

Unclassified

Security Classification

DOCUMENT CONTROL DATA - R&D

(Security classification of title, body of abstract and indexing annotation must be entered when the overall report is classified)

1. ORIGINATING ACTIVITY *(Corporate author)*
Northeastern University
Boston, Massachusetts 02115

2a. REPORT SECURITY CLASSIFICATION
Unclassified

2b. GROUP

3. REPORT TITLE
Data Transmission and Instrumentation Systems for Space Vehicles

4. DESCRIPTIVE NOTES *(Type of report and inclusive dates)*
Final Scientific Report, 1 April 1963 through 31 March 1967 Approved 23 June 1967

5. AUTHOR(S) *(Last name, first name, initial)*
Rochefort, J. Spencer
O'Connor, Lawrence J.
Sukys, Raimundas
Glazer, Arthur

6. REPORT DATE	7a. TOTAL NO. OF PAGES	7b. NO. OF REFS
30 April 1967	74	12

8a. CONTRACT OR GRANT NO.	9a. ORIGINATOR'S REPORT NUMBER(S)
AF 19 (628) - 2433 b. PROJECT NO. - 7043 c. TASK DOD Element No. 65402124 d. DOD Subelement No. P6328-850B-7043	Final Report 9b. OTHER REPORT NO(S) *(Any other numbers that may be assigned this report)* AFCRL-67-0338

10. AVAILABILITY/LIMITATION NOTICES
Distribution of this document is unlimited. It may be released to the Clearinghouse, Department of Commerce, for sale to the general public.

11. SUPPLEMENTARY NOTES	12. SPONSORING MILITARY ACTIVITY
	Air Force Cambridge Research Laboratories (CRE), L. G. Hanscom Field, Bedford, Mass. 01730

13. ABSTRACT

This report summarizes the main work carried out under this contract (April 1, 1963 through March 31, 1967). The contract effort can be grouped under programs concerned with an orbiting vehicle, a re-entry vehicle, field support for certain sounding rockets and balloons, evaluation of commercial telemetry system components, and system studies and developments related to telemetry and weather radar. The orbital vehicle effort is concerned with a telemetry subsystem, a data storage system, aspect instrumentation and determination and a commutator. The discussion of the instrumentation of a Trailblazer II rocket for a re-entry experiment includes treatment of an s-band pulsed system, an x-band PPM telemeter and certain probes. A tabulation is given of commercial airborne telemetry components tested and evaluated since detailed results are published in scientific reports which are available to authorized agencies. The field support rendered in connection with the various programs is tabulated. Specific discussion is given to a PAM/FM system, temperature studies of balloon telemetry systems, and the modification of a weather radar.

DD FORM 1 JAN 64 1473

Unclassified

Security Classification

Unclassified

Security Classification

14. KEY WORDS	LINK A		LINK B		LINK C	
	ROLE	WT	ROLE	WT	ROLE	WT
Data Transmission Satellites Re-entry Vehicle Rockets Balloons Attitude Determination Systems Studies and evaluation						

INSTRUCTIONS

1. **ORIGINATING ACTIVITY:** Enter the name and address of the contractor, subcontractor, grantee, Department of Defense activity or other organization *(corporate author)* issuing the report.

2a. **REPORT SECURITY CLASSIFICATION:** Enter the overall security classification of the report. Indicate whether "Restricted Data" is included. Marking is to be in accordance with appropriate security regulations.

2b. **GROUP:** Automatic downgrading is specified in DoD Directive 5200.10 and Armed Forces Industrial Manual. Enter the group number. Also, when applicable, show that optional markings have been used for Group 3 and Group 4 as authorized.

3. **REPORT TITLE:** Enter the complete report title in all capital letters. Titles in all cases should be unclassified. If a meaningful title cannot be selected without classification, show title classification in all capitals in parenthesis immediately following the title.

4. **DESCRIPTIVE NOTES:** If appropriate, enter the type of report, e.g., interim, progress, summary, annual, or final. Give the inclusive dates when a specific reporting period is covered.

5. **AUTHOR(S):** Enter the name(s) of author(s) as shown on or in the report. Enter last name, first name, middle initial. If military, show rank and branch of service. The name of the principal author is an absolute minimum requirement.

6. **REPORT DATE:** Enter the date of the report as day, month, year, or month, year. If more than one date appears on the report, use date of publication.

7a. **TOTAL NUMBER OF PAGES:** The total page count should follow normal pagination procedures, i.e., enter the number of pages containing information.

7b. **NUMBER OF REFERENCES:** Enter the total number of references cited in the report.

8a. **CONTRACT OR GRANT NUMBER:** If appropriate, enter the applicable number of the contract or grant under which the report was written.

8b, 8c, & 8d. **PROJECT NUMBER:** Enter the appropriate military department identification, such as project number, subproject number, system numbers, task number, etc.

9a. **ORIGINATOR'S REPORT NUMBER(S):** Enter the official report number by which the document will be identified and controlled by the originating activity. This number must be unique to this report.

9b. **OTHER REPORT NUMBER(S):** If the report has been assigned any other report numbers *(either by the originator or by the sponsor)*, also enter this number(s).

10. **AVAILABILITY/LIMITATION NOTICES:** Enter any limitations on further dissemination of the report, other than those imposed by security classification, using standard statements such as:

(1) "Qualified requesters may obtain copies of this report from DDC."

(2) "Foreign announcement and dissemination of this report by DDC is not authorized."

(3) "U. S. Government agencies may obtain copies of this report directly from DDC. Other qualified DDC users shall request through

_____."

(4) "U. S. military agencies may obtain copies of this report directly from DDC. Other qualified users shall request through

_____."

(5) "All distribution of this report is controlled. Qualified DDC users shall request through

_____."

If the report has been furnished to the Office of Technical Services, Department of Commerce, for sale to the public, indicate this fact and enter the price, if known.

11. **SUPPLEMENTARY NOTES:** Use for additional explanatory notes.

12. **SPONSORING MILITARY ACTIVITY:** Enter the name of the departmental project office or laboratory sponsoring *(paying for)* the research and development. Include address.

13. **ABSTRACT:** Enter an abstract giving a brief and factual summary of the document indicative of the report, even though it may also appear elsewhere in the body of the technical report. If additional space is required, a continuation sheet shall be attached.

It is highly desirable that the abstract of classified reports be unclassified. Each paragraph of the abstract shall end with an indication of the military security classification of the information in the paragraph, represented as *(TS), (S), (C), or (U).*

There is no limitation on the length of the abstract. However, the suggested length is from 150 to 225 words.

14. **KEY WORDS:** Key words are technically meaningful terms or short phrases that characterize a report and may be used as index entries for cataloging the report. Key words must be selected so that no security classification is required. Identifiers, such as equipment model designation, trade name, military project code name, geographic location, may be used as key words but will be followed by an indication of technical context. The assignment of links, rules, and weights is optional.

Unclassified

Security Classification